An-Najah National University
Faculty of Graduate Studies

Development of Efficient Photovoltaic Solar Cells' Various Models

By
Aya Mahmoud Abu Baker

Supervisor
Dr. Muna Hajj Yahya
Co- Supervisor
Dr. Maen Ishtaiwi

This Thesis is submitted in Partial Fulfillment of the Requirements for the Degree of Master in physics, Faculty of Graduate Studies, An-Najah National University, Nablus, Palestine.

2019

Development of Efficient Photovoltaic Solar Cells' Various Models

By

Aya Mahmoud Abu Baker

This Thesis was Defended Successfully on 21/3/2019 and Approved by:

Defense Committee Members	**Signature**
1. Dr. Muna Hajj Yahya \ Supervisor	**……………….**
1. Dr. Maen Ishtaiwi \ Co-Supervisor	**……………….**
3. Dr. Rabab Jarrar \ External Examiner	**……………….**
4. Prof. Mohammad Elsaid \ Internal Examiner	**……………….**

Dedication

To my father, my mother, my sisters and my brother, this thesis is dedicated to you with respect and love…..

Acknowledgment

First and foremost, I want to thank my parents (Mahmoud and Naimah) for their endless love, support and encouragement throughout my life.

My sisters (Raya, Heba and Basma) and brother (Mohammed), I'm very grateful to you for your moral and emotional support in my life.

I would like to sincerely thank my supervisors, Dr.Muna and Dr.Maen, for their guidance, patience and support. I consider myself very lucky for being able to work with an encouraging Drs. Like them.

To all my cousins and friends, I owe many thanks to you. I cannot list all the names here, but you are always on my mind.

Finally, I would like to thank my dear university, An-Najah National University, for being exactly what I needed. Special thanks go to the department of physics for teaching me so much – both about the world and about myself. I will forever hold you near and dear to my heart.

This thesis is just the beginning of my journey.

الاقرار

أنا الموقعة أدناه مقدمة الرسالة التي تحمل العنوان:

Development of Efficient Photovoltaic Solar Cells' Various Models

تطوير نماذج مختلفة من الخلايا الشمسية الكهروضوئية الفعالة

أقر بأن ما اشتملت عليه هذه الرسالة إنما هي نتاج جهدي الخاص، باستثناء مـــا تمــت الإشارة إليه حيث ما ورد، وإن هذه الرسالة ككل، أو أي جزء منها لم يقدم من قبل لنيــل أيـــة درجة عملية أو لقب علمياً وبحثي لدى أية مؤسسة تعليمية أو بحثية أخرى.

Declaration

The work provided in this thesis, unless otherwise referenced, is the researcher's own work, and has not been submitted elsewhere for any other degree or qualification.

Student's name:	**اسم الطالبة:**
Signature:	**التوقيع:**
Date:	**التاريخ:**

List of abbreviations and nomenclatures

RE: renewable energy

PV: photovoltaic

Si: silicon

c- Si: crystalline silicon

mc- Si or mono- Si: monocrystalline silicon

pc- Si or poly-Si: polycrystalline silicon

a- Si: amorphous silicon

OSC: organic solar cell

DC: direct current

STC: standard test conditions

BHJ: bulk heterojunction

VB: valence band

CB: conduction

E_g or W_g: band gap energy

SCR: space charge region

V_D: diffusion voltage

MPP: maximum power point

FF: fill factor of the PV cell

OPV: organic photovoltaic

LUMO: lowest unoccupied molecular orbital

HOMO: highest occupied molecular orbital

$P3HT{:}PCBM$: poly 3-hexylthiophene:phynyl-C70 butyric acid methyl ester

Model I: Single-diode – PV model

Model II: Single-diode with series resistance – PV model

Model III: Single-diode with series resistance and parallel resistances – PV model

Model IV: Double-diode with series and parallel resistances – PV model

G: solar irradiance

AM: air mass

P: output power

I: output current

J: current density

I_L or I_{pv} or I_{ph}: illumination or photo generated current

P_{max} or P_{MP}: maximum power

I_{MP}: maximum current

V_{MP}: maximum voltage

I_{sc}: short circuit current

V_{oc}: open circuit voltage

I_o or I_{sat}: saturation current

V_T or V_t: thermal voltage

A or n: ideality factor

I_D: diode current

R_s: series resistance

R_p or R_{sh}: parallel or shunt resistance

R_l: load resistance

α, β, γ: constant parameters for PV cell

QUCS: quite universal circuit simulator software

GPVDM: general purpose photovoltaic device model software

CO_2: Carbon dioxide

$CdTe$: Cadmium telluride

$CIGC$: Copper indium gallium selenide

P: Phosphorus

As: Arsenic

B: Boron

Ga: Gallium

Al: Aluminum

Table of contents

List of Tables

List of Figures

Development of Efficient Photovoltaic Solar Cells' Various Models

By
Aya Mahmoud Abu Baker
Supervisor
Dr. Muna Hajj Yahya
Co- Supervisor
Dr. Maen Ishtaiwi

Abstract

This thesis deals with three different types of photovoltaic (PV) cells namely monocrystalline silicon and polycrystalline silicon and organic PV cells. We studied four models of PV cells equivalent circuits for each of mono- and polycrystalline silicon cells by QUCS software. The input parameters were extracted from the datasheet of the cells. The main goal of this research is to conclude the most efficient model of DC PV cells that gives the highest maximum power point. This work also deals with the main factors affecting the behavior of the PV cell: the cell temperature and solar irradiance. I-V characteristic curves will be drawn properly under the variation of temperature and irradiance. Depending on varying the models of PV cells, cell temperature and irradiance we saw how efficiency and different parameters of the cell will be varied.

This thesis opens up a new field which is the organic solar cells devices or third generation of PV cells devices. The electrical simulation of an organic bulk heterojunction (BHJ) PV cell based on $P3HT:PCBM$ as an active layer was done using GPVDM software under STC. The conversion efficiency of organic BHJ cells is studied under changing the thickness of the active layer. Furthermore, the current density-voltage characteristics were obtained under changing series resistance value.

The simulation results confirmed, as expected, that monocrystalline silicon solar cells are more efficient than polycrystalline silicon solar cells but polycrystalline solar cells have higher quality than monocrystalline solar cells. It was concluded also that the non-crystalline solar cells are not as efficient as the crystalline ones but they are cheaper.

Chapter One

Introduction

Chapter One
Introduction

1.1 Background

Solar energy is an important renewable energy (RE) source. Lots of researches are directed towards the solar cells and many countries started seriously to rely on this clean, safe and renewable energy due to the concern over global warming and the depletion of fossil fuels.

Photovoltaic (PV) system or solar power systems are related to the systems which convert sunlight into electricity by the solar panels. Solar panels are made up of smaller units called solar cells or PV cells. PV cells are mostly made from Silicon (Si), which is a semiconductor material. PV systems generation is attracting a growing amount of economic and commercial interest, in spite of its relatively high cost. The PV cell production is increasing more than 40% every year [1]. This rate of growth has led to a rise in research projects on numerous aspects of photovoltaics, from the development of novel PV cells [2] to the performance analysis, sizing, performance estimation and optimization of PV energy systems [3].

In PV cell, p-n junction is sandwiched between two conductive layers. Si p-n junction is made up of two layers of monocrystalline (mc-Si): n-type silicon and p-type silicon. Also, instead of mc-Si, p-n junction can be made up of polycrystalline silicon (pc-Si). We can differentiate between these two major types of Si wafers by looking at the defect density in the bulk of Si [1].

N-type silicon has an extra electrons and p-type silicon has an extra holes. Electrons can cross the p-n junction when the two layers meet, leaving a positive charge on one side and creating a negative charge on another producing the barrier potential.

The electromagnetic radiation of solar energy can be directly converted to electricity through photovoltaic effect. When the solar cell is exposed to sunlight, photons with energy greater than the band gap energy of the semiconductor are absorbed and create some electron-hole pairs proportional to the incident irradiation. Under the influence of the internal electric fields of the p-n junction, these carriers are swept apart and create a photocurrent which is directly proportional to solar irradiation [4].

PV cell models are usually drawn from the equivalent electrical circuit. Modeling of PV cells is an important topic of this research [5].

1.2 Motivation of Thesis

Solar energy is the world's main RE source and is accessible everywhere in distinct quantities. PV panels do not have any moving parts, operate silently and generate no emissions.

Many people believe that tackling the energy problem is amongst the biggest challenges for human kind in the 21^{st} century. It is a challenge because of several problems: The first challenge the humankind is facing is a supply-demand problem. The demand is continuously growing. The world population is still rapidly growing, and some studies predict a world population of 9 billion around 2040 in contrast to the 7 billion people living on the planet today. All these people will need energy, which increases the global energy demand.

A second challenge that we tend to face is related to the fact that our energy infrastructure heavily depends on fossil fuels like oil, coal and gas. Fossil fuels are nothing but millions and millions of years of solar energy stored in the form of chemical energy. The problem is that humans consume these fossil fuels much faster than they're generated through the photosynthetic process in nature. Therefore fossil fuels aren't a sustainable energy source. The more fossil fuels we consume, the less easily obtainable gas and oil resources will be available.

A third challenge is that by burning fossil fuels we produce the so-called greenhouse gases like carbon dioxide (CO_2). The additional carbon dioxide created by human activities is stored in our oceans and atmosphere. The increase in carbon dioxide is responsible for the global warming and climate change, which can have drastic consequences of the habitats of many people [1].

A PV cell generates electricity when it is illuminated by the sun or some other light sources. Simply, the equivalent circuit of an illuminated PV cell is a current source in parallel with a single-diode. The environmental conditions have a big effect on the characteristics and overall performance of a PV module.

In figure 1.1 the global growth of photovoltaic in recent years is shown. The vertical axis shows the total produced power capacity in megawatts (MW). The horizontal axis presents the time. We can see that the solar production is increasing through years [6].

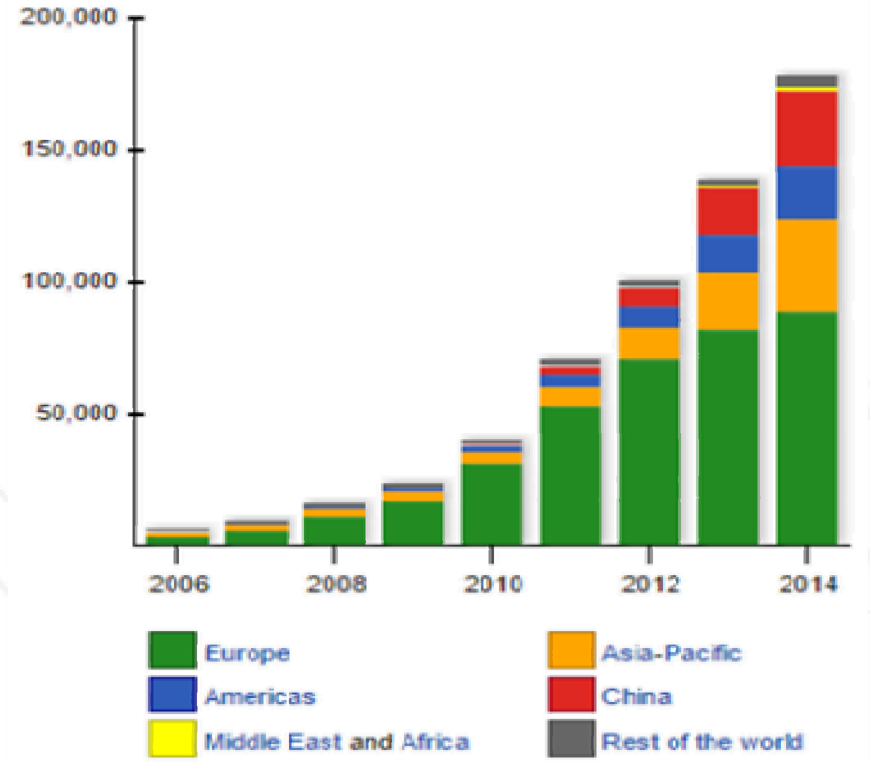

Figure (1.1): The worldwide growth of photovoltaics [6].

The notable growth of the PV industry and the elevated number of installed PV systems all over the world raised the want for simulation tools for PV systems. To understand the PV system in a better way, modeling the PV system in many operating and weather conditions is essential [7].

Simulation of PV systems is a necessary part of any engineering practice. It helps to learn about and analyze the behavior of the system also, to estimate the conversion efficiency of the PV system.

1.3 PV materials

1.3.1 Crystalline silicon (c-Si) PV technology

This is known as the first generation solar cell technology. Almost 86% of solar cell market today is based on crystalline silicon solar cells. Crystalline silicon based solar cells have a wide spectral absorption range and high carrier mobility. There are two approaches to produce crystalline silicon based solar cells; monocrystalline and multi-crystalline cells.

Monocrystalline silicon also known as single-crystalline silicon is a crystalline solid, in which the crystal sample is continuous and unbroken without any grain boundaries over the whole bulk. Monocrystalline silicon is produced using the Czochralski process (CZ process). Monocrystalline wafer cells are expensive since they are cut from cylindrical ingots. While polycrystalline silicon cells which they are less expensive than mono-Si ones, they are made up from cast square ingots- large blocks of molten silicon carefully cooled and solidified. However poly-Si solar cells are less efficient than mono-Si cells [1].

1.3.2 Thin-film PV technology

This is known as the second generation solar cell technology. Thin-film solar cells were developed to become cheaper than first generation solar cells. However, thin-film cells have a lower efficiency than crystalline silicon solar cells. An example of thin-film PV cells is amorphous silicon (a-Si) solar cell. a-Si is the non-crystalline form of silicon. It is broadly used in calculators and other small electronic devices. It is also more flexible than crystalline silicon solar cells. Thin-film technology includes $CdTe$ solar cells and $CIGS$ cells [1] [8].

1.3.3 Organic PV technology

This is known as third generation solar cell technology. The used absorber materials are either conductive organic polymers or organic molecules that are based on carbon, which may form a cyclic, a-cyclic, linear or mixed compound structure. Organic solar cells (OSCs) are cheap to produce because of the low cost of materials and the easy fabrication processes. It will be discussed more in chapter 5 [1] [8].

1.4 Literature reviews

Vun Jack Chin and his group [9] have presented a useful review paper that considers the remarkable works on the modeling and parameters estimation of PV cells for PV simulation. They performed the main ideas, features, and highlighted the advantages and disadvantages of three main PV cell models, that are, the single diode with series resistance (R_s), parallel resistance (R_p) and two diode. The work was done using both analytical and the soft computing process for the parameter estimation techniques. Their work can be considered as a reference for researches in the field of modeling and simulation of PV systems.

Bhubaneswari Parida and his group [10] introduced a review paper which shows the PV technology, its power generating ability and the various present light sensitive materials used. They also discussed the different existing evaluation methods related to the accuracy of PV devices.

Huan-Liang Tsai et al. [11] proposed a PV model using Matlab/Simulink software package. They studied the effect of sun irradiance and cell temperature on the output current and power characteristics of the PV model. The research represented PV cell, module and array by an easy use of the package.

Vivek Tamrakar and his group [12] have presented the characteristics of three PV models which they are: ideal single diode, practical single diode, and double diode. They demonstrated non-linear mathematical equations for yielding current and power curves from a single diode model. They have been used a $120\,W$ polycrystalline solar module specifications for the model evaluation.

The results obtained by Md. Nazmul Islam and Sarkar [13] point out that the fill factor and short-circuit current are decreased when increasing series resistance. The parallel resistance does reduce the open-circuit voltage. They found also that both diffusion diode and recombination diode does reduce the open-circuit voltage and fill factor. They concluded that increasing cell temperature reduces open-circuit voltage and fill factor significantly.

L.A. Dobrzański et al. [14] discussed the differences between mono- and polycrystalline silicon solar cells. Their work was based on using mathematical equations to measure parameters of PV cells and to carry out current and power curves.

Simon Lineykin and his group [15] developed a novel process of the single diode PV model estimation. They analyzed the characteristics of the solar panel provided by the manufacturer. They used a method which mixes the solution of a system of algebraic equations with optimization algorithm for extracting seven PV module parameters of the single diode model. The output parameters and current curves were obtained with an accuracy of about $0.1\% - 0.5\%$ for STC.

E. Saloux and his group [16] have been proposed a very helpful approach for design engineers to define the performance of any PV system without doing numerical calculations. They determined the electrical characteristics of PV panel. Also they studied the effect of PV panel temperature and sun irradiance on key cell parameters.

Kashif Ishaque and his group [17] had utilized the two diode model to represent a PV cell using Matlab/Simulink software. They extracted the input parameters of PV system from datasheet provided by manufacturers. They considered five PV modules of different types, multi-crystalline, mono-crystalline and thin-film concentrating on verification the accuracy of the simulator. Their work can be very useful for PV experts and design engineers who need a simple, fast and accurate PV simulator to help them design their PV systems.

Current and voltage of a $120\ W$ of monocrystalline PV module were experimentally measured by [18]. The environmental variables like temperature and irradiance were measured also and used to prove the operating current of the system. They considered the four parameter model to study the PV system considering the parallel resistance as infinite and thus neglect it. They found that the five parameter model predicts the operating current better than the four parameter model does.

E.M.G. Rodrigues and his group [19] had focused on single diode PV models. They presented a comprehensive simulation that studied the temperature dependence, solar irradiation change, diode ideality factor and series resistance impact on behavior of PV cell. Conclusions were finally drawn properly.

Minh Trung Dang and his group [20] have been carried out a survey of the enormous literatures published between 2002 and 2010 that offer solar cells based on a mixture of $P3HT$ and $PCBM$ as an active layer in organic PV cells. They reported that the most studied active layer materials around the world for the BHJ solar cell are $P3HT$ and $PCBM$. It gives a power conversion efficiency of about 5%.

Nikhil Rastogi and his group [21] have been analyzed the electrical properties of BHJ solar cell based on $P3HT$: $PCBM$ organic materials by using GPVDM software. They focused on the behavior of the simulated organic PV cell at different series resistances. They observed that the current density-voltage (J-V) curve is varied with series resistance. They found that the best J-V curve i.e. the maximum short circuit current density occurs at series resistance equals 1Ω.

Narender Singh and his group [22] have been simulated the organic solar cell based on $P3HT{:}PCBM$ electrically using GPVDM software at different charge carrier mobility. They observed that the charge carrier mobility affects the J-V characteristics. They concluded that the best J-V curve is obtained at $0.5 \times 10^{-6} m^2 v^{-1} s^{-1}$ carrier mobility.

Adam J. Moulé and his group [23] have been studied the dependence of performance of BHJ solar cells on the thickness of active layer. They made a comparison between solar cells comprised of the donor materials $P3HT$ and $OC_1C_{10} - PPV$ with the acceptor $PCBM$. They finally achieved a device with a power efficiency of 3.7% when active layer thickness is equal $225\ nm$ under STC.

1.5 Aim and objectives

The conversion of solar radiation into electrical energy by means of solar cells - in other words, the conversion efficiency of a PV cell, was developed as a part of satellite and space-travel technology. Nowadays prevailing technology utilizes the band gap of semiconductor materials to generate electrons and conduct them in a preferred direction using a p-n junction. The theoretical maximum efficiency of single junction solar cells is approximately 33%, and in practice, efficiencies as high as 25% have been achieved with Si PV devices. The overall system efficiencies of the commercially available PV panels today are in the range of 10% to 25% [24].

This research aims to figure out the most efficient model of DC PV cell with performance close to the ideal model and which is easy to apply as hardware. Also it will help industries and engineers to determine the performance of PV cells easily.

Since the experimental test of DC PV cell is expensive and unstable because it relies on weather conditions it is very useful to have simulation models of PV cell in order to use them anytime and everywhere. This research will study the behaviour of PV cells. The equivalent circuits will be analysed and studied in stable conditions with low cost.

The modelling techniques and analysing methods reviewed and examined during this research aim to provide students and researchers a set of criteria that will assist in designing a model to identify which model of PV cell has more conversion efficiency i.e. convert incident photons to DC current more efficiently.

1.5.1 Simulation of single junction crystalline silicon solar cells.

The following steps serve the research goals:

1. The DC PV cell models will be simulated using Quite Universal Circuit Simulator (QUCS) [25].
2. The ideal DC model will be built and simulated firstly.

The important parameters which affect the efficiency of the cell under the standard test conditions (STC) will be analyzed and compared to those provided by the datasheet values.

3. Study the $I - V$ characteristic curve for one model (the ideal model).
4. Introduce the losses in the solar cell:
   a. A shunt resistance and another in series can be added.
   b. Increasing the number of diodes.
5. Compare the output power and efficiency of various PV cell models.
6. Study the behavior of PV cell in various external temperatures and different solar irradiations.

These solar cells will be simulated and analyzed depending on the data sheet parameters' of the panels. The research will focus on their efficiencies to compare results in order to get the most efficient photovoltaic system.

1.5.2 Simulation of organic bulk heterojunction solar cell based on $P3HT{:}PCBM$.

1. The organic PV cell model will be simulated using general purpose photovoltaic device model (GPVDM) software [26].
2. The solar cell will be simulated firstly with an active layer thickness equals 400 nm under STC.

3. Current density-voltage (J-V) characteristics and conversion efficiency will be studied and analyzed.

4. The organic solar cell will be simulated under different values of thickness of the active layer and an efficiency comparison will be held.

5. The organic solar cell will be simulated under different series resistances.

6. J-V characteristics behavior of organic solar cell will be studied under different values of series resistances.

1.6 Thesis Outline

This thesis consists of six chapters:

Chapter 1 contains a brief introduction to solar cells, motivation of this research, previous studies and research objectives.

Some background knowledge on renewable energy, the solar radiation, PV materials, the p-n junction and the working principle of PV cells are described in chapter 2.

Also, various models used to describe the crystalline silicon PV cell are drawn and analyzed namely single-diode, single-diode with series resistance, single-diode with series and parallel resistances and double-diode with series and parallel resistances PV models. Also, the important electrical characteristics of a PV cell are presented in chapter 2.

The methodology of simulating crystalline silicon PV cells (mono-Si and poly-Si) using QUCS software and the way of extracting the input parameters from a datasheet are discussed in chapter 3.

A brief introduction to several topics concerning about organic solar cell devices or non-crystalline solar cells and the simulation of organic BHJ solar cell based on $P3HT:PCBM$ that is carried out using GPVDM software are presented in chapter 4.

A discussion on the results of the simulation of mono-Si PV cell and poly-Si PV cell under STC, a comparison between the simulated results under varying the environmental conditions and the simulation results of the $P3HT:PCBM$ BHJ solar cell are provided in chapter 5.

The conclusions drawn from the research are presented in chapter 6.

Chapter Two

The Physics of Solar Cells

Chapter Two
The Physics of Solar Cells

2.1 The family of renewable energies

Before turning to photovoltaics and solar radiation in detail, we should allocate them into the family of renewable energies (REs). The term "renewable" means that the supply of energy isn't spent [7]. In other words, renewable means "refilled" by nature in a useful amount of time [1]. The wind blows every year, again and again. The Sun rises every day and the plants grow once more after the harvest. Within the case of geothermal energy, the earth is cooling off however this will only be noticeable thousands of years in future. Figure 2.1 shows that the factual primary energies of the REs are:

- The movement of the planets.
- The heat of the Earth.
- Solar radiation.

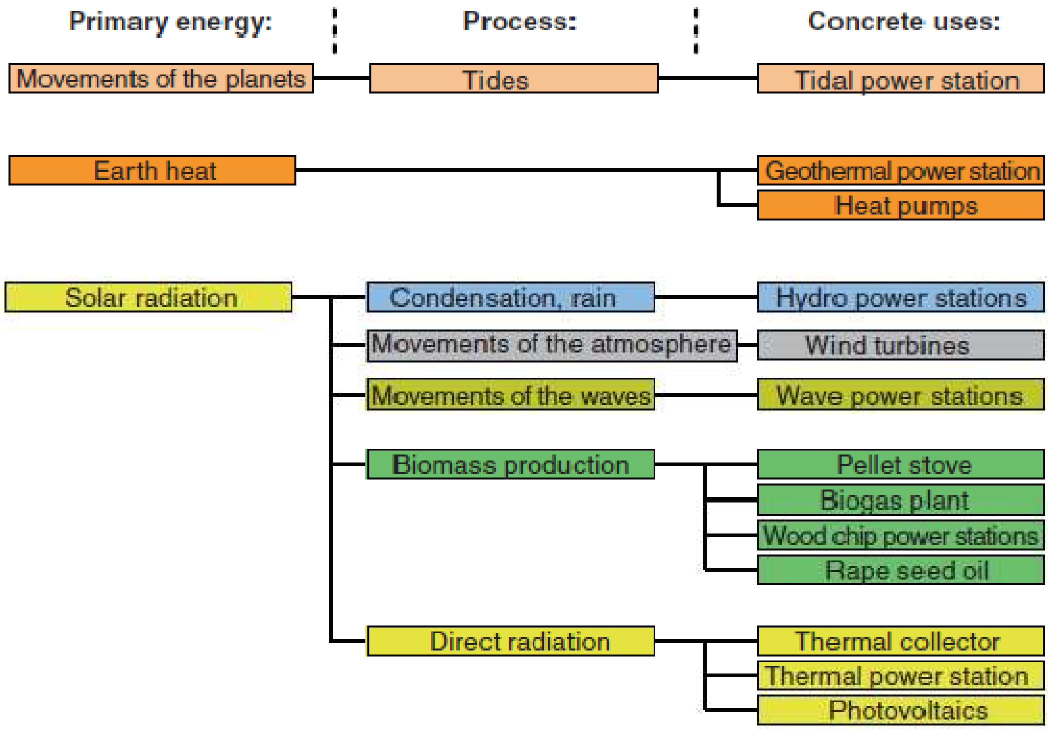

Figure (2.1): Various prospects for the use of renewable energies.

Solar radiation is that the basic for a wide range of energies. Thus, the utilization of hydropower is possible only by the condensation of water and subsequent precipitation onto land. Atmospheric movement originates mostly because of the solar radiation that is also the basis for the utilization of wind power. In the case of biomass products it's again the sunlight that causes photosynthesis, and therefore the growth of biomass is conditioned by it.

Solar radiation also can be used directly for the generation of heat, for example in a thermal collector for domestic water or domestic space heating. Thermal solar power stations generate process heat from focused sunlight so as to drive generators for the production of electricity. Last but not least, with photovoltaics, solar radiation is directly converted into electrical energy.

Photovoltaics have a very special attraction since they're the only one able to convert sunlight into electricity directly without complicated intermediate processes and without employing mechanical converters that can wear out [7].

2.1.1 What does "Photovoltaic" mean?

"Photovoltaic" is a term which is a combination of the Greek word *phós*, *phōtós* (light, of the light) and the name of the Italian physicist Alessandro Volta (1745-1825). He discovered the first practical electrochemical battery and also the unit of electric potential difference, Volt, is named after him. Therefore, a translation of the word photovoltaic could be light battery or also light source. More generally, photovoltaic is the direct conversion of sunlight into electrical energy.

2.2 The solar source

The basis of all life on Earth is that the radiation from the Sun because the solar energy is the most plentiful renewable source. The use of photovoltaics additionally depends on the availability of sunlight.

The Sun is the star at the center of the solar system. It represents a huge fusion reactor in whose inside each four hydrogen atoms are melted into one helium atom. During this atomic fusion temperatures of around 15 million °C are created. The energy freed is released into space in the form of radiation [7].

This radiation is called the solar radiation. It consists of the electromagnetic waves emitted by the Sun. Solar energy is in the form of electromagnetic radiation with the wavelengths ranging from approximately $290\,nm$ to over $3200\,nm$, which correspond to ultraviolet (less than $400\,nm$), visible (400 and $700\,nm$), and infrared (over $700\,nm$). Most of this energy is concentrated in the visible and the near-infrared wavelength range. The incident solar radiation, sometimes called insolation, is measured as irradiance, or the energy per unit time per unit area (or power per unit area). The unit most often used is watt per square meter (W/m^2) [27]. So, to summarize up:

- Solar radiation: is all the radiant energy emitted by the sun.
- Solar irradiance (G): is the power per unit area received from the Sun in the form of electromagnetic radiation measured in space or at the Earth's surface.
- Insolation (S): is the total solar radiation that reaches the earth's surface. It is measured by the amount of solar energy received per unit time per unit area.

Not the entire direct sunlight incident on earth’s atmosphere arrives at the earth’s surface (figure 2.2 [27]). As shown in the figure the atmosphere attenuates many parts of the spectrum [28].

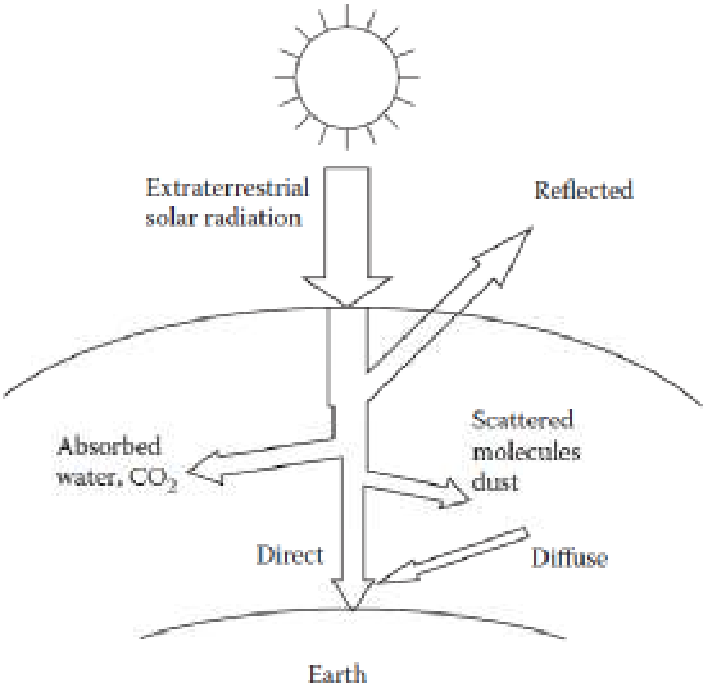

Figure (2.2) Attenuation of solar radiation as it passes through the atmosphere [27]**.**

According to figure 2.2, there are two main components of solar radiation received on earth [28]:

- Direct radiation: which depends on the distance the rays travel (air mass).
- Diffuse radiation: it is demonstrated in figure 2.2.

2.2.1 The solar spectrum

It is main to know the spectral distribution of the solar radiation, i.e. the number of photons of a particular energy as a function of the wavelength λ or the spectral irradiance of a wavelength spectrum ($E_\lambda(\lambda)$) [1].

Every hot body provides off radiation to its surroundings. According to Plank's Law of Radiation, the surface temperature determines the spectrum of the radiation. The Sun has a surface temperature equals approximately $6000\,K$ that leads to the black body spectrum shown in figure 2.3 (dashed line) [7].The extraterrestrial spectrum is already different. It is referred to as the $AM0$ spectrum, because "zero" atmosphere is traversed. $AM0$ is also illustrated in figure 2.3.

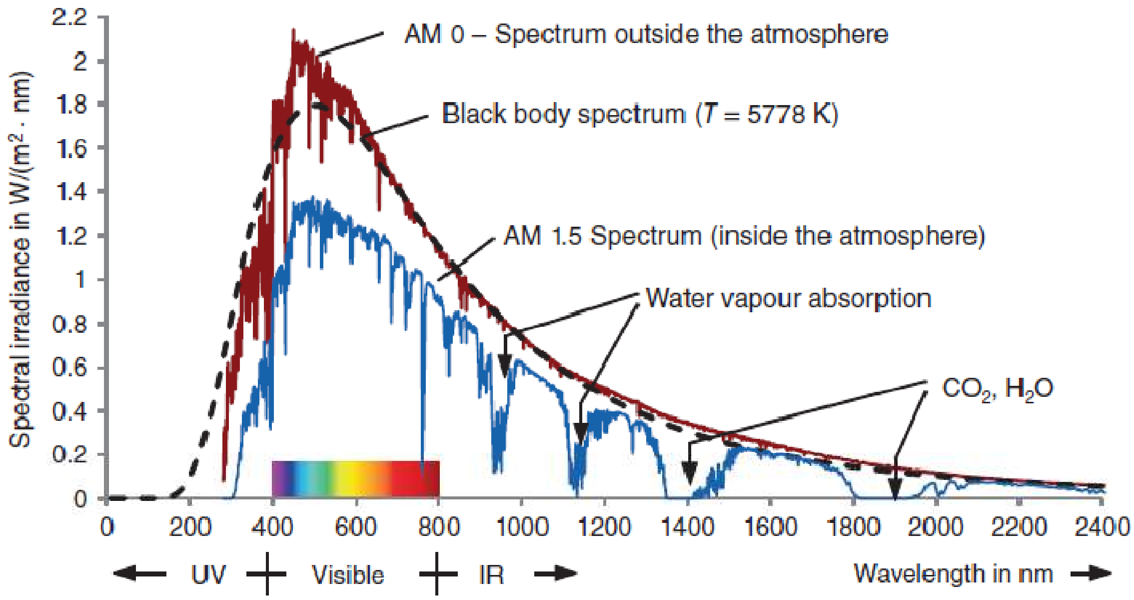

Figure (2.3); Different solar spectra: the blackbody spectrum of a blackbody at 5778 K, the extraterrestrial AM0 spectrum and the AM1.5 spectrum [7]**.**

When radiation passes through the atmosphere of the earth, it's attenuated. The most necessary parameter that determines the solar irradiance under a clear sky conditions is that the distance that the sunlight has to travel through the atmosphere. The distance is the shortest when the Sun is at the zenith, i.e. directly overhead. The ratio of an actual path length of the sunlight to this minimal distance is known as the optical air mass

(AM). So when the Sun is at its zenith, the air mass is unity and the spectrum is called air mass one ($AM1$) spectrum (figure 2.4 [29]) When the Sun is at an angle θ with zenith, AM is given by [1]:

$$AM = \frac{1}{cos\theta} \quad (2.1)$$

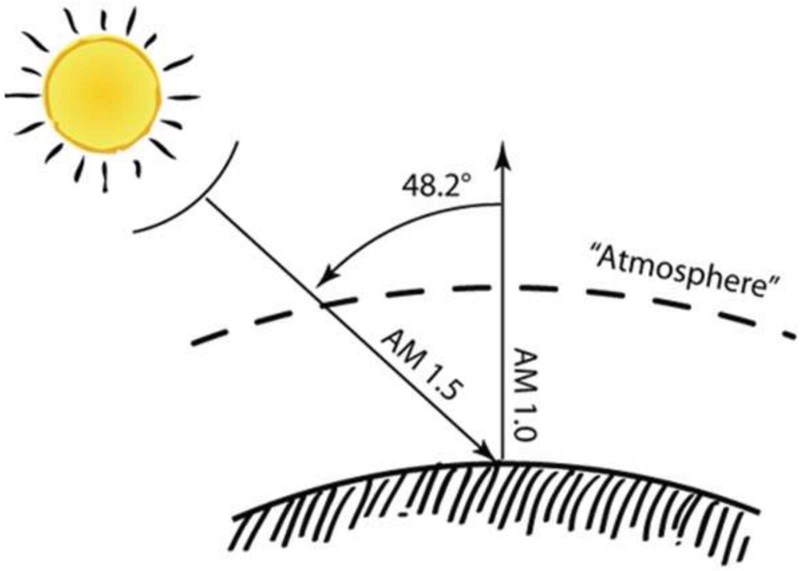

Figure (2.4): Explanation of the term *Air Mass* [29]**.**

2.2.2 The standard test conditions (STC)

It is important to define a reference solar conditions that allow a comparison of all the different solar cells and PV modules' parameters provided on manufacturer's datasheet [1]. So the standard test conditions are specified as follow:

- Full Sun radiation (radiation strength $G = G_{STC} = 1000\, W/m^2$)
- Reference cell temperature for performance rating ($T_{cell} = T_{C\_STC} = 25°C$)

- Standard light spectrum (AM 1.5). As it arrives in spring and autumn and can be viewed as an average year's spectrum [7].

2.3 The material of solar cells

2.3.1 Introduction

As was mentioned previously, PV effect is the basis of the conversion of light to electricity in PV, or solar, cells. PV technology requires materials that firstly should absorb light "which is pure energy"; and this light should impart enough energy to some electrons within the material in order to free them. A built-in-potential barrier should also present in the PV cell material in order to act on the electrons and to produce a voltage, which can be used to drive a current through a circuit. These requirements on material properties make semiconductors particularly very suitable for solar cell technology [28].

We will take silicon (Si) cell as a model. Si is a widely used as the active material in solar cells; understanding the Si solar cell is a good basic work for understanding any PV cell. We shall start by reviewing some of silicon's basic characteristics.

The Si atom has fourteen electrons coordinated in such a way that the outer four can be given to, accepted from, or shared with another atom. These outer four electrons are called valence electrons ($v.e's$). Big numbers of Si atoms will bond together to create a solid, through their $v.e's$. As a solid every Si atom typically shares each of its four $v.e's$ with another Si atom. Each basic silicon unit, forming a tetrahedral arrangement, thereby contains five atoms (Si atom plus the four others it shares electrons with) [28].

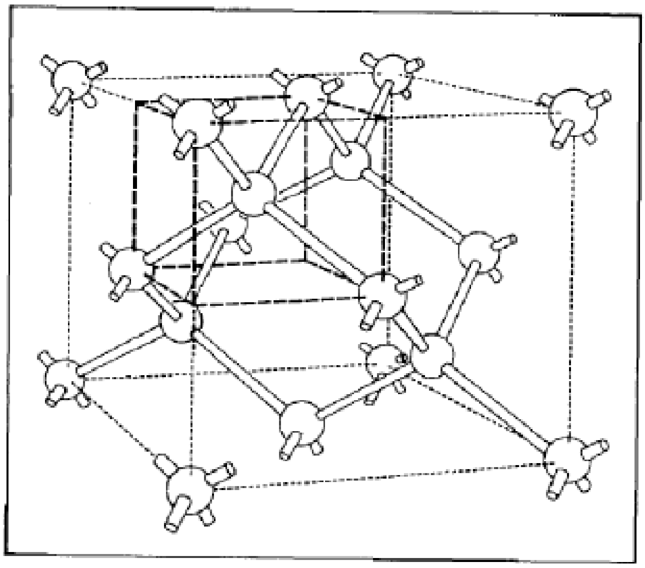

Figure (2.5) the silicon crystal arrangement.

The fixed formation of a solid's atoms i.e. each atom in the solid is held in place at a constant distance and angle with each of the atoms which it shares a bond. This formation is called a crystal lattice. Not all solids are crystalline however some can have multiple crystalline forms. A representation of the Si crystal lattice arrangement is shown in figure 2.5 [28].

Valence electrons that participate in the covalent bonds, have their allowed energies in the valence band (VB) and the allowed energies of electrons freed from the covalent bonds form the conduction band (CB). The VB is separated from the CB by a band of forbidden energy levels [1].

The maximum attainable VB energy is denoted by E_v. Also, the minimum attainable CB energy is denoted by E_c. The energy difference between the edges of those two bands is named as the band gap energy or band gap, E_g or W_g and it is a very important material parameter (figure 2.6). Si has an energy gap equals 1.1 eV at room temperature [1].

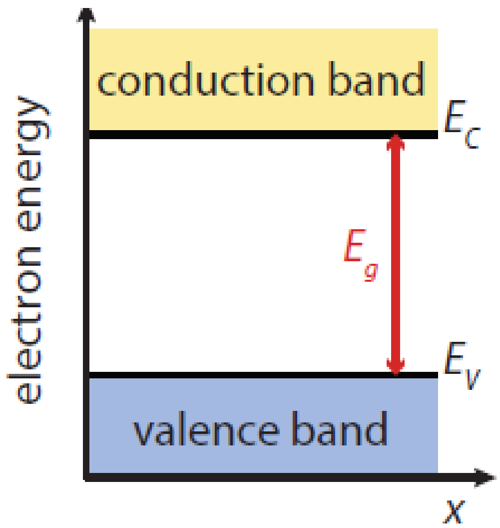

Figure (2.6): the basic energy band diagram [1].

2.3.2 Doping of the material

To make a material to conduct, $v.e's$ in the VB should be freed i.e. the bonds should be broken and an electron-hole pair will be generated by applying a work on the material with a sufficient energy. This can be done by:

- Heating the material.
- Illuminating the material with a suitable light.
- Doping the material with suitable impurities.

In order to produce practical and useful devices from semiconductors, one has to dope the material by adding specific impurities. By doping we can get:

- N-type or p-type semiconductor.
- A change in the electron and hole concentration in the material.

In order to produce n-type Si, pentavalent impurity atoms will be added to Si for example: P and As. While for p-type semiconductor we add trivalent atoms such as B,Ga and Al to Si [2]. N-type and p-type doping are illustrated in figures 2.7 and 2.8. For more details see for example [28] and [7].

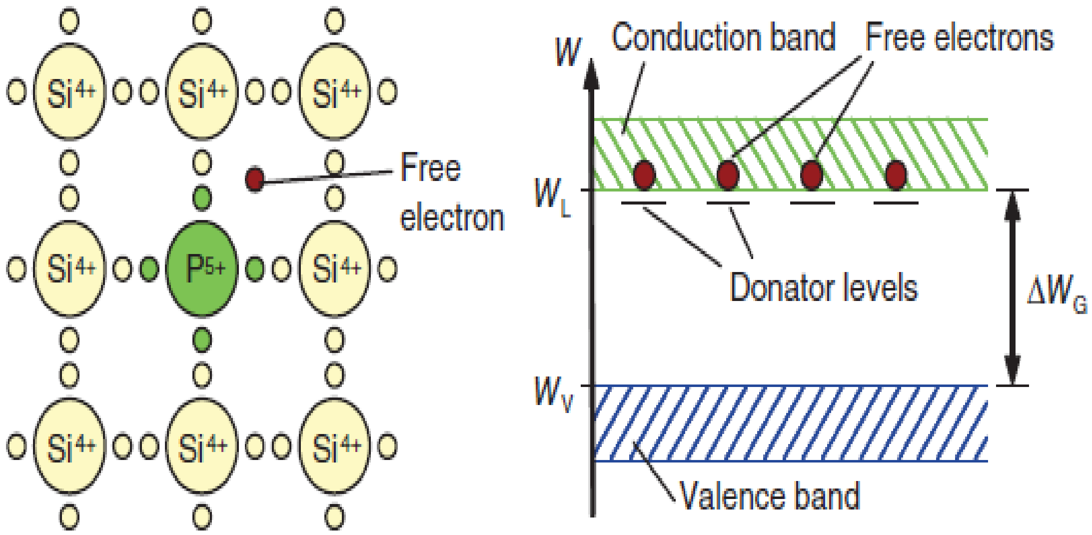

Figure (2.7): n-type doping of Si crystal with a phosphorus atom: one of the five $v.es$ of the P atom is available as a free electron and a new energy level is formed beneath the CB edge [7].

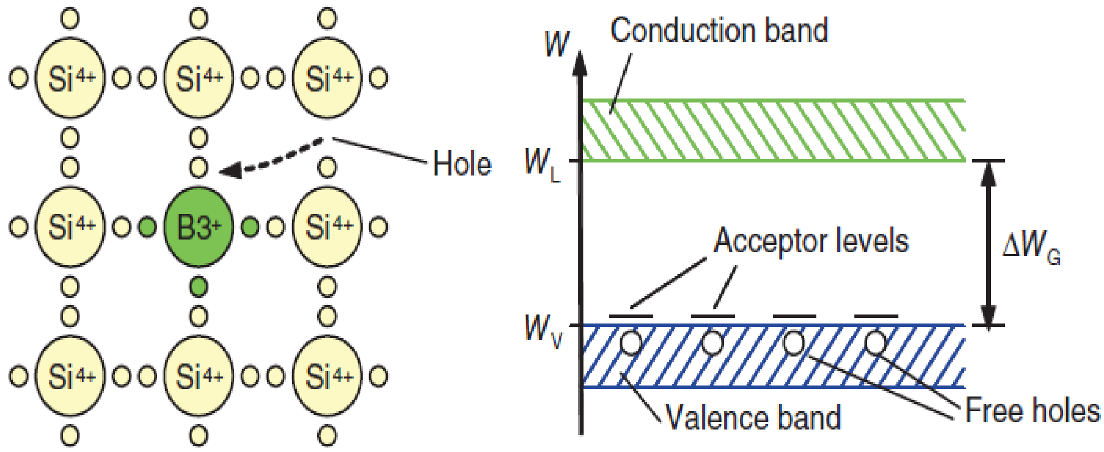

Figure (2.8): p-doping of Si crystal with a boron atom. B atom offers one of the four links opened since B atom has only three $v.es$. A neighboring electron moves into this vacancy and a hole is generated [7]**.**

2.4 The p-n junction

P-N junction is formed when n-type semiconductor and p-type semiconductor meet. The processes are shown in figure 2.9. Both n-type and p-type regions are electrically neutral. On the n-side there is an excess of free electrons. When the two regions are in contact the free electrons on the left side diffuse due to the concentration graded from the diffusion current across the junction region into the p-doped region and there they recombine with the holes. Holes in the right side diffuse to the left into the n-type material where they recombine with the electrons. Due to the rising number of superfluous fixed charges in the junction region, an electrical field finally comes into existence. This electric field leads again to the electrons being pushed to the left and the holes to the right until a new balance is built up in which diffusion and field current cancel each other and a space charge region (SCR) exists at the p-n junction.

This space charge region causes a potential difference between the right and left borders of the space charge region that is called the diffusion voltage (V_D).

So, doping semiconductor materials make them conduct electrical current as well as simple metals. Also make n-type semiconductor in contact with p-type semiconductor will yield materials with very special properties [7].

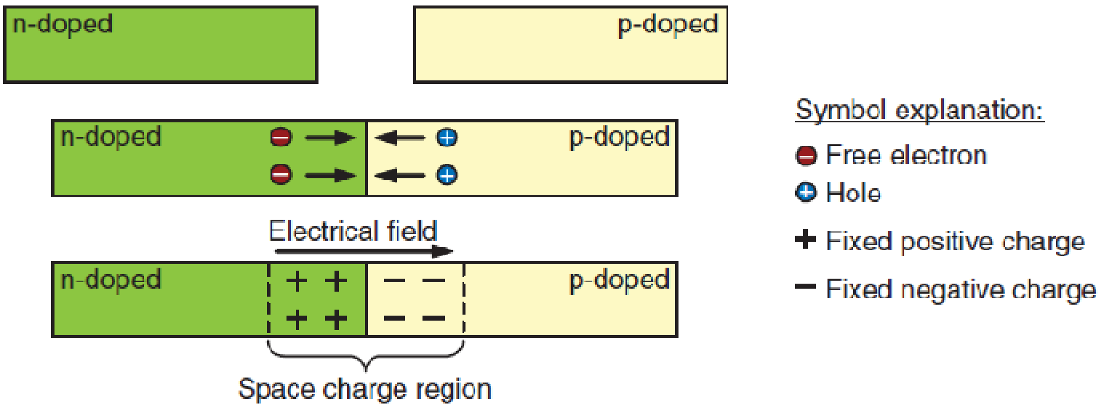

Figure (2.9) formation of SCR, when n-type and p-type semiconductors are brought together to form a junction.

2.5 Working principle of a solar cell

When light "photons" is incident on a solar cell's surface, electrons will be excited and an electron-hole pairs will be formed. Then the electric field in the junction will separate those electrons and holes. When they reach the end contacts of p-n material, an electrical current will flow through an external load. Hence, the radiative energy of the photon is directly converted into electrical energy [1].

The photon energy is given by:

$$E_\lambda = hf = h\frac{c}{\lambda} \quad (2.2)$$

Where:

- f is the frequency of the light
- λ is the wavelength
- c is the speed of light in vacuum
- h is the plank's constant

This energy must be sufficient enough to excite electrons i.e. it should be greater than the energy gap $E_g (E_\lambda > E_g)$ in order to excite electrons from the VB into CB of the semiconductor.

A typical single-crystal silicon p-n junction solar cell is shown in figure 2.10 [28]. As shown in figure 2.10, single junction solar cell consists of several layers. It is mainly consists of a conducting grid on the top surface of the solar cell and it is usually composed of metal; just below the top layer there is an antireflective coating layer in order to reduce losses and it is colored by black. The back electrical contact or the back-electrode covers the whole back side of the solar cell also it is composed of a metal with high conductivity. Between these two layers a p-n junction is sandwiched; n-type silicon about 1 μm thick also it called collector; a very narrow junction field region where no free charge carriers exist; and a p-type silicon layer which is termed also as silicon base layer and it is about $500\ \mu m$ thick [28].

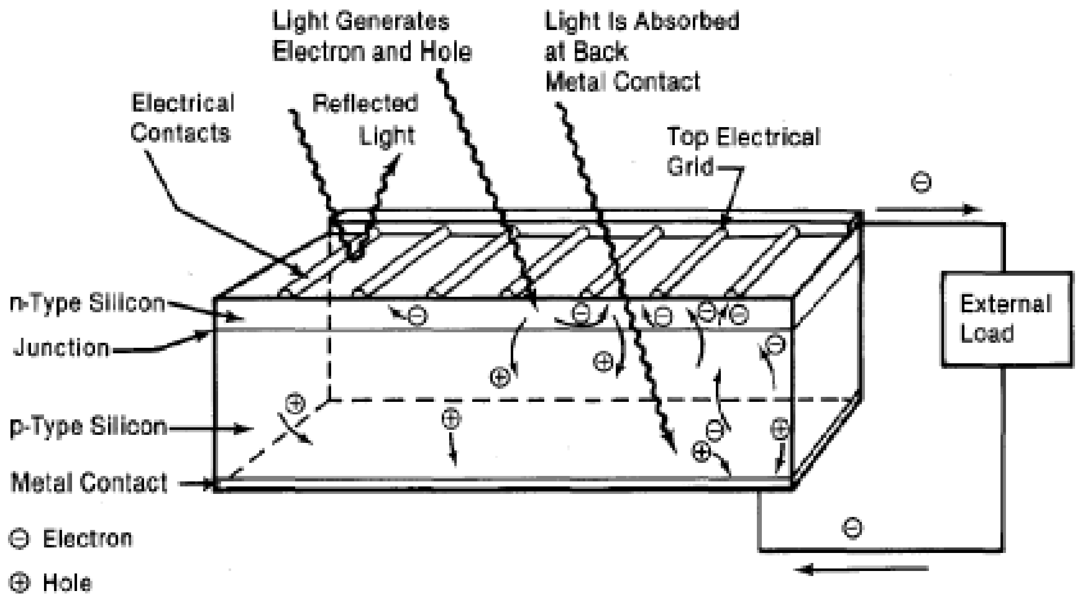

Figure (2.10): Light incident on the cell creates electron-hole pairs, which are separated due to the potential barrier, creating a voltage that drives a current through an external circuit [28].

2.6 Loss mechanism

Due to loss mechanisms not all the incident solar energy participates in the energy-to-electricity conversion process [1]. The single junction theoretical limit of solar cell conversion efficiency was firstly calculated by Shockley and Queisser in 1961 [24]. According to [24] the maximum obtainable efficiency for a single junction solar cell which composed of one material is approximately 30% (figure 2.11).

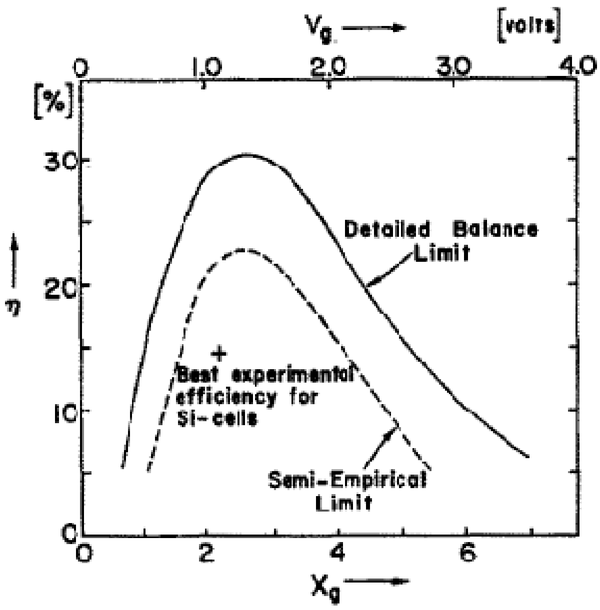

Figure (2.11): theoretical efficiency and its dependency on band gap [24]**.**

In addition, this theoretical limit of efficiency was obtained under several assumptions. Shockley-Queisser limit considers only band to band recombination (will be discussed below). Also it neglects all the optical losses.

So to be more realistic we should discuss the optical and electrical losses that occur in solar cells and how we can get the best efficiency result.

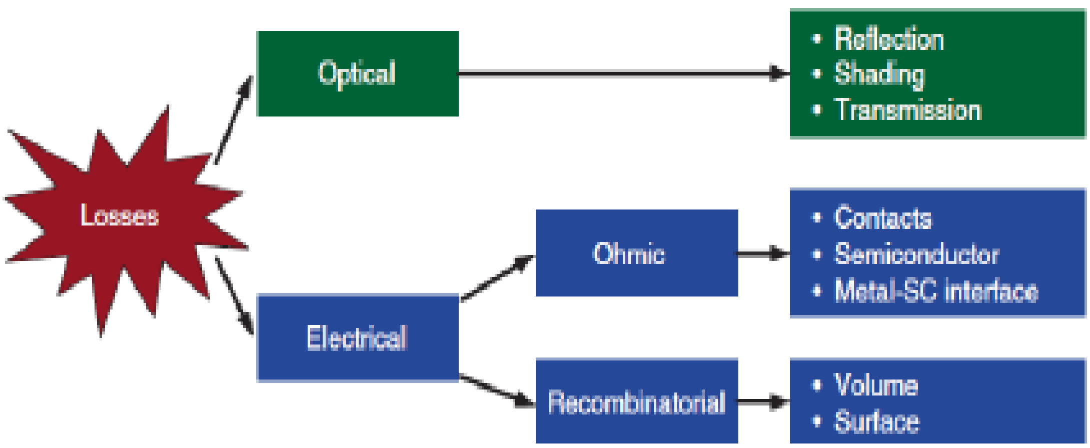

Figure (2.12): The losses in solar cells.

As shown in figure 2.12 loss mechanisms in single junction solar cells are:

- Optical loss involves losses like: reflection on the cell surface, shading and transmission. The inability to convert photons with energies less than the band gap energy ($E_\lambda < E_g$) into electricity is called the transmission loss [1].

- The thermalisation of photons of energies larger than the band gap energy ($E_\lambda > E_g$) [1].

- The electrical loss happens in the grid contact on the top of the cell surface. Ohmic loss occurs in the semiconductor material and it is related to the concentration of dopants in the material. An increase in n-doping for example will bring an improvement in conductivity but in the same time more recombination in the doped area. Also Ohmic loss involves losses at metal-semiconductor junction termed as Schottky contact.

- Recombination loss which occurs through one of three recombination mechanisms; band to band recombination: where an electron in CB recombines with a hole in the VB and release a photon. Auger recombination: also in this recombination an electron in CB recombines with a hole in VB but rather than releasing a photon this mechanism release an electron into the CB. Shockley-Read-Hall or SRH recombination which occurs in semiconductors doped with impurities.

Due to the impurities in the semiconductor a new energy state is located between the CB and VB. If an electron or hole is trapped by this state and then a hole or an electron moves up from VB into this intermediate state the recombination occurs.

2.7 Characteristics of solar cell

The model of PV cell can be used to simulate a PV module, because PV module is an association of cells in series and parallel, there are several models of a single junction Si PV cell. These models will be simulated and modeled in order to determine the most efficient model to get the best performance of a PV module.

Solar cells are basically p-n junction diode structured in a special way in order to receive the incident solar radiation and convert it to electrical energy. So, to study solar cell characteristics we need to study p-n junction diode. They both share a similar operating principle. The solar cell in darkness is a p-n diode, whose dark characteristics set the limits for the illuminated characteristics. From the principle point of view [2]:

An illuminated solar cell ≡ A short-circuit cell under light + A biased p-n diode.

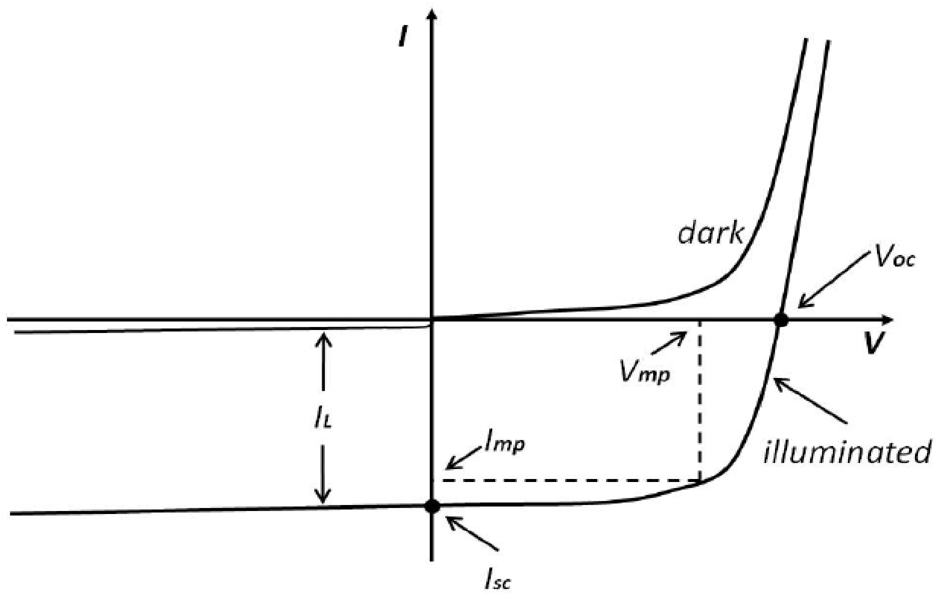

Figure (2.13): I-V characteristics of an ideal diode solar cell when non-illuminated (dark) and illuminated [3].

As shown in figure 2.13 [3], under dark the photon generated current is zero. The PV cell behavior under dark is thus the I-V characteristic curves of diode under forward and reverse bias conditions respectively.

The noteworthy point here is that the device diode behaves with positive current and positive voltage in first quadrant (forward biased diode) and with negative current and negative voltage in third quadrant (reverse biased diode) [4].

Dark curve general equation is given by:

$$I_D = I_o \left[\exp\left(\frac{V}{AV_T}\right) - 1\right] \quad (2.3)$$

Where,

I_D: The diode current

I_o: The reverse saturation current

V: The output voltage

A: The ideality factor

$V_T = \frac{kT}{q}$ is the thermal voltage

The effect of solar radiation (illumination) on PV cell is shown in figure 2.13. The illuminated I-V curve is the dark curve but shifted to the down by a value equal to I_L (illumination current). I_L can be written also as I_{pv}.

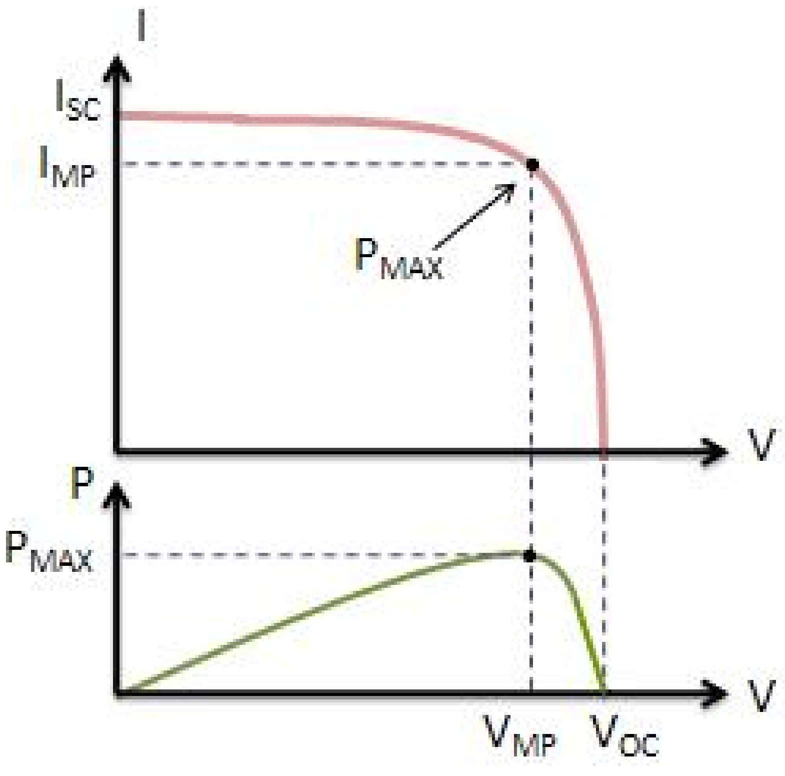

Figure (2.14): Typical *I* -*V* and *P*-*V* curves for a PV cell [5].

I-V characteristic curve of a typical PV cell is shown in figure 2.14 [5]. The current axis (where $V = 0$) is the short-circuit current, and the intersection with the voltage axis (where $I = 0$)is the open-circuit voltage.The power as a function of voltage is also shown in Figure 2.14.

The maximum power that can be obtained corresponds to the rectangle of maximum area under the I-V curve. At the maximum power point (MPP) the power is P_{MAX} or P_{MP}, the current is I_{MP}, and the voltage is V_{MP} [30].The difference between figure 2.13 and 2.14 is that the axis of current is flipped up in the second figure. In industry of PV cells and modules it is conventional to study I-V curve in the first quadrant as shown in figure 2.14.

Solar cell has many important parameters which can be described by applying basic electrical analysis techniques to the I-V general relation of solar cell. They are modelled as follows:

2.7.1 Short-circuit current

The short-circuit current,I_{sc}, is the current that flows through the external circuit when the electrodes of the solar cell are short circuited. The short-circuit current of a solar cell depends on the photon flux density incident on the solar cell, which is determined by the spectrum of the incident light. I_{sc} depends also on the area of the solar cell.

2.7.2 Open- circuit voltage

According to figure 2.14, when solar cell current equals zero, the solar cell voltage is at its greatest voltage available from a solar cell which is the open circuit voltage of the solar cell V_{oc}.

V_{oc} is the voltage at which no current flows through the external circuit; i.e. when the solar cell terminals are open or not connected to a load. It is the largest voltage that a solar cell can deliver under any given illumination.

An ideal p-n junction cell $V_{oc}$is:

$$V_{oc} = A\, V_T ln\left[1 + \frac{I_{pv}}{I_o}\right] = A\, V_T ln\left[1 + \frac{I_{sc}}{I_o}\right] \quad (2.4)$$

Where,

V_{oc} : The open circuit voltage

V: The output voltage

A: The ideality factor

$V_T = \frac{kT}{q}$ is the thermal voltage

I_o: The reverse saturation current

I_{pv} is the current generated by the sun

I_{sc} is the short circuit current

Equation 2.4 shows that V_{oc} depends on the saturation current (I_o) and the photo-generated current (I_{pv}). Since the saturation current depends on the recombination within the PV cell, V_{oc} is a measure of the recombination in the device.

The natural log in the expression indicates that V_{oc} is less dependent on irradiance than the short circuit current is. The open circuit voltage of a solar cell is proportional to the natural logarithm of the irradiance (G) [7].

Silicon solar cells on high quality monocrystalline material have open-circuit voltages of up to $730\,mV$ under one sun and $AM1.5$ conditions, whereas commercial devices on polycrystalline silicon usually have open-circuit voltages around $600\,mV$.

According to [24], V_{oc} increases as bandgap energy E_g increases. Also efficiency increases as V_{oc} increases until the current starts to drop.

2.7.3 Maximum power

The maximum power is that the area of the product of the maximum current and voltage as shown in equation below:

$$P_{MP} = V_{MP} * I_{MP} \quad (2.5)$$

Figure 2.14 also represents the greatest current and voltage of a typical solar cell.

2.7.4 Fill factor

The fill factor FF, is a parameter that, accordingly with V_{oc} and I_{sc}, determines the largest power yielded by a solar cell. The FF is the ratio of P_{MP} from the solar cell to the product of V_{oc} and I_{sc}.

$$FF = \frac{P_{MP}}{V_{oc} * I_{sc}} = \frac{V_{MP} * I_{MP}}{V_{oc} * I_{sc}} \quad (2.6)$$

Where:

- P_{MP} in $Watts$ (W)
- V_{oc} and V_{MP} in $Volts$ (V)
- I_{sc} and I_{MP} in $Ampere$ (A)
- FF is dimensionless

Graphically, the FF is a measure of the "squareness" of the solar cell and is also the area of the largest rectangle which will fit in I-V curve as shown in figure 2.15. FF is a measure for the quality of a cell; typical values for silicon cells are between 0.75–0.85 and in the region of thin film materials they are between 0.6–0.75 [7]. An empirical formula of FF is used for the PV module with arbitrary values of resistances is given as follows [31]:

$$FF = FF_0\left(1 - \frac{R_s}{V_{oc}/I_{sc}}\right) \quad (2.7),$$

$$FF_0 = \frac{v_{oc} - \ln(v_{oc} + 0.72)}{1 + v_{oc}} \quad (2.8),$$

Where FF_0 is the fill factor of the ideal PV module without any resistive effects; R_s is the series resistance; v_{oc} is the normalized value of open circuit voltage to the thermal voltage and it is given by:

$$v_{oc} = \frac{V_{oc}}{nKT/q} \quad (2.9)$$

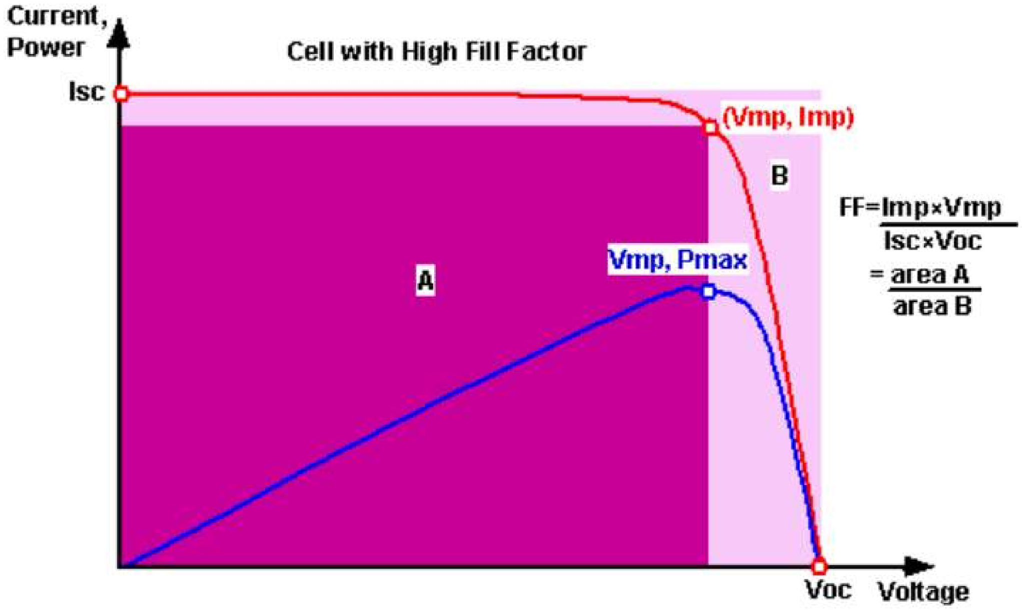

Figure (2.15): The fill factor gives the relationship of the area of square A to the background surface or B square [32]**.**

2.7.5 Efficiency

Efficiency or the conversion efficiency η, is defined as the ratio of the largest power generated by the solar cell ($P_{MP} = V_{MP} * I_{MP}$) to the input or incident or optical power P_{in}.

$$\eta = \frac{P_{MP}}{P_{in}} = \frac{V_{MP} * I_{MP}}{P_{in}} = \frac{V_{oc} * I_{sc} * FF}{P_{in}} = \frac{V_{oc} * I_{sc} * FF}{G * A} * 100 \quad (2.10)$$

With:

- A is the surface area of the solar cell (m^2)

- G is the solar irradiance (W/m^2)

Typical efficiencies of crystalline silicon cells are between 10 and 25%.

2.7.6 The effect of temperature on solar cells and the temperature coefficients (TC)

Similar to other semiconductor devices, solar cells are sensitive to temperature. An increase in temperature of a semiconductor will reduce its bandgap this will increase the thermal movement of the electrons built into the lattice. During this case a lot of electrons are torn from their bands and get into the conduction band and that therefore the intrinsic carrier concentration (n_i) rises. Higher n_i also results in arise in saturation current (I_o). This does affect the solar cell according to:

$$V_{oc} = AV_T \ln \frac{I_{sc}}{I_o} \quad (2.11)$$

According to the above equation the increased saturation current leads to a reduction in V_{oc}. The most affected parameter in a solar cell by the increasing of temperature is V_{oc}. As shown in the figure below (figure 2.16) [32].

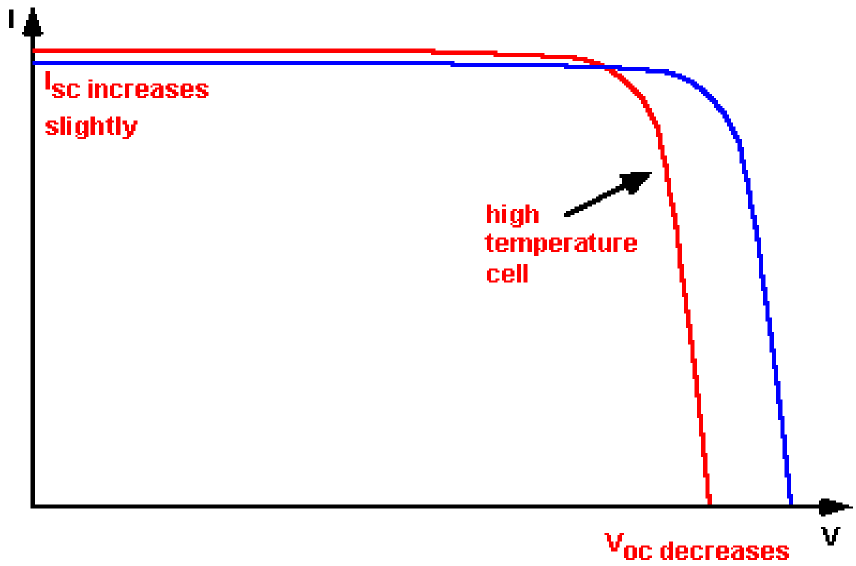

Figure (2.16): The effect of increasing temperature on the I-V characteristics of a solar cell [32].

V_{oc} decreases with increasing temperature because of the temperature dependence on I_o which is given for one side of a p-n junction by:

$$I_o = qA\frac{D{n_i}^2}{LN_D} \quad (2.12)$$

Where:

q is the charge of an electron (C)

A is the area (m^2)

D is the diffusivity of the minority carrier given for silicon as a function of doping (m^2/s)

L is the minority carrier diffusion length (m)

N_D is the donor concentration at n-side and

n_i is the intrinsic carrier concentration

Many of the parameters in the above equation have some temperature dependence. However the biggest effect is due to n_i. it depends on the band gap energy (lower band gaps give a higher n_i also it depends on the energy which the carriers have (higher temperatures giving higher n_i).

The equation for n_i is given by:

$${n_i}^2 = 4\left(\frac{2\pi kT}{h^2}\right)^3 ({m_e}^* {m_h}^*)^{3/2}\, exp\left(\frac{-E_{G0}}{kT}\right) = B\,T^3\, exp\left(\frac{-E_{G0}}{kT}\right) \quad (2.13)$$

Where:

T is the temperature in kelvin

h, k are constants

m_e^*, m_h^* are effective masses of electrons and holes respectively

E_{G0} is the band gap at $T = 0\ K$ for silicon $E_{G0} = 1.17\ eV$

B is a constant which is essentially independent of temperature.

Now, by substituting the above equation in the saturation current one and assuming that the temperature dependencies of the other parameters can be neglected, gives:

$$I_o = qA\frac{D}{LN_D}B\,T^3\exp\left(\frac{-E_{G0}}{kT}\right) \approx B'T^{\gamma}\exp\left(\frac{-E_{G0}}{kT}\right) \quad (2.14)$$

Where:

B' is a temperature independent constant.

A constant, γ is used instead of the number 3 to incorporate the possible temperature dependencies of the other material parameters. For silicon solar cells near room temperature, I_o approximately doubles for every $10\ °C$ increase in temperature [32]. Now for calculating the reduction in V_{oc} due to increasing I_o the above equation will be substituted in the equation of V_{oc} given the following one:

$$V_{oc} = \frac{kT}{q}\ln\left(\frac{I_{SC}}{I_o}\right) = \frac{kT}{q}[\ln I_{SC} - \ln I_o]$$
$$= \frac{kT}{q}\ln I_{SC} - \frac{kT}{q}\ln\left[B'T^{\gamma}\exp\left(\frac{-qV_{G0}}{kT}\right)\right]$$
$$= \frac{kT}{q}\left(\ln I_{SC} - \ln B' - \gamma\ln T + \frac{qV_{G0}}{kT}\right) \quad (2.15)$$

Where: $E_{G0} = qV_{G0}$ and by differentiating the above equation with respect to T and assuming that $\frac{dV_{oc}}{dT}$ does not depend on $\frac{dI_{SC}}{dT}$. $\frac{dV_{oc}}{dT}$ is denoted by β and it is given by:

$$\beta = \frac{dV_{OC}}{dT} = -\frac{\gamma k}{q}\ln T - \frac{\gamma k}{q} = \frac{V_{OC} - V_{G0}}{T} - \gamma\frac{k}{q} \quad (2.16)$$

For the Si cell $E_{G0} = 1.2\ eV$ and using $\gamma = 3$

$$\frac{dV_{OC}}{dT} \approx -2.2\ mV\ per\ K\ for\ Si$$

For a typical open circuit voltage of $600mV$ there is thus a temperature coefficient $TC(V_{OC})$ of approximately $0.4\%\ per\ K$. The open circuit voltage V_{OC} of a Si solar cell is reduced by $2.2mV\ per\ Kelvin$, which corresponds to a temperature coefficient of approximately $-0.4\%\ per\ Kelvin$ [7].

So,

$$\beta = \frac{1}{V_{oc}}\frac{dV_{oc}}{dT} \approx -0.004\ per\ K\ for\ Si \approx -0.4\%/K$$

The position is completely different within the case of I_{sc}. Increasing the temperature does reduce the band gap energy and then more photons (even energy-poor ones) will have enough energy to create $e^- - h^+$ pairs. So I_{sc} will increase slightly with increasing temperature. The temperature dependence of the short-circuit current from a silicon solar cell is [32]:

$$\alpha = \frac{1}{I_{SC}}\frac{dI_{SC}}{dT} \approx 0.0006\, per\ K\ for\ Si \approx 0.06\%/K$$

The temperature dependency of the FF is given by:

$$\frac{1}{FF}\frac{dFF}{dT} \approx \left(\frac{1}{V_{OC}}\frac{dV_{OC}}{dT} - \frac{1}{T}\right) \approx -0.0015\, per\ K\ for\ Si \approx -0.15\%/K$$

Then the effect of temperature on P_{MP} is:

$$\gamma = \frac{1}{P_{MP}}\frac{dP_{MP}}{dT} = \frac{1}{V_{OC}}\frac{dV_{OC}}{dT} + \frac{1}{FF}\frac{dFF}{dT} + \frac{1}{I_{SC}}\frac{dI_{SC}}{dT} \quad (2.17)$$

$$\gamma \approx -\frac{0.004}{K} + \frac{0.0006}{K} - \frac{0.0015}{K} \approx -0.005\, per\ K\ for\ Si$$

2.7.7 Solar cell dependence on the solar irradiance

An increase in irradiance does affect the output power and efficiency of the cell. The short circuit current increases linearly when increasing the solar irradiance. Figure 2.17 shows how I-V characteristics are affected by varying irradiance.

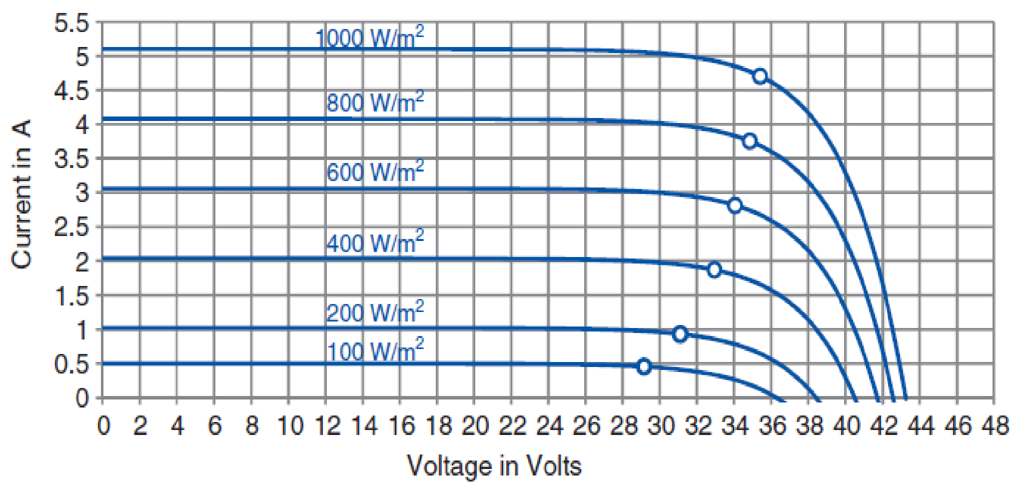

Figure (2.17) I-V characteristic curve of SW-165 module at various irradiances and constant module temperature of 25℃ [7].

As shown in the above figure when sun irradiance increases the open circuit voltage, short circuit current and fill factor will be increased. In the case of SW-165 module the MPP is reduced from $165\,W$ at $1000\ W/m^2$ to $31\,W$ at $200\ W/m^2$. Thus the efficiency has been reduced by -6%. This reduction in efficiency is also provided in the datasheet of the module.

2.8 Single-diode – PV model (ideal)

To develop an accurate equivalent circuit for a single junction Si PV cell, it is necessary to understand the physical configuration of the elements of the cell as well as the electrical characteristics of each element. Single-diode – PV model equivalent circuit is a current source in parallel with a single-diode. The configuration of the simulated ideal solar cell with single-diode is shown in figure 2.18 [33].

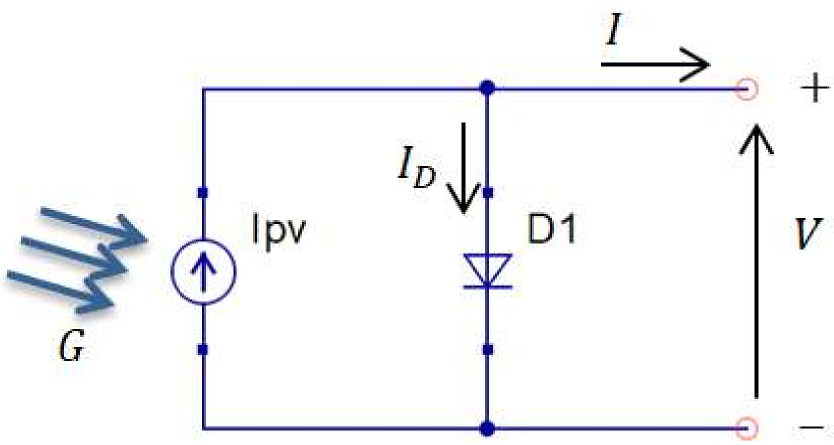

Figure (2.18): Single-diode – PV model

This model is the most simplified form of a PV cell, the output voltage and current relations are given by:

$$I_{pv} = I + I_D \quad (2.18)$$

$$I = I_{pv} - I_D \quad (*)$$

From Shockley diode equation, diode current (I_D) is given by:

$$I_D = I_o\left[\exp\left(\frac{V}{AV_T}\right) - 1\right] \quad (2.19)$$

So equation (*) becomes

$$I = I_{pv} - I_o\left[\exp\left(\frac{V}{AV_T}\right) - 1\right] \quad (2.20)$$

The output of the current source (I) is directly proportional to the light falling on the cell which increases linearly with solar irradiance.

Where:

- I_{pv} is the current generated by the incidence of light
- I_o is the diode reverse bias saturation current
- $V_T = \frac{N_s kT}{q}$ is the thermal voltage of a PV module having N_s cells connected in series; q is the electron charge; k is the Boltzmann constant; T is the temperature of the p-n junction and A the diode ideality factor.

The diode ideality factor A indicates how closely the diode follows the ideal diode equation. The value of A greater than 1 represents non-ideal condition, whereas $A = 1$ represents ideal behavior of the diode.

A solar cell can at least be characterized by I_{sc},V_{oc} and A. For the same irradiance and *p-n* junction temperature conditions, I_{sc} is the greatest value of the current generated by the cell, which is given by

$$I_{sc} = I = I_{pv} \text{ for } V = 0 \quad (2.21)$$

V_{oc} is the greatest value of the voltage at the cell terminals. Under the same irradiance and solar cell temperature conditions, V_{oc} can be written as:

$$V = V_{oc} = A\, V_T ln\left[1 + \frac{I_{sc}}{I_o}\right] \text{ for } I = 0 \quad (2.22)$$

The output power is given by

$$P = V\left\{I_{sc} - I_o\left[exp\left(\frac{V}{AV_T}\right) - 1\right]\right\} \quad (2.23)$$

2.9 Single-diode with series resistance – PV model

This model has a resistance in series with diode as shown in figure 2.19. In real, the output current generated by solar cell will pass through the emitter and base of the solar cell. As was shown in the previous chapter, top and back metal contacts in solar cell have a resistance. Also, a contact resistance is between the metal contacts and silicon. So, more accuracy can be introduced to the model by adding a series resistance R_s [19]. R_s reduces the short circuit current and fill factor [13].

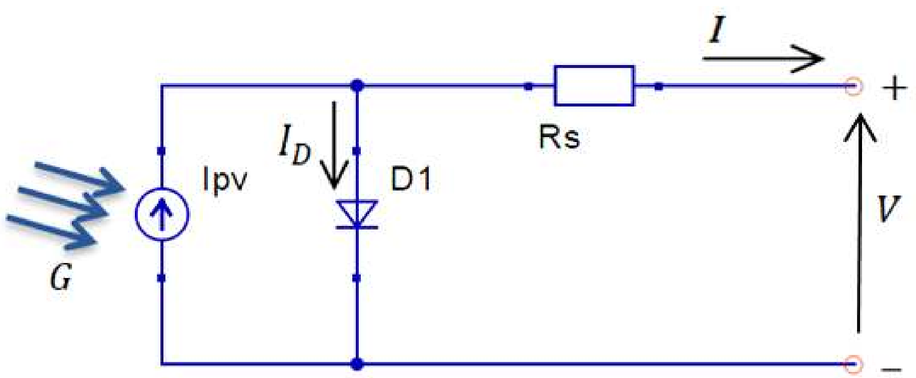

Figure (2.19): Single-diode with series resistance – PV model

Under stable external condition i.e. for the same temperature and irradiation, the I-V characteristics of this solar cell model are given by [33]:

$$I = I_{PV} - I_o\left[exp\left(\frac{V + IR_s}{AV_T}\right) - 1\right] \quad (2.24)$$

I_{sc} is given by:

$$I_{sc} = I = I_{PV} - I_o\left[exp\left(\frac{I_{sc}R_s}{AV_T}\right) - 1\right] \text{ for } V = 0 \quad (2.25)$$

R_s is small and negligible in computing the above equation [33].

V_{oc} is given by:

$$V = V_{oc} = AV_T\, ln\left[1 + \frac{I_{sc}}{I_o}\right] \text{ for } I = 0 \quad (2.26)$$

And the output power is given by:

$$P = V\left\{I_{sc} - I_o\left[exp\left(\frac{V + IR_s}{AV_T}\right) - 1\right]\right\} \quad (2.27)$$

2.10 Single-diode with series and parallel resistances – PV model

Figure 2.20 shows the Single-diode with series and parallel resistances – PV model which is commonly used in many studies and provides sufficient accuracy for most applications [33].

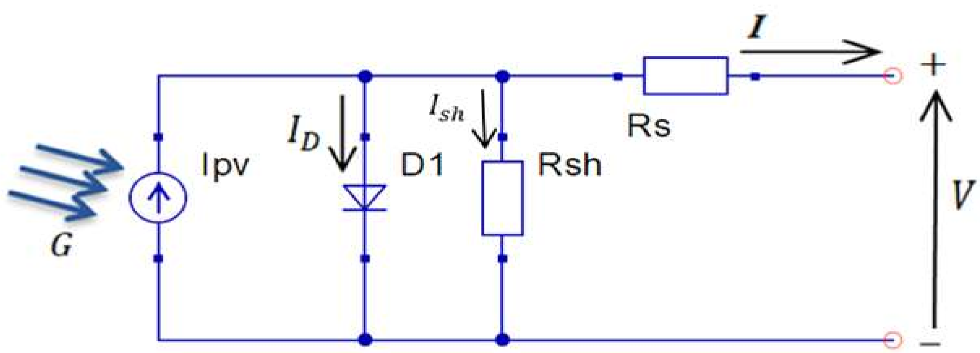

Figure (2.20): Single-diode with series and parallel resistances – PV model

Indeed, the electrical equivalent of the solar cell is based on a diode, adding two resistors to account for internal losses. As previously mentioned, R_s is the series resistance which takes into account the ohmic losses of the material, the metallization and the contact metal/ semiconductor; R_{sh} represents resistance leakage current from currents between the top and bottom of the cell, by the board in particular and within the material by irregularities or impurities [34].

According to [33] the previous model of PV cell doesn't adequately represent the behavior of the cell when subjected to environmental variations, especially at low voltage [34]. So, Single-diode with series and parallel resistances – PV model is more practical model i.e. will yield an accurate simulation results.

The output current of this model is given by:

$$I = I_{PV} - I_o\left[exp\left(\frac{V + IR_s}{AV_T}\right) - 1\right] - \left(\frac{V + IR_s}{R_{sh}}\right) \quad (2.28)$$

2.11 Double-diode with series and parallel resistances – PV model

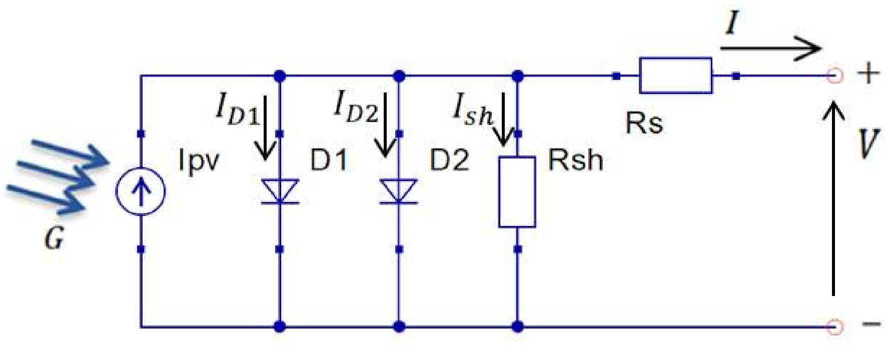

Figure (2.21): Double-diode with series and parallel resistances – PV model

The equivalent circuit of this model is shown in figure 2.21. A new diode D_2 is added in parallel with D_1.

I is given by:

$$I = I_{PV} - I_{D1} - I_{D2} - I_{sh} \quad (2.29)$$

Where:

$$I_{D1} = I_{o_1}\left[exp\left(\frac{V + IR_s}{A_1V_T}\right) - 1\right] \quad (2.30)$$

$$I_{D2} = I_{o_2}\left[exp\left(\frac{V + IR_s}{A_2V_T}\right) - 1\right] \quad (2.31)$$

Where I_{o_1} and I_{o_2} the diffusion and saturation currents respectively; $A_1$and A_2 are the diffusion and recombination diode ideality factors.

So, I is given by:

$$I = I_{PV} - I_{o_1}\left[exp\left(\frac{V + IR_s}{A_1V_T}\right) - 1\right] - I_{o_2}\left[exp\left(\frac{V + IR_s}{A_2V_T}\right) - 1\right] - \left(\frac{V + IR_s}{R_{sh}}\right) \quad (2.32)$$

The ideality factor of the first diode (A_1) is usually taken as 1 and the second diode ideality factor (A_2) is taken as 2. This assumption is done based on the approximation of Shockley–Read–Hall (SRH) recombination in the space-charge layer of the photodiode [13].

2.12 Improved calculation method for computing I_{pv} and I_o.

There are many approaches when determining the appropriate method to model the single junction Si PV cell. In this research the input equations of I_{pv} and I_o are used in papers like [17] and [35]. The I_{pv}, as mentioned previously, depends linearly on the solar irradiance and it depends also on the cell temperature. It is given by the following equation [36]:

$$I_{pv} = \left(I_{pv_{STC}} + \alpha \Delta T\right) \frac{G}{G_{STC}} \quad (2.33)$$

Where:

- I_{pv_STC} in Ampere is the photo generated current under STC.
- $\Delta T = T - T_{STC}$, ΔT is in Kelvin where T_{STC} is the cell temperature under STC ($T_{STC} = 25$°C).
- G is the surface irradiance of the cell where G_{STC} is the irradiance under STC ($G_{STC} = 1000\, W/m^2$).
- α (in %/°C) is the short circuit current coefficient, it is a constant and normally provided by the datasheet.

An improved equation to describe the saturation current with taking the variation of temperature into consideration is given by [35], [37]:

$$I_o = \frac{I_{pv}}{\exp\left[(V_{oc\_STC} + \beta \Delta T)/AV_T\right] - 1} \quad (2.34)$$

Where β (in %/°C) is the open circuit voltage coefficient, it is a constant and normally given by the datasheet.

The following table summarizes the equations within the four models for both monocrystalline and polycrystalline solar cells based on datasheet:

Table (2.1): input equations used to simulate PV cells under STC ($T = 25$°C and $G = 1000\,W/m^2$)

Equations	Model I	Model II	Model III	Model IV
$I_{pv} = (I_{pv\_STC} + \alpha\Delta T)\dfrac{G}{G_{STC}}$	✓	✓	✓	✓
$I_o = \dfrac{I_{pv}}{\exp\left[(V_{oc\_STC} + \beta\Delta T)/AV_T\right] - 1}$	✓ $(A = 1)$	✓ $(A = 1)$	✓ $(A = 1)$	✓ $(A = 1)$
$I_{o_2} = \dfrac{I_{pv}}{\exp\left[(V_{oc\_STC} + \beta\Delta T)/AV_T\right] - 1}$				✓ $(A = 2)$
$V_T = \dfrac{N_s kT}{q}$	✓	✓	✓	✓
$R_S = \left(1 - \dfrac{FF}{FF_0}\right)\left(\dfrac{V_{OC}}{I_{SC}}\right)$		✓	✓	✓
R_p is large			✓	✓

Chapter Three

Methodology

Chapter Three
Methodology

In this chapter modelling and simulation of PV cells' various models will be presented and discussed. For modelling and simulation QUCS is being used, due to its wide presence and it is easy to understand.

All the equivalent circuits of PV cells and modules being discussed below consist of three major components: DC current source (power source), semiconductor material i.e. diode, and a load resistance.

The following assumptions are being taken under consideration:

- The simulation of the equivalent circuits is done under the standard test conditions (STC) i.e. at $G = 1000\ W/m^2$ and $T = 25\ C^{\circ}$.
- SPICE model of diode is used:

3.1 SPICE simulator

SPICE, simulation program with Integrated circuit Emphasis, is a general-purpose analog electronic circuit simulator. It is used in Integrated circuits to check the completeness of circuit designs and to predict circuit behavior. SPICE was developed by Nagel and Pederson of University of California, Berkeley, in 1973 [38]. With time, SPICE became popular and adopted by various institutions and it is commonly used in simulation of PV cells as in [13].

In this research, SPICE model of the diode is used in all the equivalent circuits' simulation.

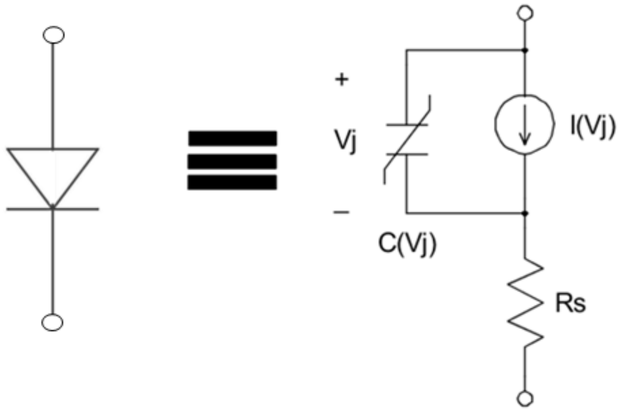

Figure (3.1): SPICE diode model: SDIODE

Figure 3.1 shows the equivalent circuit of SDIODE. Parameters of this diode are provided in table 1 in APPENDIX [39].

The model of diode simulation includes ohmic series resistance R_s and zero bias junction capacitance C_{j_0}, to adjust to PV cell model must change them to 0 Ω and 0 F respectively as shown in table A.1 in appendix A.

3.2 simulation steps within QUCS

In order to envision PV system design and the steps of simulation, a block diagram is built as shown in figure 3.2.

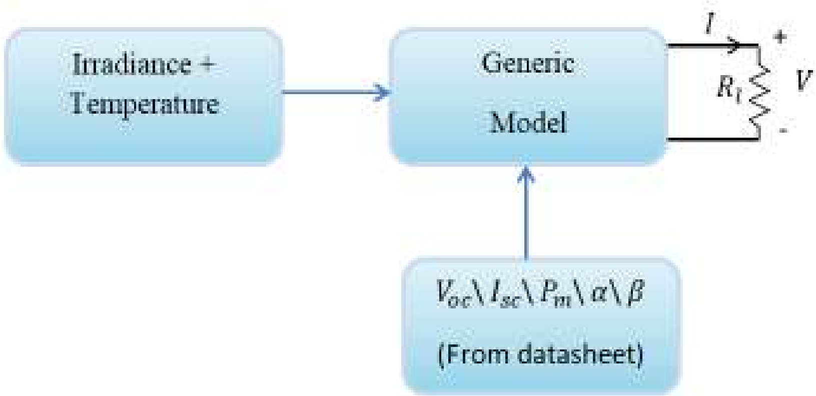

Figure (3.2): The design of the model as a block diagram [40].

According to the block diagram shown in figure 3.2 [40], the input parameters are irradiance and temperature or "external conditions". Other parameters are extracted from datasheet of the PV module under STC. The generic model contains the DC current source in parallel with diode. In this research four generic models of single junction PV cell will be simulated and discussed. The following simulation steps were obeyed in this research to attain goals:

- Step 1: drawing the equivalent circuit.
- Step 2: datasheet of solar module and extracting the input parameters used for the simulation of one solar cell.
- Step 3: inserting equations.
- Step 4: establishing the kind of analysis.

3.3 Single-diode – PV model (Model I "ideal")

I. The equivalent circuit

Figure 3.3 shows the equivalent circuit of the first model of a PV cell. As mentioned before each model contains three main parts: firstly, the dc current source. Secondly is the diode (symbolled as $D1$). It is in parallel with the first component and with the load resistance R_l which is the third component.

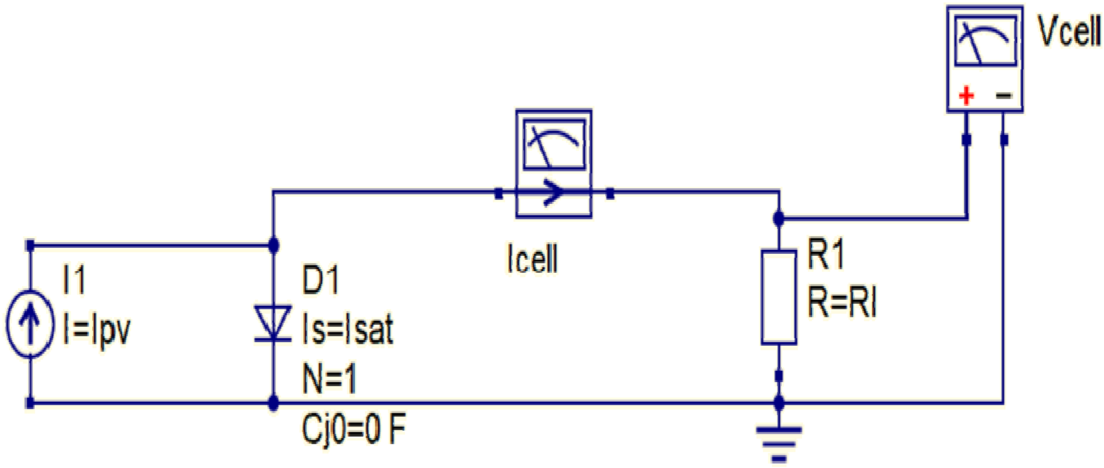

Figure (3.3): Single-diode – PV model equivalent circuit using QUCS.

The used components in the equivalent circuit can be found in the Components tab. It is located at far left of the schematic area. The ground symbol and resistor ($R1$) can be found in the Components tab in the lumped components category. The dc current source is found in the Components tab in the sources category. Furthermore, diode symbol can be found in the Components tab in the nonlinear components category. The ammeter and voltmeter are added in order to plot the I-V curve. They can be found also in the Components tab in the probes category.

II. Extracting input parameters from datasheet

Initially to simulate the equivalent circuit of one PV cell by QUCS, input parameters should be defined and inserted in simulation platform. Five parameters should be obtained from the datasheet at STC: $V_{oc\_stc}, I_{oc\_stc}, P_{m\_stc}, \alpha \; and \; \beta$. The external parameters under STC are: irradiation (G) and temperature(T), and the outputs are: value of voltage and current (I-V curve).

Therefore, these parameters are used to model the PV cell. Table 3.1 shows the electrical parameters of I-106/12 Solar Panel from Isofoton [41].

Table (3.1): Specifications of I-106/12 Solar Panel from Isofoton [41]**.**

Parameters	**Value**
Maximum power module (P_m)	$106\ W$
Short current circuit module (I_{sc})	$6.54\ A$
Voltage open circuit module (V_{oc})	$21.6\ V$
Temperature coefficient of I_{sc} (α)	$0.042\ \%/℃$
Temperature coefficient of V_{oc} (β)	$-0.328\ \%/℃$
Series cell	36
Parallel cell	2
Cell type	Monocrystalline Cell

Most of the manufacturers' datasheets provide information of PV module under STC, so for PV cells new values will be calculated. Equations 3.1 and 3.2 show the relation between V_{oc} and I_{sc} for module and number of series cells and parallel cells.

$$V_{oc\_cell} = \frac{V_{oc\_module}}{N_{cells\_series}} \quad (3.1)$$

$$I_{sc\_cell} = \frac{I_{sc\_module}}{N_{cells\_strings}} \quad (3.2)$$

Then,

$$V_{oc\_cell} = \frac{21.6}{36} = 0.6\ V$$

$$I_{SC\_cell} = \frac{6.54}{2} = 3.27\ A$$

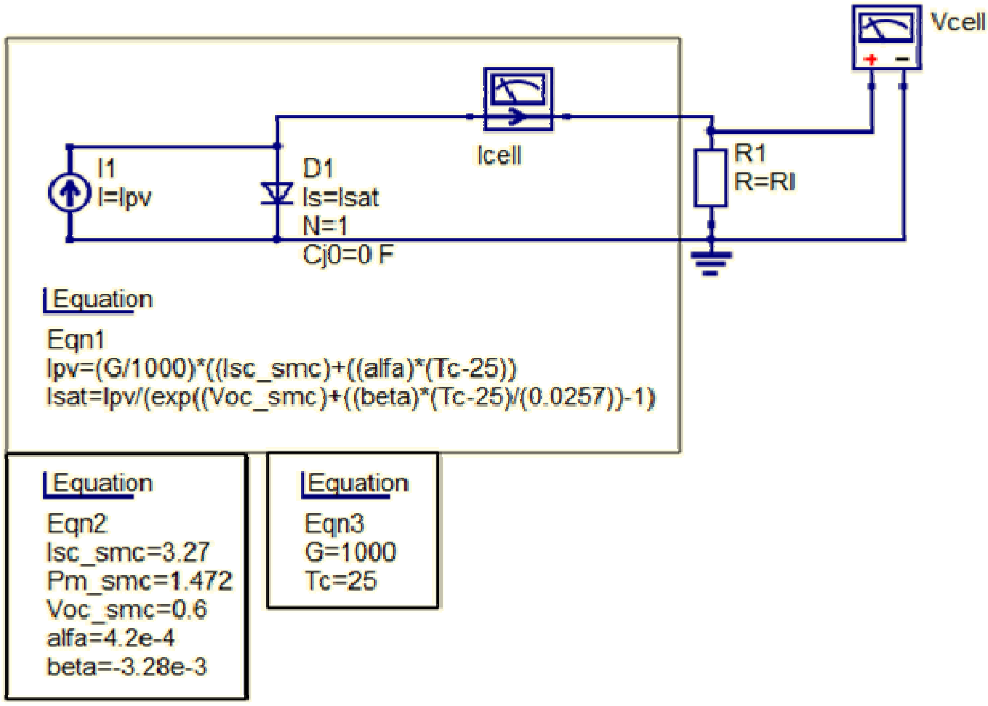

Figure (3.4): Generic model of PV cell with the extracted parameters and input equations.

The simulated circuit is shown in figure 3.4. Eqn2 and Eqn3 contain the input parameters from datasheet. In Eqn1 the equations of I_{pv} and I_{sat} are introduced.

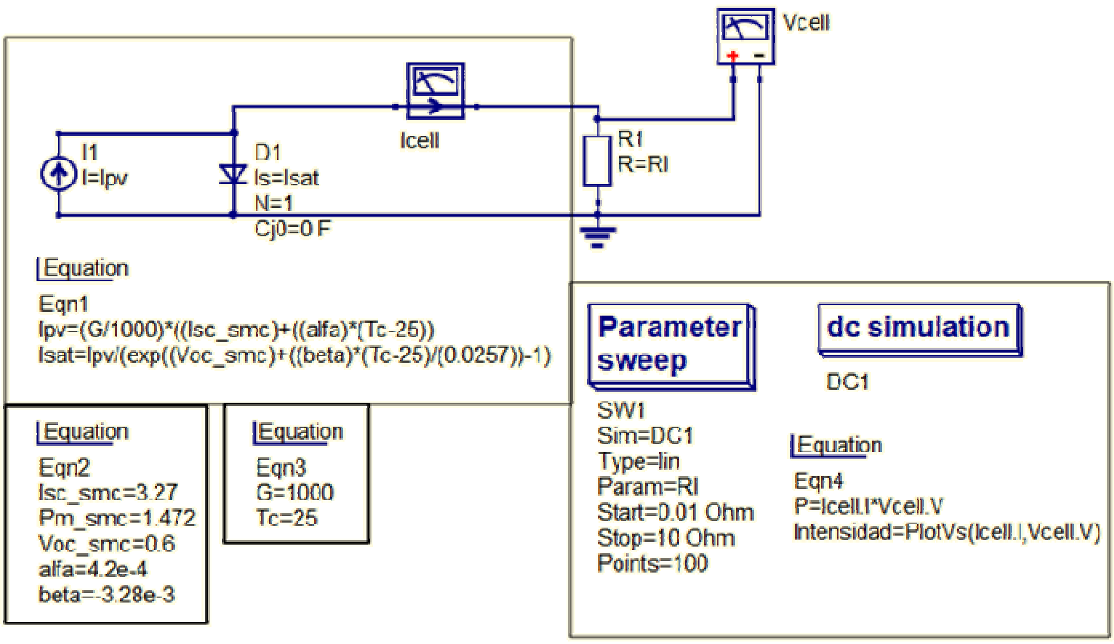

Figure (3.5): PV cell in its last configuration.

In the final step characteristic curves of model I will be set up by using DC simulation and the parameter sweep as shown in figure 3.5. They can be found in the Components tab in the simulations category.

The parameter sweep contains the instance name of the DC simulation DC1 which is going to be swept. The parameter which is swept is R_l(the load resistance) and is put into the Param property of the parameter sweep.

The parameter R_l is also put into the R property of the ohmic resistance $R1$.

3.4 Single-diode with series resistance – PV model (Model II)

In this model a new parameter is defined which is series resistance, R_s. As shown in figure 3.6 in the schematic area Eqn2 defines the series resistance.

R_s can be calculated from the empirical relationship between V_{oc} and I_{sc} with R_s, given by:

$$R_S = \left(1 - \frac{FF}{FF_0}\right)\left(\frac{V_{oc}}{I_{sc}}\right) \quad (3.3)$$

This equation give a value of R_s which is approximately $0.013\ Ohm$.

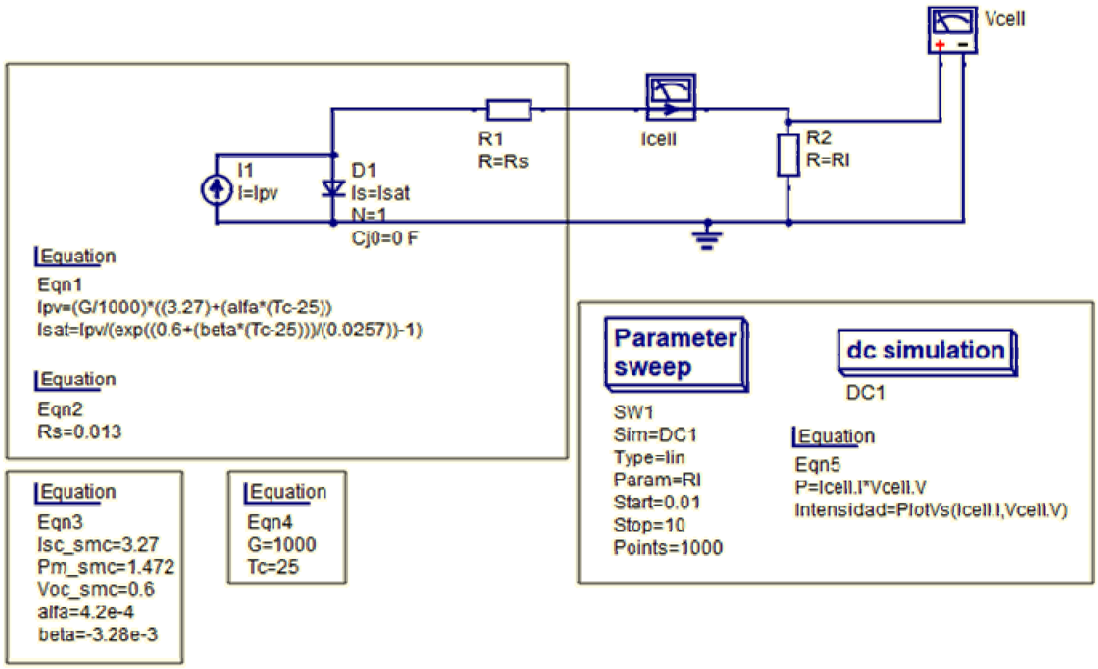

Figure (3.6): Single-diode with series resistance – PV model

3.5 Single-diode with series and parallel resistances – PV model (Model III)

In this model a new parameter is added to the equivalent circuit in parallel with the dc current source which is shunt resistance R_{sh}. Leak currents at the edges of the solar cell as well as any point short circuits of the p-n junction are modeled by R_{sh}.

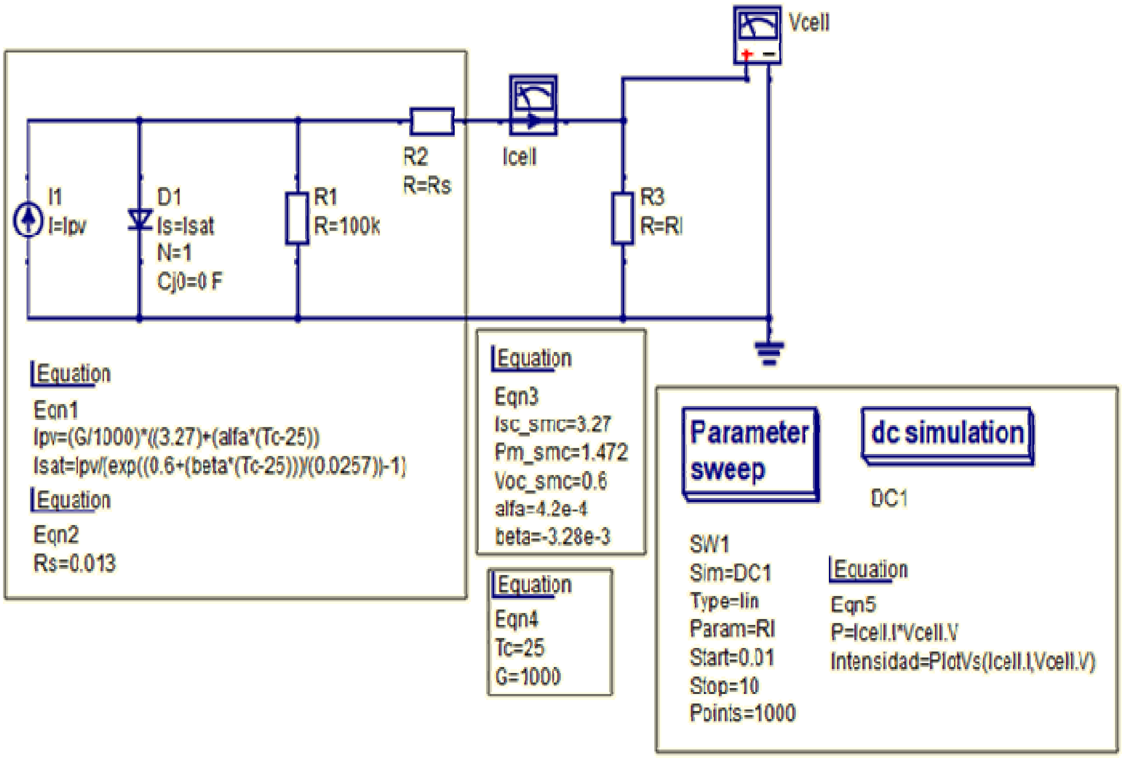

Figure (3.7): Model III schematic diagram

3.6 Double-diode with series and parallel resistances – PV model (Model IV)

In the four models of PV cell, the saturation current in the diode is generally the same. Also, in the previous three models "one-diode models" the ideality factor was equal to 1. However, in model IV the ideality factor of the second diode is greater than 1 ($A = 2$). In other words, in two-diode model the recombination current is not neglected. The diffusion current is modeled by a diode (D_1) with $A = 1$ and a recombination current through an extra diode (D_2) with $A = 2$ in parallel with the first diode [7]. (Figure 3.8)

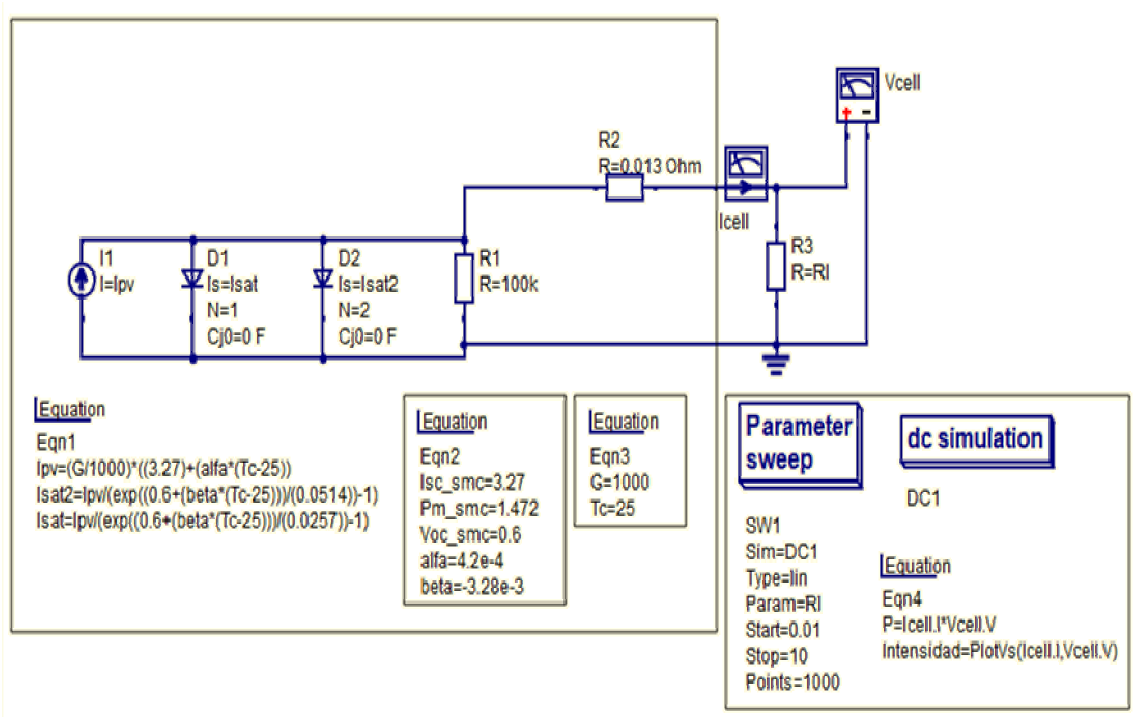

Figure (3.8): Double-diode – PV model for possible exact modeling of the solar cell characteristic curve

3.7 The effect of temperature and irradiance

All simulations was done under stable environmental conditions i.e. constant G and T. Model III will be simulated under different cell temperatures in order to examine how the behavior of PV cell is changed by changing temperature. Also it will be simulated under different irradiance values and constant cell temperature.

3.8 Polycrystalline silicon solar cells

Lastly, single junction silicon solar cells made up from polycrystalline silicon will be simulated. A comparison will be presented between first generation and second generation solar cells to conclude which is the most efficient. Steps in section 3.2 will be followed again and the parameters of PV cell will be extracted from a new datasheet shown below [42].

Table (3.2): Specifications of Solar Panel –Polycrystalline (SPM050-P) [42]**.**

Parameters	Value
Maximum power module (P_m)	$50\ W$
Short current circuit module (I_{sc})	$2.84\ A$
Voltage open circuit module (V_{oc})	$21.3\ V$
Temperature coefficient of I_{sc} (α)	$0.05\ \%/℃$
Temperature coefficient of V_{oc} (β)	$-0.35\ \%/℃$
Number of cells	36 (4×9)
Cell type	Polycrystalline silicon solar cells

Chapter Four

Introducing and Modelling of Organic Bulk Heterojunction Based on $P3HT:PCBM$ PV Cells

Chapter Four

Introducing and Modelling of Organic Bulk Heterojunction Based on $P3HT$: $PCBM$ PV Cells

4.1 Introduction

Organic PV solar cells (OPVs) based on solution processed bulk-heterojunctions (BHJs) of semiconducting polymers have been taking a high concentration in the last decade as a source of renewable energy [20]. They were proposed for the first time in 1995 [43]. Semiconducting polymers are light weighted, flexible and relatively inexpensive fabrication cost materials. This had motivated researches to focus on this field of solar cells. More than 1953 publications in the year of 2010 were published concerning the OPVs [20]. The most dominant material used as an active layer in organic BHJs is the mixture of P3HT (poly 3-hexylthiophene) and PCBM (phynyl-C70 butyric acid methyl ester) (P3HT:PCBM). The conversion efficiency of solar cells composed of these materials had reached about 6% [44]. The efficiency of organic solar cells is relatively low comparable with crystalline silicon solar cells, this is due to the low charge mobility and poor conductivity of organic materials.

4.1.1 Aim

The scope of this research is to simulate organic BHJ solar cell under STC by GPVDM (general purpose photovoltaic device model) software answering the following questions:

- Do organic cells behave as crystalline silicon solar cells?

- How thickness of active layer of the solar cell does affect efficiency of the cell and which thickness is the best?
- Does the series resistance have an impact on conversion efficiency?

4.2 Working principle and device structure.

The structure of BHJ solar cell consists mainly of the active layer sandwiched between cathode and anode layer. In this research active layer is a blend of two conjugate polymers of an electron donor or p-type ($P3HT$) and an electron acceptor or n-type ($PCBM$). This blend of polymers molecules is termed as bulk heterojunction (BHJ) that's why the solar cell is named as BHJ solar cell. The device structure is shown figure 4.1 [21].

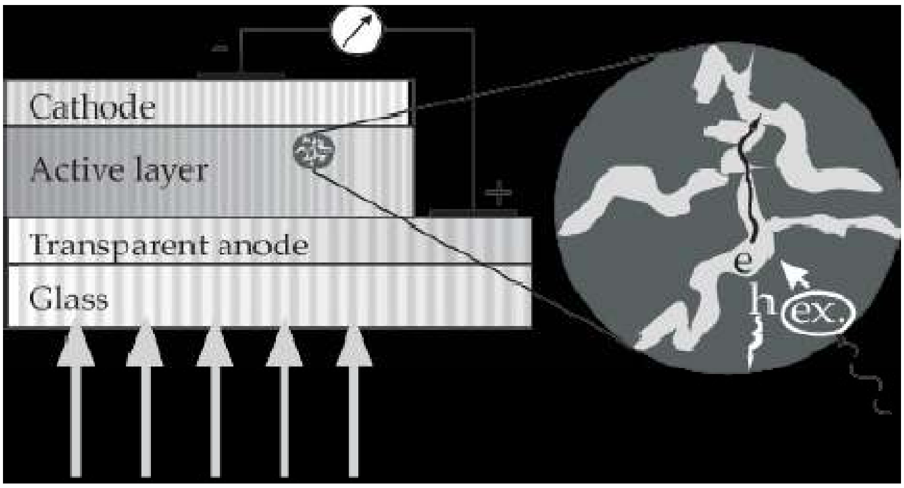

Figure (4.1): Device structure of BHJ solar cell [21].

Figure 4.1 shows a clear view of the BHJ structure and the interface between acceptor and donor materials is shown also. This interface plays an important role in the process of creating electrical current. When light hits donor molecules in BHJ, electrons will be excited from highest occupied molecular orbital (HOMO) energy level to lowest unoccupied molecular orbital (LUMO) energy level. Excited electron is always accompanied with a creation of a hole at HOMO level of the donor molecule; this electron-hole pair is called “exciton”. Exciton has diffusion length of about $4-10\ nm$ in conjugated polymers. This exciton diffuses to donor-acceptor interface, where a dissociation of the exciton happens and then carriers are transported to anode and cathode in order to deliver them to the external circuit. To a better understanding, the following diagram illustrates working principle (figure 4.2) [45].

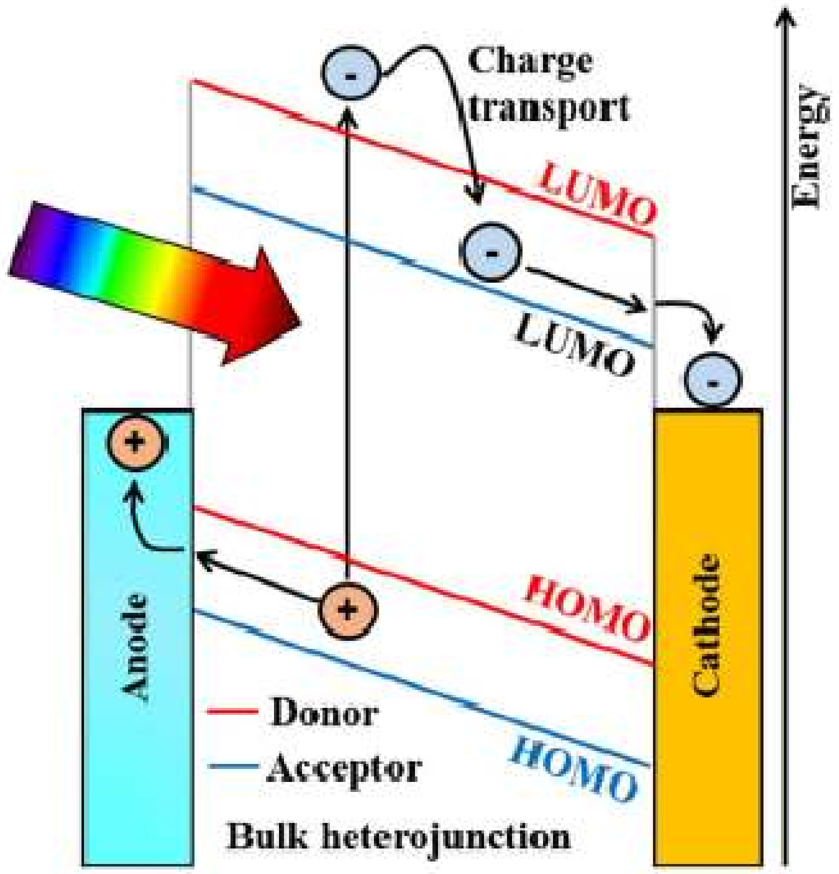

Figure (4.2) the band diagram form of BHJ solar cell structure [45].

The principle of working can be described by the following steps:

1. Light absorption and exciton creation.

The conjugated polymers have a high absorption coefficient but only 60% of the incident light is absorbed due to low charge-carrier mobility in organic materials then low photocurrent is generated. In order to enhance current generated in the cell, low band gap materials (lower than $2\ eV$) must be used within the active layer in device [45]. Exciton created after light absorption has a binding energy in the range of $0.1 - 1.4\ eV$ [46].

2. Exciton diffusion to the interface and dissociation of it at surface

Electron-hole pair has to diffuse within the donor material until reaching donor –acceptor interface in order to dissociate into free charge carriers. The energy offset between LUMO orbital in donor material and LUMO orbital in acceptor material does break the coulomb attractive force between electron and hole that results in dissociation of excitons and forming free electron and free holes. This energy offset should be in the range of $0.1 - 1.4\ eV$ to overcome the binding energy of excitons. Moreover, the difference in HOMO energy level of donor material and LUMO level of acceptor material creates built-in electric fields that enhance the separation of excitons into electrons and holes.

3. Carriers transport and delivery to external circuit

After creation of free charges the freed electrons are accepted by the material with lower LUMO level and holes are accepted by the material with higher HOMO. The charge carriers now move towards their respective electrodes. Thus, electrons move towards the cathode and holes move towards the anode [45]. The work function of the anode should match with the HOMO of the donor material, while the work function of the cathode must match with the LUMO of the acceptor material. Work function is the amount of energy required to remove an electron from a material [47]. The structure of organic solar cell is shown in figure 4.3 [22].

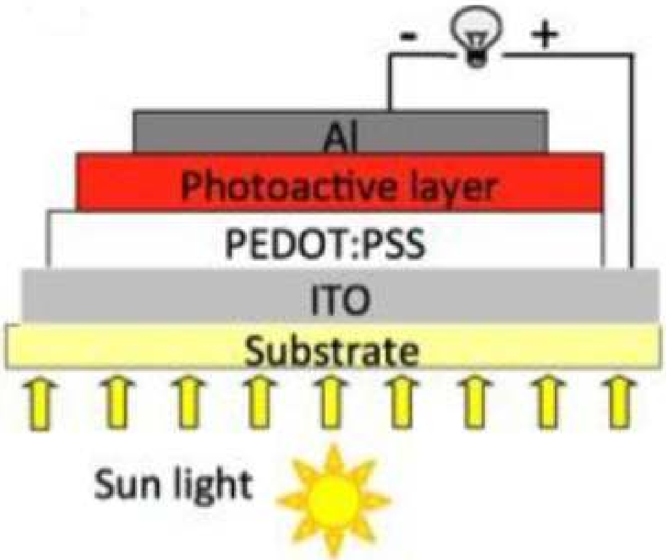

Figure (4.3): structure of BHJ solar cell [22]**.**

Most common material used for cathode is aluminum or low work function metals such as calcium, magnesium and copper. For anode, high work function metal oxides are commonly used, for example, indium tin oxide, and noble metals such as gold and platinum. In order to modify the work function of anode, a buffer layer of a high work function is added. This layer is made up of PEDOT:PSS or poly (3, 4-ethylenedioxy thiophene) poly (styrenesulfonate). It has a work function of 5.2 eV and it works as an electron blocking layer to enhance the work function of the anode and the hole transport through the device. In other words, it blocks electrons and holes transfer in wrong directions.

4.3 Electrical simulation

The electrical simulation of organic solar cell is done in this research using GPVDM software [48]. It helps researchers to simulate devices and changing parameters in an easy way. This helps scientists and engineers to understand how their devices work and how they can improve it theoretically and experimentally. The organic BHJ solar cell ITO/PEDOT: PSS/P3HT: PCBM/Al simulation configuration by GPVDM is shown in figure 4.4.

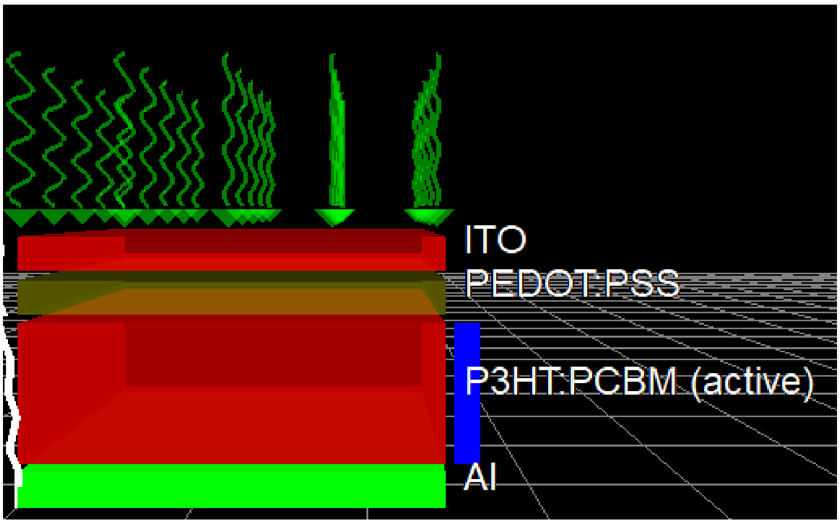

Figure (4.4) device structure of BHJ solar cell by GPVDM.

To describe charge carrier transport, the bi-polar drift-diffusion equations are solved in position space for electrons,

$$J_n = q\mu_e n_f \frac{\partial E_{LUMO}}{\partial x} + qD_n \frac{\partial n_f}{\partial x} \quad (4.1),$$

And holes,

$$J_p = q\mu_h p_f \frac{\partial E_{HOMO}}{\partial x} - qD_p \frac{\partial p_f}{\partial x} \quad (4.2)$$

Those two equations are solved in position space for electrons and holes. Where:

- J_n, J_p: are the electron and hole current density.
- μ_e, μ_h: are the electron and hole mobility.
- n_f, p_f: are the concentration of electron and hole along the Fermi level.
- E_{LUMO}, E_{HOMO}: are the energy of LUMO and HOMO level.

In this model there are two types of electrons (holes): free electrons (holes) and trapped electrons (holes). The free electrons (holes) have a finite mobility of $\mu_e^o(\mu_h^o)$ and trapped electrons (holes) cannot move at all and they have a mobility of zero. To calculate the average mobility, it is assumed to take the ratio of free to trapped carriers and multiply it by the free carrier mobility, which is given by:

$$\mu_e(n) = \frac{\mu_e^o\, n_{free}}{n_{free} + n_{trap}} \quad (4.3)$$

Thus if all carriers were free the average mobility would be μ_e^o and if all carriers were trapped the average mobility would be zero. Note that only $\mu_e^o(\mu_h^o)$ are used in the model for computation and $\mu_e(n)$ is an output parameter. It is consider that the excitons dissociation probability at the donor-acceptor hetero junction is high enough so that excitons concentration at the donor-acceptor interface is zero. Thus, only the excitons generated with a distance of excitons diffusion length from the heterojunction can contribute to the photo-current generation.

4.4 Characteristics of organic solar cell

The behavior of I-V characteristic curve of organic solar cell is similar to that of crystalline silicon solar cell mentioned in previous chapters. The output current voltage curve is shown in the figure 4.5 [21].

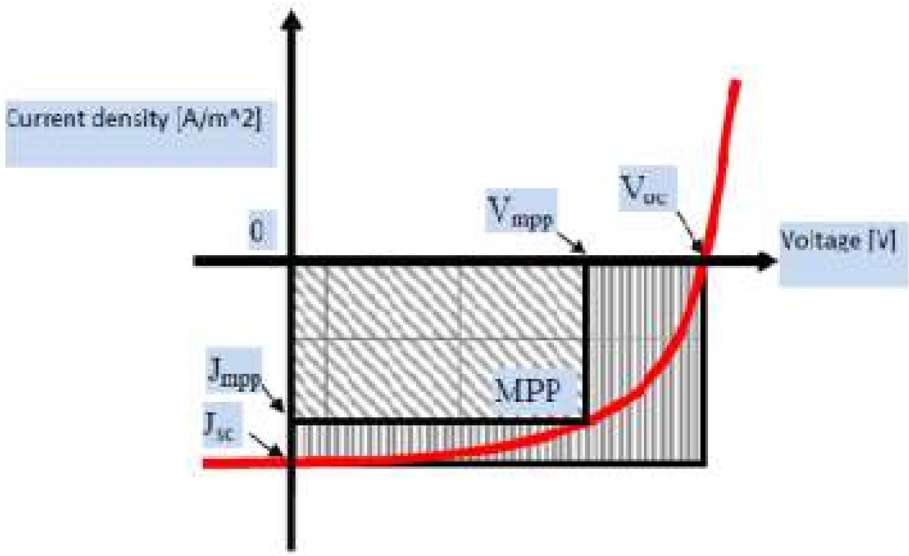

Figure (4.5): J-V characteristic curve [21]**.**

The curve in figure 4.5 shows the behavior of BHJ solar cell under illumination. In dark the curve is shifted up and the solar cell operates as a diode. Under illumination the short circuit current density (J_{SC}) is zero at zero potential difference between anode and cathode. J_{SC} contributes to the efficiency of the solar cell due to light generated charge carriers. It depends on the light intensity, spectrum of the incident light and collection probability by the electrodes. Whereas V_{OC} depends on the saturation current, current generated through radiation and the band gap of materials donor and acceptor are made up from. V_{OC} is given by the difference in LUMO energy level of acceptor and HOMO energy level of donor. V_{OC} also affects efficiency of the organic solar cell. All electrical parameters was discussed in chapter 2 are shown also in figure 4.5. Also the filling factor is given by:

$$FF = \frac{V_{max} J_{max}}{V_{oc} J_{sc}} \quad (4.4)$$

Subsequently the efficiency is given by:

$$\eta = \frac{FF\ V_{oc} J_{sc}}{P_{in}} \quad (4.5)$$

4.4.1 Other parameters improves efficiency

- **Series resistance**

The series resistance (R_s) has a very important effect on J-V characteristic curve of organic BHJ solar cell device. It has been found that an increase in R_s will decrease FF and efficiency of the solar cell due to a decrease in short circuit current density [49]. Many factors could increase R_s significantly such as: the transparent electrode (ITO) and carriers transporting inter - layers of different kinds, also the interfaces between the active layer material and inter layers (metallic contact).

- Thickness of the active layer

As mentioned before, active layer in organic solar cells has low carrier mobility and an incomplete absorption of incident light power (P_{in}).

These two parameters limit the PV cell efficiency. They are directly affected by the thickness of active layer (L). Increasing L will increase path length for incident light. This will increase the absorption of the device according to:

$$A = -\log\left(I_o e^{-\frac{4\pi k L}{\lambda}}\right) \quad (4.6)$$

Where,

- A is the measured absorbance
- I_o is the incident irradiance
- k is the extinction coefficient of the material.

So increasing thickness of active layer will generate a high number of charges and a higher absorption will occur. However, as L lengthened the photogenerated electrons and holes will travel a larger distance through the active layer so as to reach their respective electrodes. Assuming a constant recombination lifetime, the free charges will have a higher chance of recombination before reaching the electrodes. By using this qualitative image we will expect that for a given donor-acceptor mixture, as L will increase, the photocurrent will be raised because of greater charge generation and will be limited by higher recombination.

Chapter Five

Simulation results and discussion

Chapter Five
Simulation results and discussion

5.1 Introduction

This chapter provides the simulation results with a discussion on the results with regards to conversion efficiency of inorganic and organic solar cells. It is divided into three main parts; first part presents the simulation results for single junction monocrystalline silicon solar cell (I-106/12 from Isofoton) – various models, second part of the chapter contains simulation of different PV cell models of single junction polycrystalline silicon solar cell (SPM050-P). The final part deals with the results of bulk heterojunction (BHJ) organic solar cell.

The performance of mono- and polycrystalline Si solar cells under the standard test conditions will be analyzed; this includes an observation of the output current versus voltage curve and calculation of vital parameters of solar cell which they are: maximum power point (MPP), the fill factor (FF) and the conversion efficiency (η).

Since the temperature and solar irradiation affect PV cell parameters, the behavior of solar cell will be analyzed under different climatic conditions. After which a comparison between monocrystalline and polycrystalline Si solar cells will be held.

An illuminated p-n junction has an equivalent circuit based on the conventional single-diode equivalent electrical circuit drawn from a light generated DC current source connected in parallel with a diode. This model is named single- diode model or the ideal model. However, going deeper into electrical losses in the solar cell, a series resistance, parallel resistance and a second diode are added to the equivalent circuit of the ideal model. These losses in the solar cell drop the conversion efficiency. In this research the performance of “non-ideal” PV cells is very essential in order to know the behavior of the panel.

In this research, $P3HT{:}PCBM$ is used as an active layer in the structure of BHJ organic solar cell. This work focuses on the electrical simulation of organic solar cells. The current density versus voltage (J-V) output curve of the solar cell reflects the behavior of the device. After which we focus on simulation studies on the influence of parameters of organic solar cell such as: thickness of active layer and series resistance. The study considers thickness dependence of the performance of BHJ organic solar cell and how efficiency is affected. Furthermore, the organic solar cell will be electrically simulated under different series resistances and J-V output curves will be analyzed.

5.2 Simulation results of single junction mono- Si (first generation) solar cells.

Monocrystalline Si solar cells have a square shape with missing corners and they are often having a black color. They are more efficient than polycrystalline Si solar cells. Mono- Si cells are made by forming Si into bars and cut them into wafers. Si used to make mono- Si solar cells is single- crystal Si i.e. the cell is formed from a single crystal so; the electrons which generate the electrical current have more space to move. This section provides the simulation results of four different equivalent circuits of I-106/12 monocrystalline solar cell that represent the behavior of the PV device. The electrical parameters will be extracted from the output curves to analyze the performance of the solar cell under STC. Such parameters are P_{max}, FF and efficiency. Moreover, parameters provided by datasheet like V_{oc} and I_{sc} are studied under changing the environmental conditions.

5.2.1 Simulation results of model I (ideal)

Power versus load resistance (P-R_l) output curves are presented firstly and the MPP of this model will be extracted. Power is the product of the terminal voltage and its corresponding current flowing in the solar cell ($P = IV = I^2R$). Output current of solar cell is dependent upon both internal losses in the device and environmental conditions such as temperature and sun irradiation.

Model I or the ideal model as mentioned previously is the most simplified model of solar cell. It composed of a DC current source in parallel with a diode made up from Si with an ideality factor equals 1. Figure 5.1 shows the resulting power obtained under STC ($25℃$ and $1000\ W/m^2$).

The maximum power point $P_{max} = 1.62\ W$ is larger than that on the manufacturer's datasheet ($P_{max} = 1.47\ W$).This behavior is expected since no losses or recombination are considered. It is the ideal behavior of this solar cell.

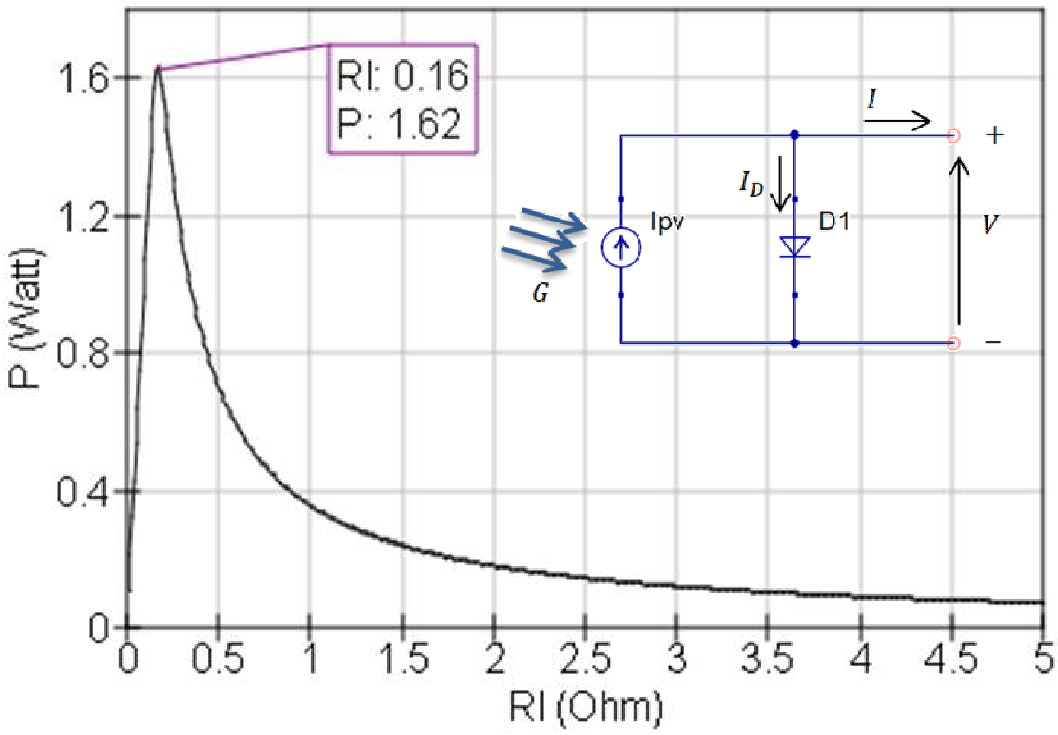

Figure (5.1): power curve of model I of mono-Si under STC (25℃ and $1000\ W/m^2$).

5.2.2 Simulation results of model II

Adding a series resistance (R_s) to the ideal model introduces more accurate results. Series resistance is added to represent some sources of electrical losses in solar cell such as contact resistance of metal-semiconductor on the back and top surfaces of the device and the resistance of base semiconductor material. Series resistance reduces the fill factor of PV cell, accordingly the efficiency will reduce. It was mentioned in chapter 2 the empirical formula used to calculate R_s. It is given by:

$$R_s = \left(1 - \frac{FF}{FF_0}\right)\left(\frac{V_{OC}}{I_{SC}}\right) \quad (5.1)$$

Where,

$$FF_0 = \frac{v_{oc} - \ln(v_{oc} + 0.72)}{1 + v_{oc}} \quad (5.2),$$

Where FF_0 is the fill factor of the ideal PV module or cell without any resistive effects; R_s is the series resistance; v_{oc} is the normalized value of open circuit voltage to the thermal voltage and it is given by:

$$v_{oc} = \frac{V_{oc}}{nKT/q} \quad (5.3)$$

Where n is the ideality factor and it is equal 1 in this case, K is the Boltzmann constant ($K = 1.38 \times 10^{-23} m^2 kg\ s^{-2} K^{-1}$), T is the cell's temperature in Kelvin ($T = 298K$) and q is the electron charge ($q = 1.602 \times 10^{-19} coulombs$). The values of V_{OC} and I_{SC} substituted in the equation of R_s and in FF formula are the extracted values from datasheet. After substituting the resulted R_s is approximately $0.013\,\Omega$. The output power curve for model II was simulated also at STC as shown in figure 5.2. The maximum power point ($P_{max} = 1.47\,W$) coincided with that on the manufacturer's datasheet. The maximum output power is obtained when the resistance of the load is equal to $160\ m\Omega$.

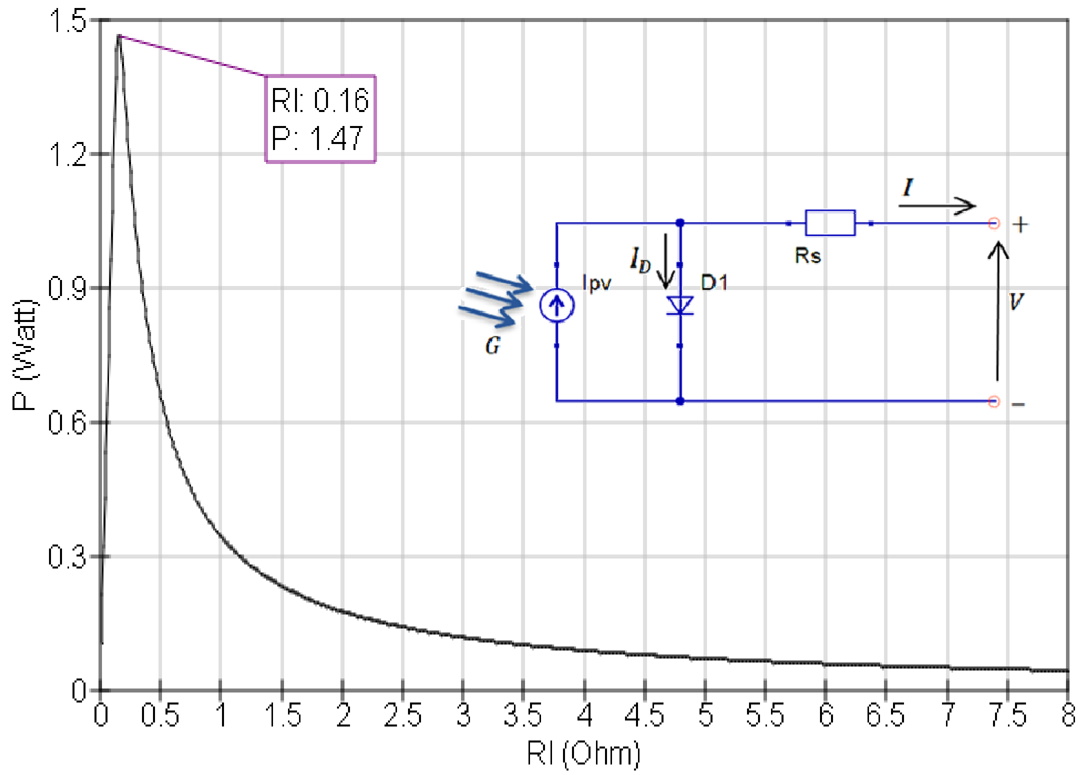

Figure (5.2): power curve of model II of mono-Si under STC (25℃ and $1000\ W/m^2$).

5.2.3 Simulation results of model III

The effect of leakage current through the PV cell caused by impurities or defects in the manufacturing process can be presented by a shunt resistance (R_{sh}). It is added in parallel to the DC current source and the diode. This model also keeps on the series resistance. R_{sh} reduces the efficiency of the solar cell since it provides a new path to the electrical current to flow in. in this research we are using a large value of R_{sh} in order to reduce the leakage current as possible. The performance of model III at STC is shown in figure 5.3. When model III is compared to model II, it is expected that they have the same maximum power point since the shunt resistance is large.

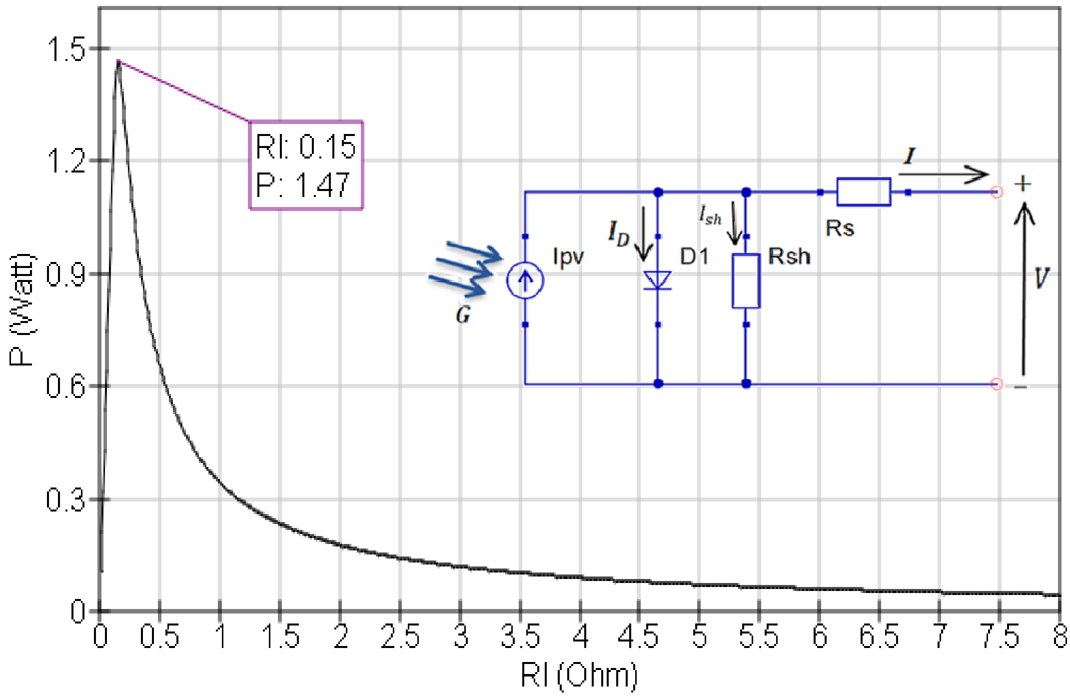

Figure (5.3): power curve of model III of mono-Si under STC (25℃ and 1000 W/m^2).

It seems that shunt resistance doesn't affect MPP of a PV cell but according to [50] R_{sh} plays an important role when PV device operates as current-source generator. It was seen that the model II that neglects the effects of R_{sh} was inadequate to fit experimental I-V and P-V data in current-source operation.

5.2.4 Simulation results of model IV

In model IV, a second diode is connected in parallel with the first diode. This diode is attached in order to include the recombination in the p-n junction at low voltages. The ideality factor of the second diode is 2. Figure 5.4 confirms that recombination does reduce the output maximum power and the efficiency.

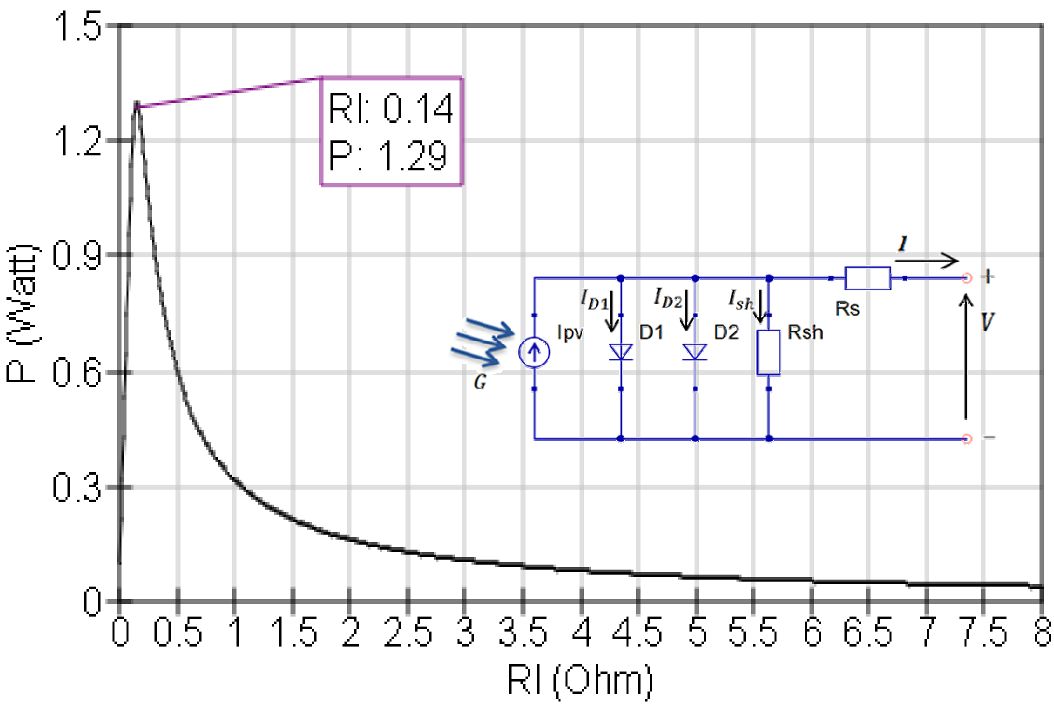

Figure (5.4): power curve of model IV of mono-Si simulated at STC (25℃ and $1000\ W/m^2$).

As shown in figure 5.4, the maximum power point has been reduced and it equals 1.29 W occurs at 140 $m\Omega$. Maximum power is less than that value provided by the datasheet so, taking into consideration the recombination current affects MPP and reduces the efficiency of the device.

5.2.5 A model comparison

Four models of mono- Si solar cell were simulated using QUCS software and the behavior of the PV cell was observed under the standard test conditions. To sum up the results, table 5.1 contains each PV cell model that have been simulated with its peak point and the load resistance that the maximum output power occurs at it.

As expected, the maximum value of output power obtained in this research is achieved by model I. This result thus obtained is compatible with what this model is commonly named “the ideal model” since it assumes no recombination and no internal losses are present in the cell. Both models II and III share the same MPP because the shunt resistance was assumed very large. In model IV the MPP is decreased due to losses caused by recombination as was mentioned before.

Table (5.1): the simulated mono-Si PV cells models’ MPPs.

Model	$P_{max}(W)$	$R_l(m\Omega)$
I(ideal)	1.62	160
II	1.47	160
III	1.47	150
IV	1.29	140

The simulated mono- Si solar cell (I-106/12 from Isofoton) total power curves at STC are shown below (figure 5.5). The P-R_l curves of the single junction mono- Si solar cell provide the following insight: a high R_{sh} value and low R_s value ensures that the MPP remains unchanged. It can be observes that MPP of model II and III resembles the one provided by the manufacturer on the datasheet.

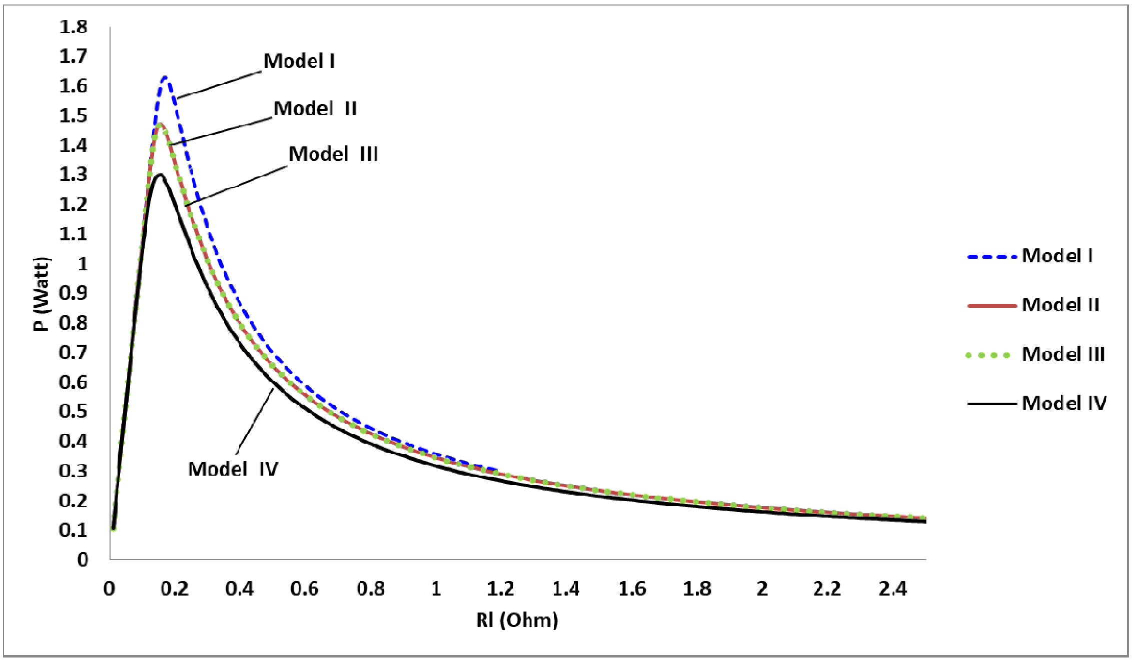

Figure (5.5): mono-Si total cell power curves under STC (25℃ and 1000 W/m^2).

5.2.6 Efficiency calculation

The efficiency or conversion efficiency is an important parameter used to compare the performance of one solar cell to another. It is defined as the ratio of the output energy generated by the solar cell to the input energy provided by the sun. The conversion efficiency is calculated according to:

$$\eta = \frac{P_{MP}}{P_{in}} = \frac{V_{MP} * I_{MP}}{P_{in}} = \frac{V_{oc} * I_{sc} * FF}{P_{in}} = \frac{V_{oc} * I_{sc} * FF}{G * A} * 100 \quad (5.4)$$

Where V_{oc} is the open circuit voltage and it is the maximum voltage that solar cell can provide when the terminals of PV cell are not connected to any load, I_{sc} is the short circuit current; which is the maximum current provided by the PV cell when the output terminals are shorted together. The area of solar cell (A) in this research is assumed to be $100\,mm \times 100\,mm$. FF is the fill factor and it is calculated from:

$$FF = \frac{I_{MP}V_{MP}}{I_{sc}V_{oc}} \quad (5.5)$$

And G equals $1000\ W/m^2$ (STC).The I-V characteristics for various models of mono-Si solar cell (I-106/12 from Isofoton) were implemented in QUCS under STC and they are shown in figure 5.6.

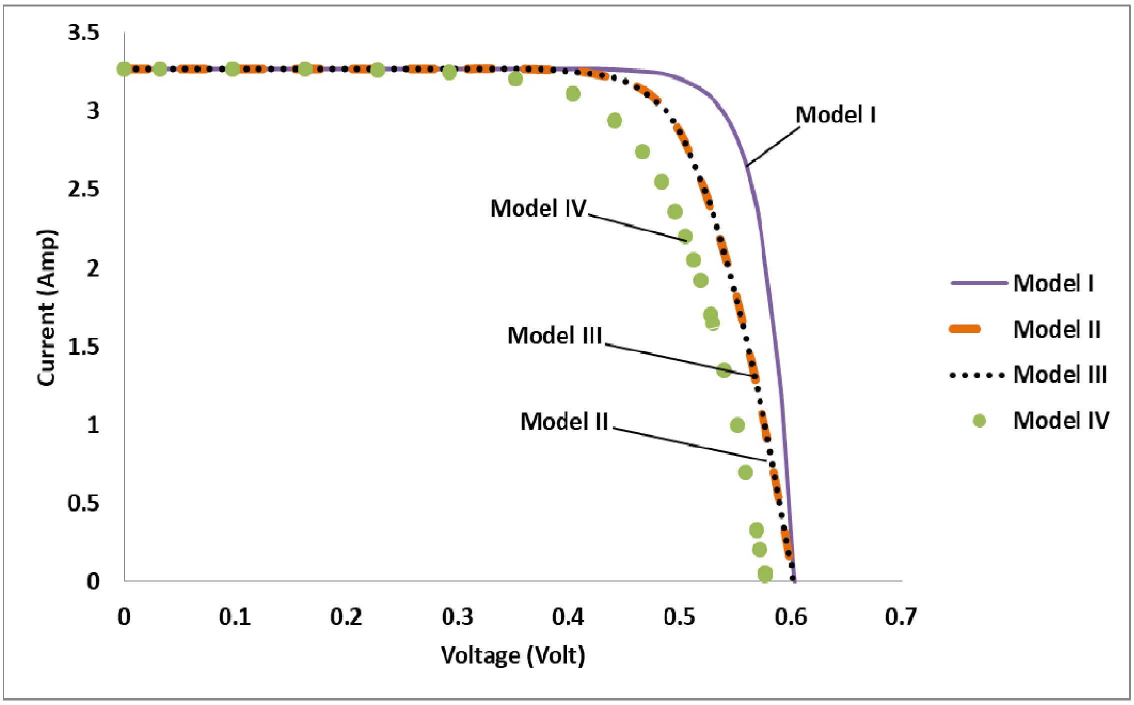

Figure (5.6): single junction mono-Si total I-V curves under STC (25℃ and $1000\ W/m^2$).

It can be seen from figure 5.6, as expected, the good match between I-V curves and P-R_l curves which was shown in figure 5.5. It is very important to know the maximum point (V_{MP},I_{MP}) from the I-V characteristic of a solar cell. Since current times voltage equals power ($P = I \times V$), I-V curves can help in providing the information required to make a solar cell then a solar system operates as close as possible to its MPP.

I. Efficiency calculation of model I

In order to calculate the efficiency of the ideal model, the fill factor must be calculated firstly. The fill factor (FF) is the ratio of maximum obtainable power by a solar cell (P_{MP}) to the product of the open circuit voltage times the short circuit current ($V_{oc} \times I_{sc}$). FF value gives an idea of the behavior of the solar cell. The closer the value of FF to one, the more power the cell can provide and the more efficient the cell it is. Typically FF values are between 0.7 and 0.8. Figure 5.7 shows the I-V curve of model I separately.

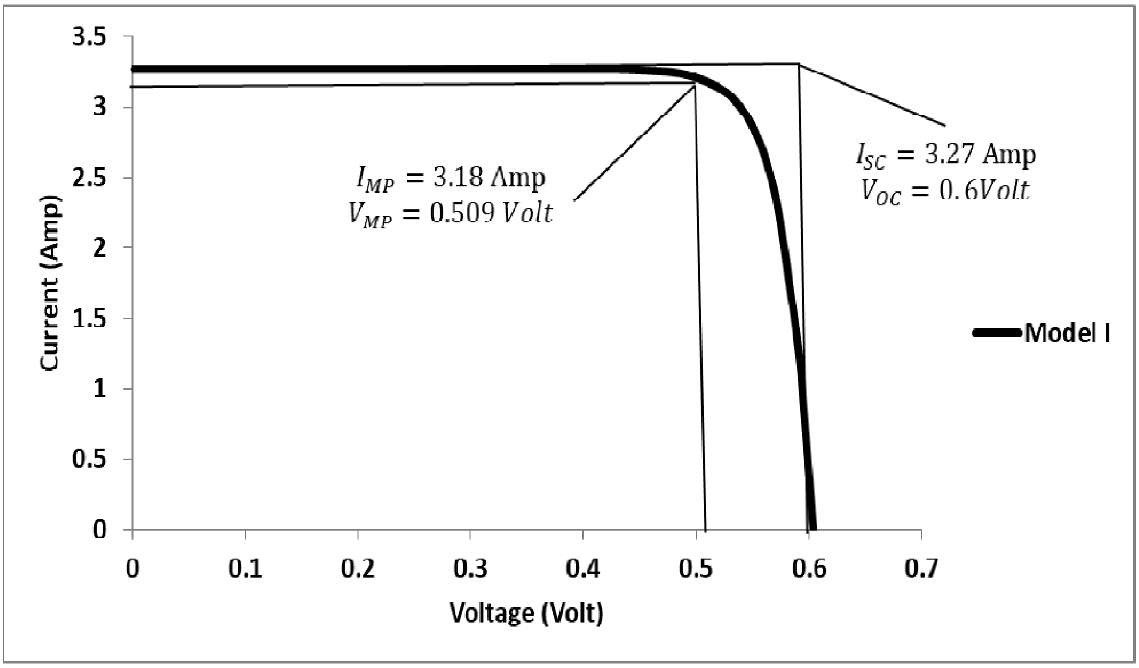

Figure (5.7): I-V sweep of the ideal mono-Si solar cell under STC (25℃ and $1000\ W/m^2$).

According to figure 5.7, the FF is represented graphically by the I-V curve. The FF is the ratio of the small rectangular to the bigger one. The fill factor of the first model of mono-Si PV cell (I-106/12 from Isofoton) under STC according to figure 5.7 is:

$$FF = \frac{1.62}{1.96} = 0.82$$

This value is acceptable since it matched the calculations. The efficiency is:

$$\eta = 16.1\%$$

This is the theoretical efficiency obtained by the cell since it is an ideal model.

II. Efficiency calculation of model (II+III)

The fill factor is affected by the series resistance (R_s) and shunt resistance (R_{sh}). Decreasing the value of R_s and increasing the value of R_{sh} lead to a higher FF, consequently resulting a higher efficiency. Figure 5.8 shows the resulting I-V curve of single-diode with series resistance model of mono-Si solar cell (I-106/12 from Isofoton) namely model II.

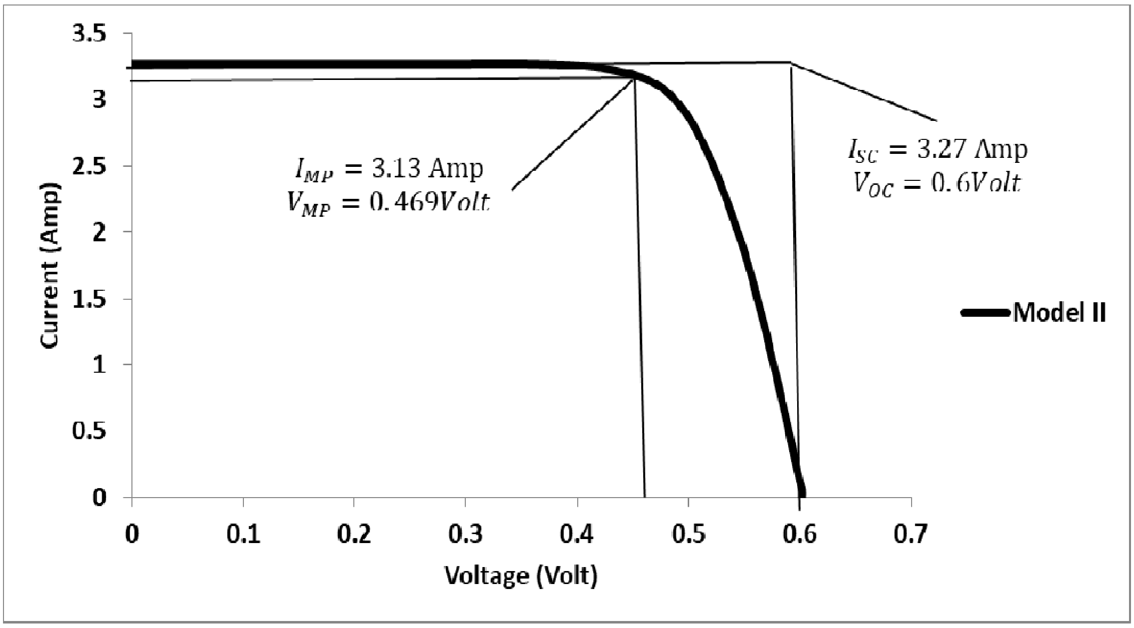

Figure (5.8): The resultant I-V sweep of mono-Si solar cell (model II) under STC (25°C and 1000 W/m^2).

The fill factor of the single-diode with series resistance – PV model of mono-Si solar cell according to figure 5.8 is:

$$FF = \frac{1.47}{1.96} = 0.75$$

$$\eta = 14.7\%$$

It can be noticed, as expected, a reduction in values of FF and η due to the addition of R_s to the circuit. This result is consistent with literature reviews and the information provided in the manufacturer's datasheet. Moreover, since model II and model III (single-diode with series and parallel resistances) have the same MPP then they share the same value of FF and η.

III. Efficiency calculation of model IV

The FF is affected also by the internal losses caused by the junction recombination in the cell. These losses reduce the value of FF and η due to a drop in the output power generated by model IV as was shown in the previous section. Figure 5.9 presents the output I-V curve of model IV.

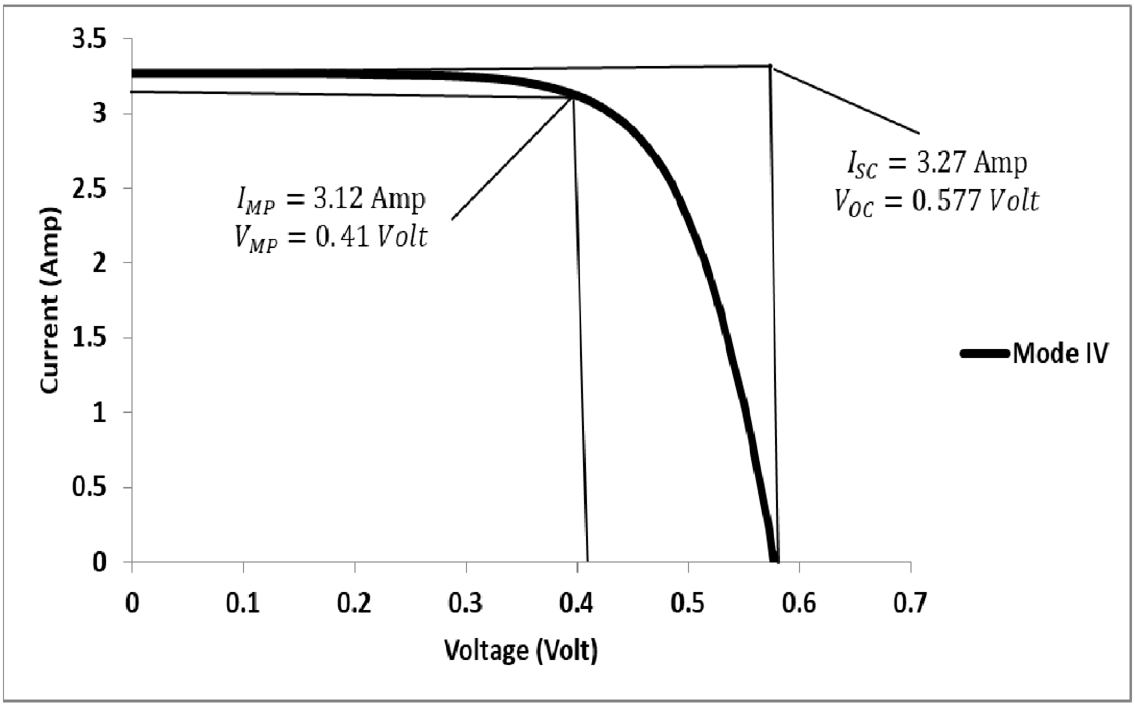

Figure (5.9): the resultant I-V sweep of the double-diode mono-Si PV cell (model IV) under STC (25°C and $1000\ W/m^2$).

The fill factor of the double-diode with series and parallel resistances – PV model for monocrystalline Si solar cell according to figure 5.9 is:

$$FF = \frac{1.28}{1.88} = 0.68$$

It is obvious, as expected, the drop of FF caused by the existence of a second diode in parallel with the first one. This leads for sure to a reduction in the efficiency of the solar cell:

$$\eta = 12.8\%$$

To sum up, the findings so far are quite convincing, and thus the calculated data of monocrystalline solar cell's various models at STC is summarized in table 5.2.

Table 5.2: simulation results of mono-Si (I-106/12) solar cell's various models simulated under STC (25°C and $1000\ W/m^2$).

Model	FF	η
I(Ideal)	0.82	16.1%
II	0.75	14.7%
III	0.75	14.7%
IV	0.68	12.8%

5.2.7 Variation of characteristics with temperature.

The performance of a PV cell is affected by varying cell's temperature. That because temperature affects the parameters of the solar cell such parameters are P_{max}, FF, I_{MP}, V_{MP}, V_{oc} and I_{sc}. As temperature increases, V_{oc} decreases significantly then the output power will be reduced. I_{sc} increases slightly by increasing the temperature, this because more electron-hole pairs are created at higher temperatures. So the most dominant effect of temperature is on V_{oc} with a negative temperature coefficient. V_{oc} is given by the relation:

$$V_{oc} \cong \frac{kT}{e} \ln\left[\frac{I_{pv}}{I_o}\right] \quad (5.6)$$

When temperature is increased, band gap is decreased then carrier concentration (n_i) will increase so that I_o then the open circuit voltage will decrease.

The performance of mono-Si solar cell (I-106/12) at a constant level of irradiance ($G = 1000\,W/m^2$) and at three different temperatures is shown in figure 5.10. it is clear from the figure that open circuit voltage decreases as the temperature increases. Also, there is a significant drop in the power output of the PV cell as temperature increases.

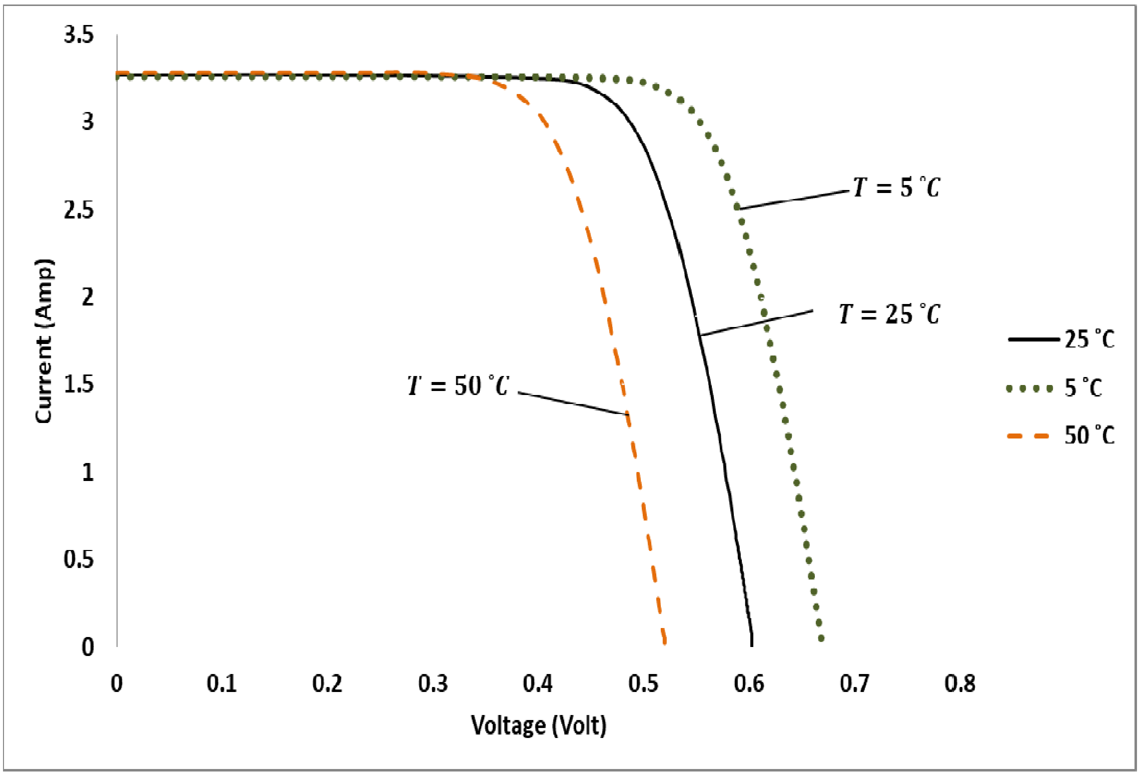

Figure (5.10): mono-Si PV cell I-V curves at different temperatures and at a constant irradiance.

As we can see from the above figure that the short circuit current rises slightly when the temperature is increased while open circuit voltage decreases with increasing temperature. The I_{sc} varied from $3.27 - 3.28\ A$ whereas the V_{oc} varies from $0.668 - 0.52\ V$. Table 5.3 includes simulation results of mono-Si solar cell that show how the parameters of PV cell are varied with increasing the cell temperature. As expected, maximum power, the fill factor and efficiency decreases with increasing temperature.

Table (5.3): simulation results for mono-Si solar cell (I-106/12) with respect to temperature ($G = 1000\ W/m^2$).

T (°C)	$I_{SC}(A)$	$V_{OC}(V)$	$P_{max}(W)$	FF	η %
5	3.27	0.668	1.6	0.73	16 %
25	3.27	0.6	1.47	0.75	14.7 %
50	3.28	0.52	1.2	0.71	12.1 %

5.2.8 Variation of characteristics with irradiance.

To study the effect of sun irradiance on the performance of the PV cell the values of irradiance are changed to three different values and the temperature is kept constant ($T = 25°C$). The variation of I-V characteristics with respect to irradiance are shown in figure 5.11. It is clear from figure 5.11 that as the irradiance is changed, V_{oc} is barely changing but I_{sc}changes dramatically linearly.

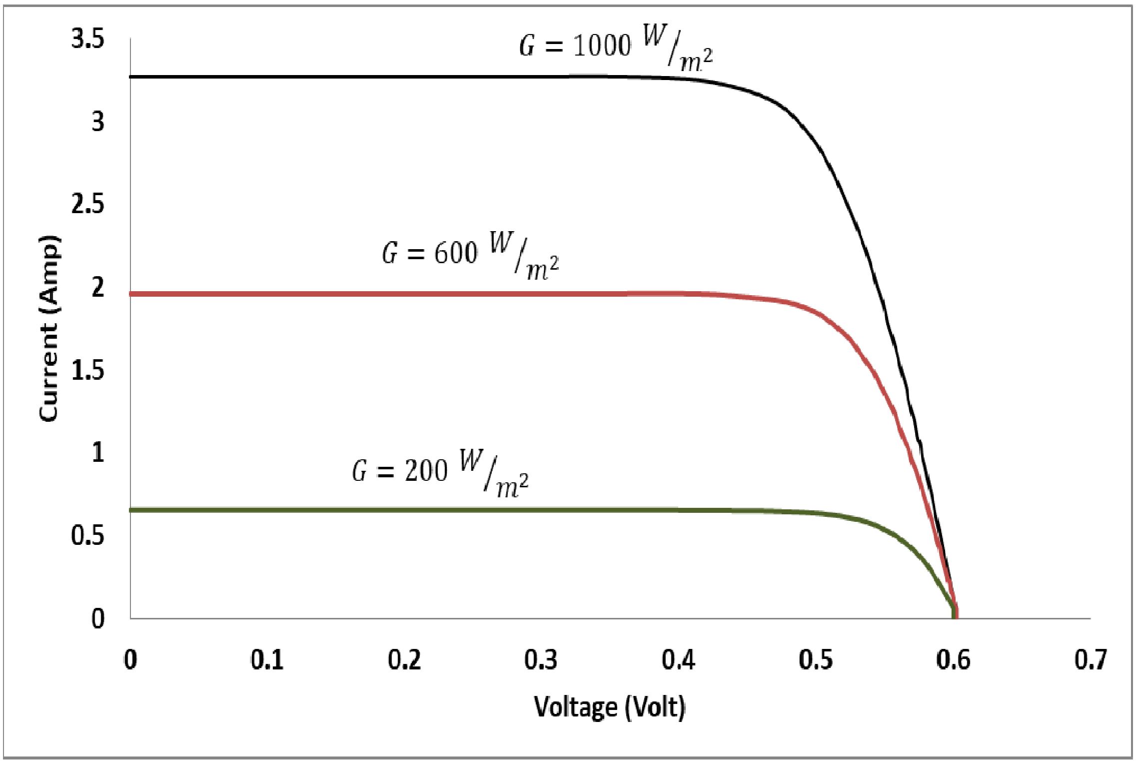

Figure (5.11): mono-Si PV cell I-V curves at different values of irradiance and at fixed temperature.

As irradiance increases, I_{sc}increases from $0.654\ A$ to $3.27\ A$. Also, an increase in irradiance does result in an increase in P_{max}, FF and efficiency. The simulation results with respect to irradiance are summarized in table 5.4.

Table 5.4: simulation results for mono-Si solar cell (I-106/12) with respect to irradiance ($T = 25$°C).

$G\ (W/m^2)$	$I_{SC}(A)$	$V_{OC}(V)$	$P_{max}(W)$	FF	η %
200	0.654	0.6	0.26	0.66	2.5 %
600	1.96	0.602	0.807	0.68	8.07 %
1000	3.27	0.602	1.47	0.74	14.7 %

5.2.9 Outcomes of section II

The following points are the results of observation of the graphs and tables:

I. PV cell – model I has the highest value of conversion efficiency. This was expected since it is the ideal model.

II. Mono-Si PV cell model III (the nearest to real behavior) yields a conversion efficiency of approximately 15%. This value is acceptable since the range of efficiency of market solar cells is between 15% and 20%.

III. As expected, PV cell that has the highest efficiency has the highest FF.

IV. An increase in cell temperature results in a drop in power and a drop in efficiency of the cell.

V. As expected, short circuit current is slightly affected with increasing temperature as open circuit voltage does.

VI. Increasing temperature does result in a decrease in open circuit voltage.

VII. An increase in irradiance results in an increase of power and efficiency of the cell.

VIII. As expected, open circuit voltage is not affected with increasing irradiance as short circuit current does.

IX. Increasing the irradiance does result in a raise of short circuit current of the cell.

X. As expected recombination current of diode does drop the value of open circuit voltage of the cell and the fill factor.

5.3 Simulation results of single junction poly- Si solar cell.

Polycrystalline silicon solar cells are square shaped with a blue color instead of the black color of mono-Si cells. Poly-Si cells are made also from Si. It is made by melting many fragments of Si together to form the wafers. The polycrystalline Si solar cell includes many crystals in it; this offers a small space for electrons to move. As a result, poly-Si solar cells have a lower conversion efficiency than mono-Si cells. Although the low conversion efficiency of poly-Si cells compared to mono-Si solar cells, their low price gives them an advantage. In this section the simulation results of four different equivalent circuits of SPM050-P polycrystalline solar cell that represent the behavior of the PV device are provided. The poly-Si solar cell was simulated also by QUCS software. Solar cell I-V characteristic curves will be carried out and analyzed under STC firstly. After which the performance of poly-Si PV cell will be studied under varying temperature and irradiance values.

5.3.1 Simulation results of model I (ideal)

Model I or the ideal model is a DC current source in parallel with a diode with an ideality factor equals 1. The resultant power curve of model I is shown in figure 5.12.

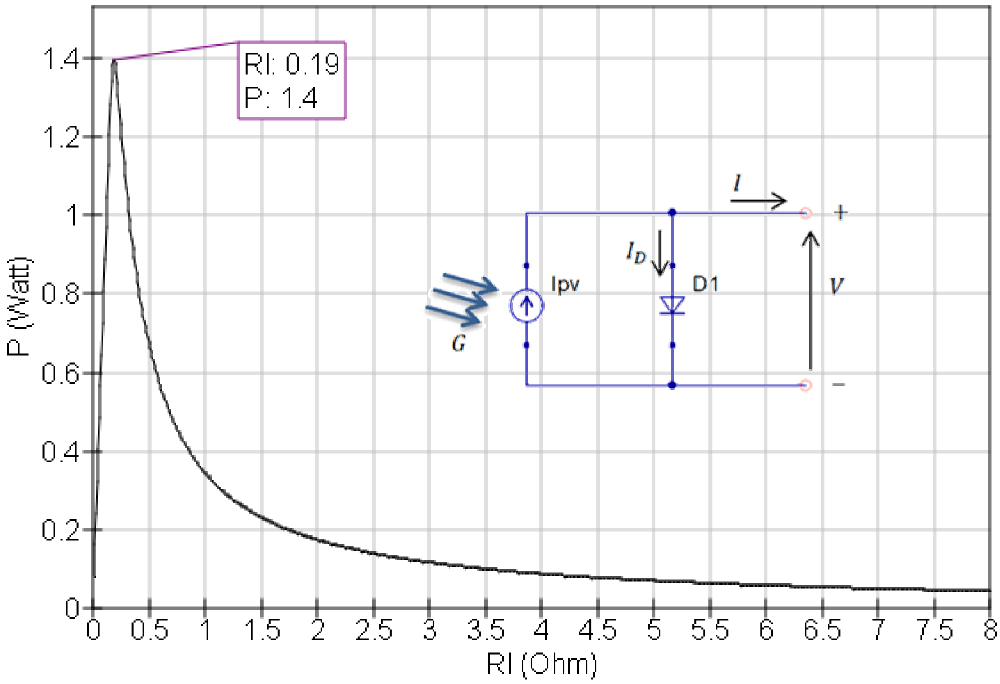

Figure (5.12): power curve of model I of poly-Si solar cell (SPM050-P) under STC (25°C and 1000 W/m^2).

Figure 5.12 presents the circuit configuration of model I with the resultant power curve. As is clear from figure 5.12 the MPP is 1.4 W at load resistance equals 190 $m\Omega$.

5.3.2 Simulation results of model II

The second model is a DC current source in parallel with a diode connected in series with a resistance (R_s). Figure 5.13 depicts the output power generated by model II under STC. From figure 5.13 we see that the MPP is 1.29 W. This result was expected since the existence of R_s drops the output power generated by a cell. The maximum power also coincides with that on the manufacturer's datasheet.

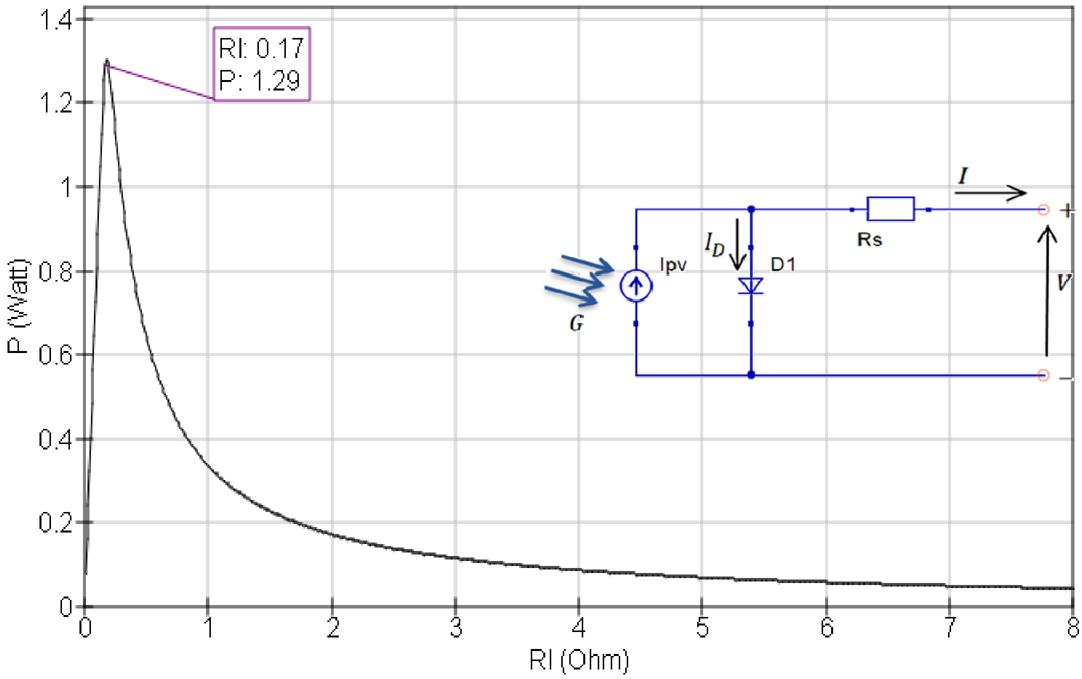

Figure (5.13): power curve of model II of poly-Si solar cell (SPM050-P) under STC (25°C and $1000\ W/m^2$).

5.3.3 Simulation results of model III

Model III is a single diode with series and parallel resistances - PV model. The equivalent circuit and the power curve are shown in figure 5.14.

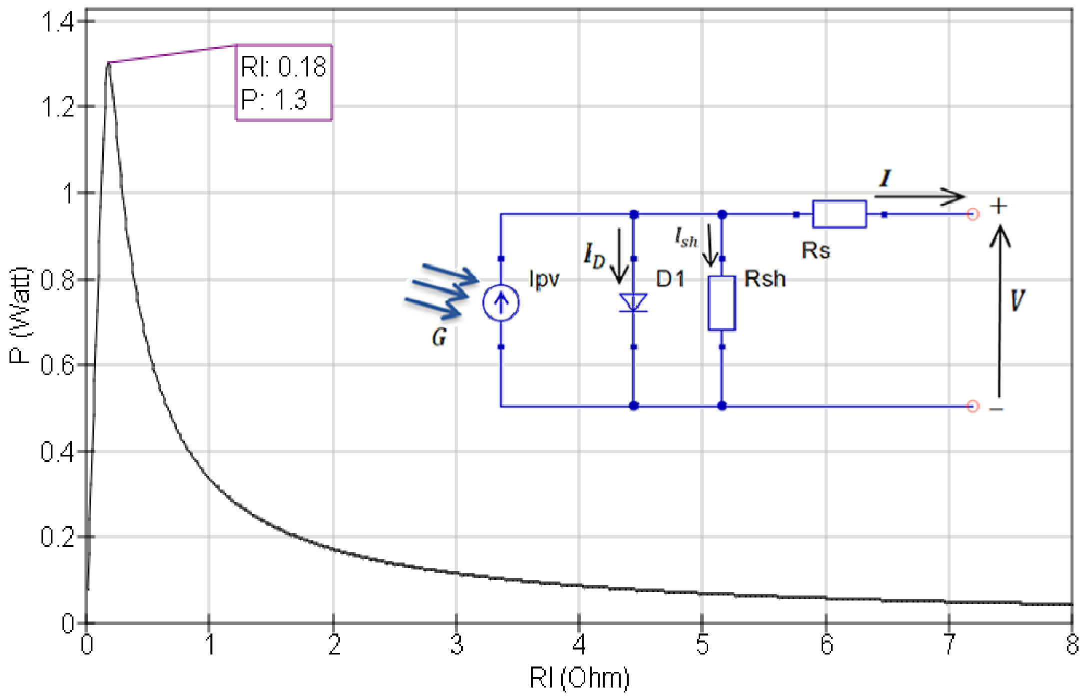

Figure (5.14): power curve of model III of poly-Si solar cell (SPM050-P) at STC (25°C and 1000 W/m^2).

According to figure 5.14, the maximum power model III can generate equals 1.3 W. This result concurs with the value of output power which has generated by model II since the shunt resistance is assumed to be very large. Thus, it is very close to the value of maximum power provided on the datasheet of the cell.

5.3.4 Simulation results of model IV

This model considers the internal losses in the solar cell caused by recombination mechanisms in addition to the impact of series and shunt resistances. Model IV is a DC current source connected in parallel with two diodes. The first and second diodes have an ideality factor of 1 and 2 respectively. Model IV is named as double-diode with series and parallel resistances – PV model. Figure 5.15 represents the power curve obtained by QUCS.

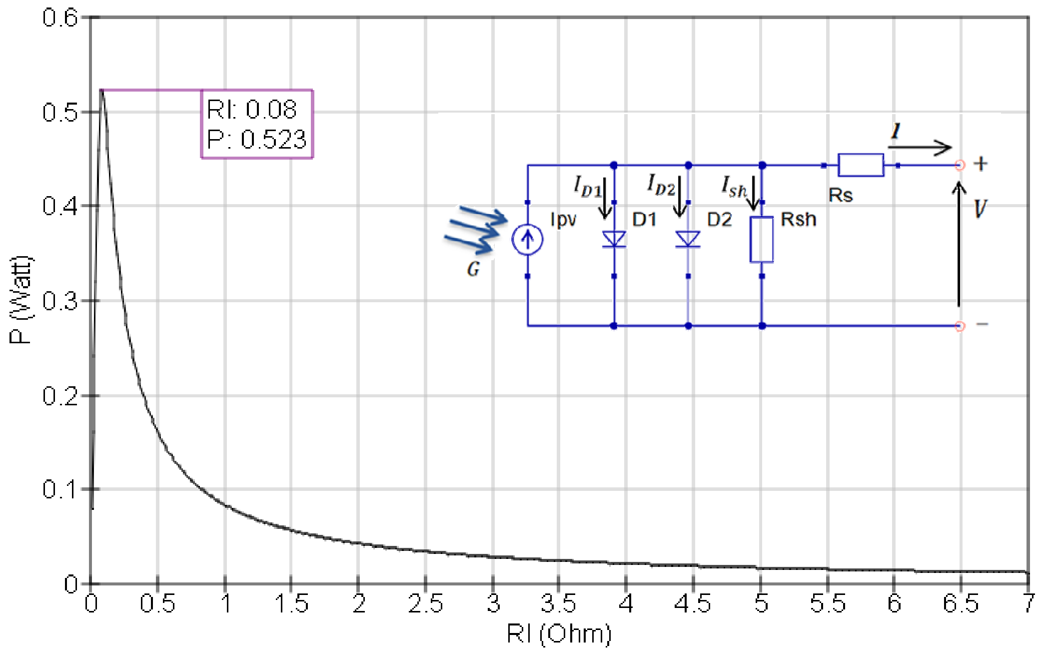

Figure (5.15): power curve of model IV of poly-Si solar cell (SPM050-P) at STC (25℃ and 1000 W/m^2).

The figure above indicates a drop in the MPP. This will result in a drop in the FF and efficiency as will be seen in the next section.

5.3.5 A model comparison.

The findings so far are summarized in table 5.5. It provides the resulted maximum power points and their load resistances obtained at STC.

Table (5.5): The four models of poly-Si (SPM050-P) simulated at STC with respect to MPP and R_l.

Model	$P_{max}(W)$	$R_l(m\Omega)$
I(ideal)	1.4	190
II	1.29	170
III	1.3	180
IV	0.523	80

It is evident that the performance of poly-Si solar cell is similar to that of mono-Si. However, the value of maximum power points obtained by poly-Si cell is less than that one generated by mono-Si. The power curves of the four models of poly-Si are illustrated in figure 5.16.

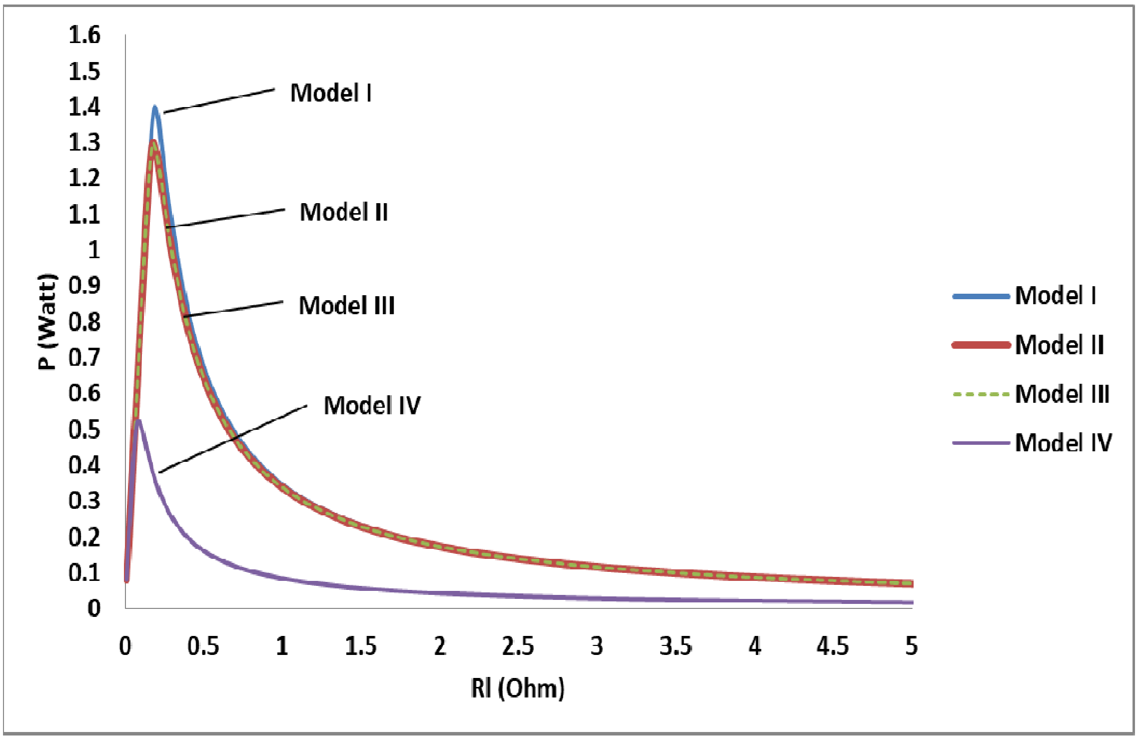

Figure (5.16): the power curves of the four models of poly-Si (SPM050-P) simulated at STC ($T = 25$°C and $G = 1000\,W/m^2$).

5.3.6 Efficiency calculation.

In the same manner that has been done in efficiency calculation of monocrystalline PV cells, the same process is followed in polycrystalline PV cells. Efficiency can be calculated from:

$$\eta = \frac{P_{MP}}{P_{in}} = \frac{V_{MP} * I_{MP}}{P_{in}} = \frac{V_{oc} * I_{sc} * FF}{P_{in}} = \frac{V_{oc} * I_{sc} * FF}{G * A} * 100 \quad (5.7)$$

Where FF is calculated from:

$$FF = \frac{I_{MP}V_{MP}}{I_{sc}V_{oc}} \quad (5.8)$$

As mentioned previously, the I-V characteristic is a graph of output current versus voltage obtained by a PV cell. It can tell about the ability of a PV cell to convert sunlight energy into electricity. It helps also in determining the MPP that can be generated by a PV cell so that it can operate as close as possible to P_{max} so that the performance of the solar cell is enhanced.

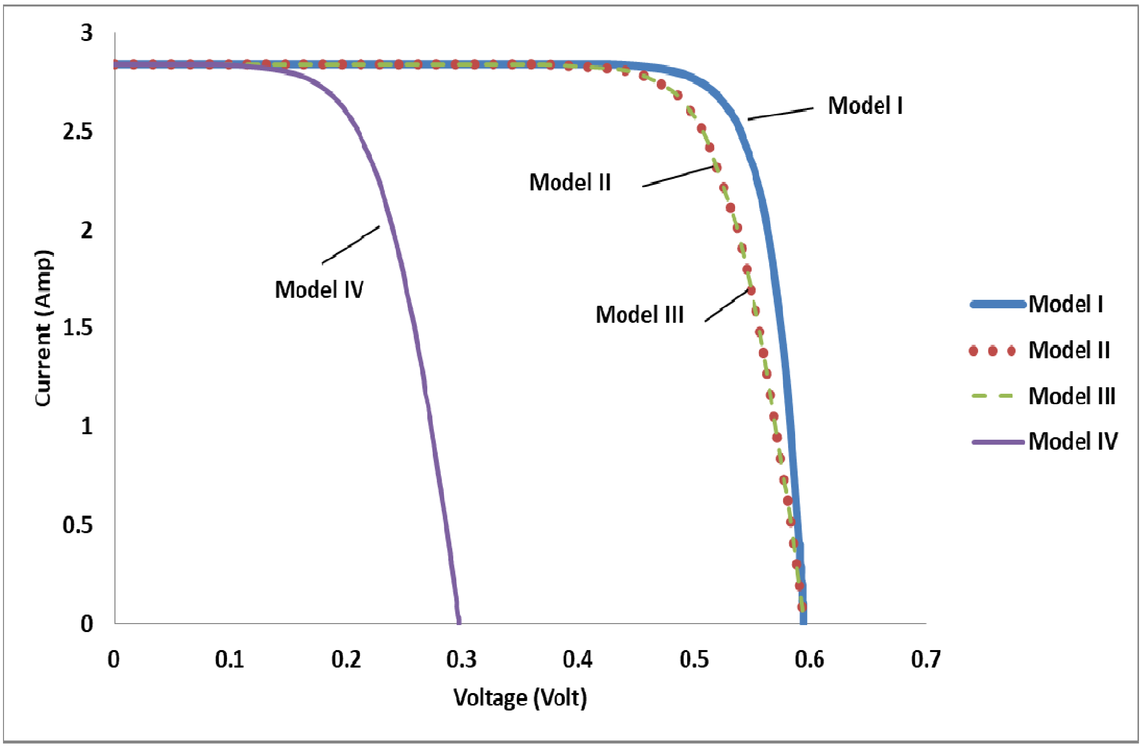

Figure (5.17): I-V curves of poly-Si solar cell (SPM050-P) simulated at STC ($T = 25$°C and $G = 1000\, W/m^2$).

I. Efficiency calculation of model I

The I-V curve of the ideal model of poly-Si solar cell simulated under STC is shown in figure 5.18. The FF can be extracted graphically by dividing the area of the small rectangular by the area of the bigger one.

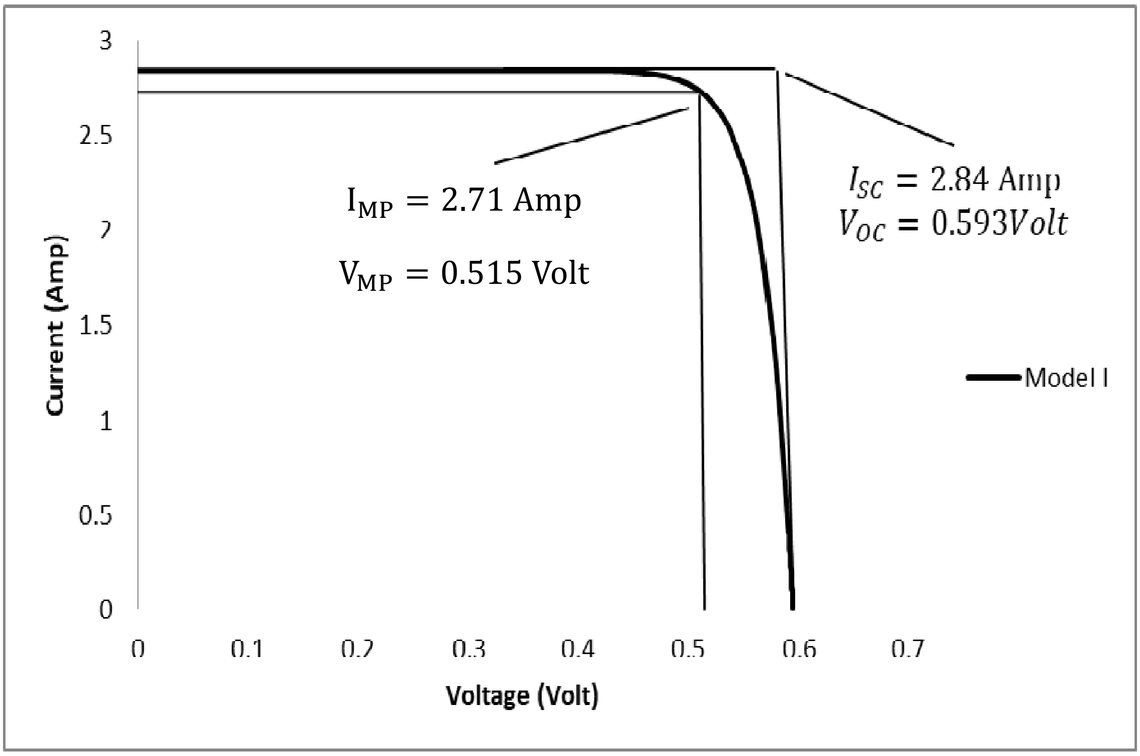

Figure (5.18): I-V sweep of the ideal model of poly-Si solar cell simulated under STC.

The fill factor of poly-Si PV cell according to figure 5.18 is:

$$FF = \frac{1.4}{1.68} = 0.83$$

And then the efficiency is:

$$\eta = 14\%$$

The results are quite convincing and it can be seen, as expected, that the efficiency of model I of poly-Si solar cell is less than efficiency of model I of mono-Si solar cell.

II. Efficiency calculation of model (II+III)

Resistive losses in a solar cell reduce the FF and efficiency. Both model II and model III share the same I-V characteristic curve. Figure 5.19

shows the output curve. The curve outlines that the MPP decreases due to losses in the cell. Moreover, the resultant MPP is very close to that value provided by the datasheet.

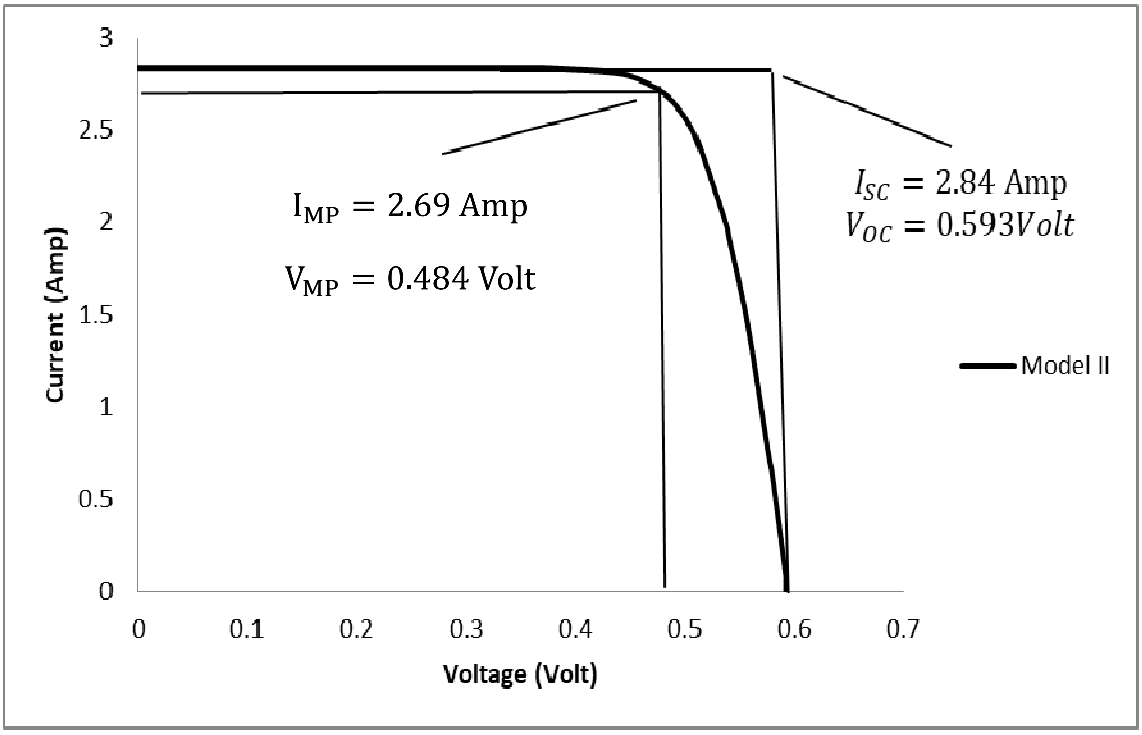

Figure (5.19): I-V sweep of model II and model III of poly-Si solar cell simulated under STC.

According to the above figure (5.19) the FF for model II and model III of poly-Si PV cell is:

$$FF = \frac{1.3}{1.68} = 0.77$$

So the efficiency is:

$$\eta = 13\%$$

This result is acceptable and very similar to the value provided in datasheet.

III. Efficiency calculation of model IV

Last but not least, the double-diode with series and parallel resistances of poly-Si cell has been simulated by QUCS under STC. The I-V curve is shown in figure 5.20. The curve illustrates a clear drop in the value of MPP. This will drop the FF and efficiency of the solar cell.

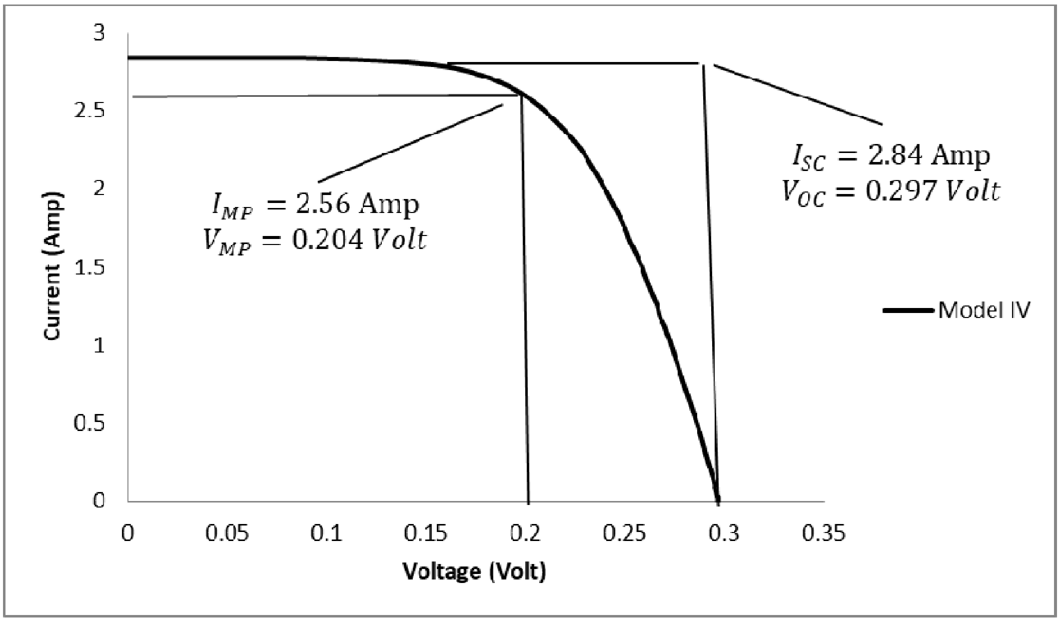

Figure (5.20): I-V sweep of model IV of poly-Si solar cell simulated under STC.

From figure 5.20 the FF for model IV is:

$$FF = \frac{0.523}{0.84} = 0.62$$

Thus the efficiency is:

$$\eta = 5.2\%$$

Table 5.6 summarizes the findings of different models of poly-Si (SPM050-P) solar cell at STC. As expected, model I has the highest FF and efficiency. Also, a drop in the output maximum power does result in a reduction of efficiency of the solar cell.

Table (5.6): simulation results of poly-Si (SPM050-P) solar cell's various models simulated under STC (25℃ and $1000\ W/m^2$).

Model	FF	η
I (ideal)	0.83	14%
II	0.76	12.9%
III	0.77	13%
IV	0.62	5.2%

5.3.7 Variation of characteristics with temperature.

As was mentioned previously, the environmental conditions have a huge influence on the characteristics of the PV cell. QUCS was used also to simulate the polycrystalline Si solar cell under different values of temperature. The performance of poly-Si solar cell under three different temperature and a fixed irradiance ($G = 1000\,W/m^2$) is presented in figure 5.21. The figure depicts, as expected, an increase in temperature results in a drop in P_{max}, FF and efficiency. Moreover, V_{oc} decreases when increasing temperature and there is a clear increase in I_{sc} as temperature increases. Table 5.7 summarizes the findings.

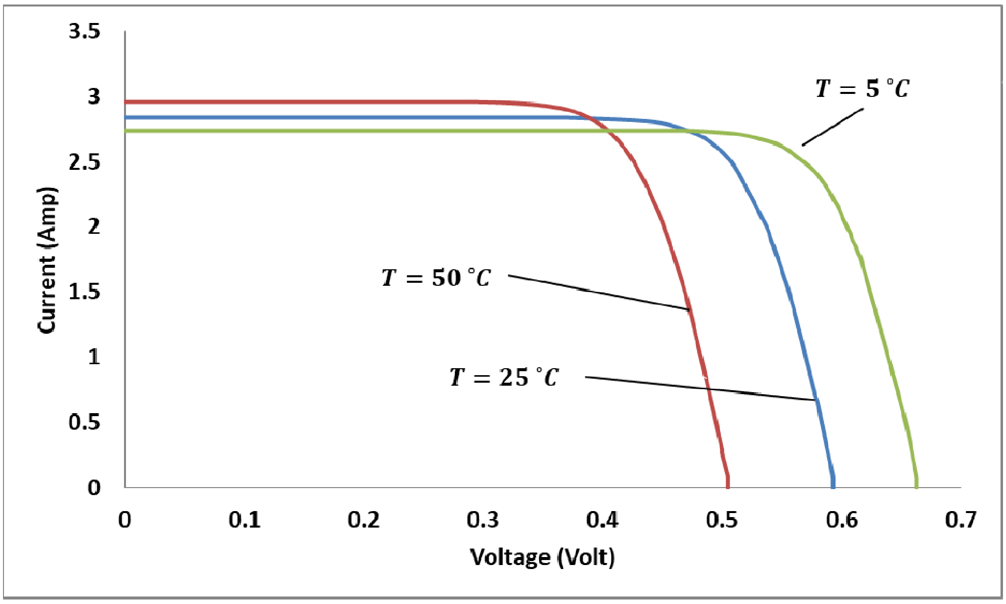

Figure (5.21): poly-Si PV cell I-V curves at different temperatures and at a constant irradiance.

Table (5.7): simulation results for poly-Si solar cell (SPM050-P) with respect to temperature ($G = 1000\, W/m^2$).

T (°C)	$I_{SC}(A)$	$V_{OC}(V)$	$P_{max}(W)$	FF	η %
5	2.74	0.663	1.4	0.79	14 %
25	2.84	0.593	1.3	0.77	13 %
50	2.96	0.505	1.1	0.73	11 %

5.3.8 Variation of characteristics with irradiance.

To study the behavior of poly-Si solar cell with respect to irradiance, the temperature is kept fixed 25℃ and the irradiance was changed. I-V output curves were studied under three different values of irradiance which they are $200\ W/m^2$, $600\ W/m^2$ and $1000\ W/m^2$. Figure 5.22 illustrates the performance of PV cell under varying irradiance. As expected, an increase in irradiance results in increase the value of output power. This leads to an increase in FF and efficiency of PV cell when the irradiance is increased. V_{oc} has been increased slightly when increasing the irradiance while it is clear that I_{sc} is increased when the irradiance is increased. Table 5.8 shows the effect of irradiance in numbers.

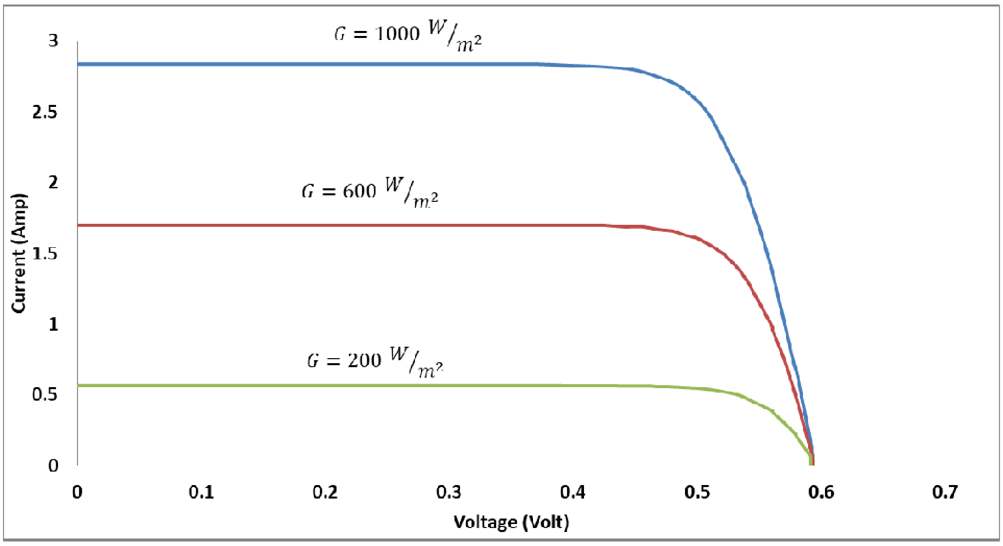

Figure (5.22): poly-Si PV cell I-V curves at different values of irradiance and at fixed temperature.

Table (5.8): simulation results for poly-Si solar cell (SPM050-P) with respect to irradiance ($T = 25$℃).

$G\ (W/m^2)$	$I_{SC}(A)$	$V_{OC}(V)$	$P_{max}(W)$	FF	η %
200	0.568	0.591	0.26	0.77	3 %
600	1.7	0.593	0.8	0.79	8 %
1000	2.84	0.593	1.3	0.77	13 %

5.3.9 Outcomes of section III

Table (5.9): a comparison between mono-Si and poly-Si solar cells simulated by QUCS under STC.

	$\boldsymbol{Mono-Si}$				$\boldsymbol{Poly-Si}$			
Model	I(ideal)	II	III	IV	I(ideal)	II	III	IV
$\boldsymbol{FF}$	0.82	0.75	0.75	0.68	0.83	0.76	0.77	0.62
$\boldsymbol{P_{max}(W)}$	1.62	1.47	1.47	1.29	1.4	1.29	1.3	0.523
$\boldsymbol{\eta}$	16.1%	14.7%	14.7%	12.8%	14%	12.9%	13%	5.23%

I. Poly-Si solar cells in general have efficiency range in 13% and 16%.

II. In response to the change in environmental conditions poly-Si solar cell has a similar behavior to that in mono-Si solar cell.

III. Recombination current decreases open circuit voltage of poly-Si solar cell.

IV. The table above concludes it up. Referring to [7], crystalline silicon cells' efficiencies are ranged between $15\ and\ 22$ %. The resulted efficiencies in this research are approximately in this range. Crystalline silicon solar cells with higher V_{oc} or I_{sc} or FF will have higher efficiencies according to:

$$\eta = \frac{V_{oc} * I_{sc} * FF}{P_{in}} \quad (5.9)$$

V. Both model II and model III have the nearest efficiency to that of the ideal model (model I).

VI. As expected, mono-Si solar cell has higher conversion efficiency than poly-Si solar cell. This is, as mentioned previously, due to the fact that mono-Si cells produce a larger space in crystal for the electrons to move and conduct the electrical current. However, crystals of poly-Si solar cells impede the flow electricity due to the small room they provide. Also, the black color of mono-Si gives it an advantage since it enhances the absorption of sunlight.

5.4 Simulation results of organic PV cell using GPVDM

5.4.1 Input parameters

GPVDM software has facilitated the study of different types of solar cell specially the organic PV cells. Before running any desired simulation, input parameters should be specified. The simulated organic bulk heterojunction solar cell's structure is shown in the below figure ($x - y$ cross section).

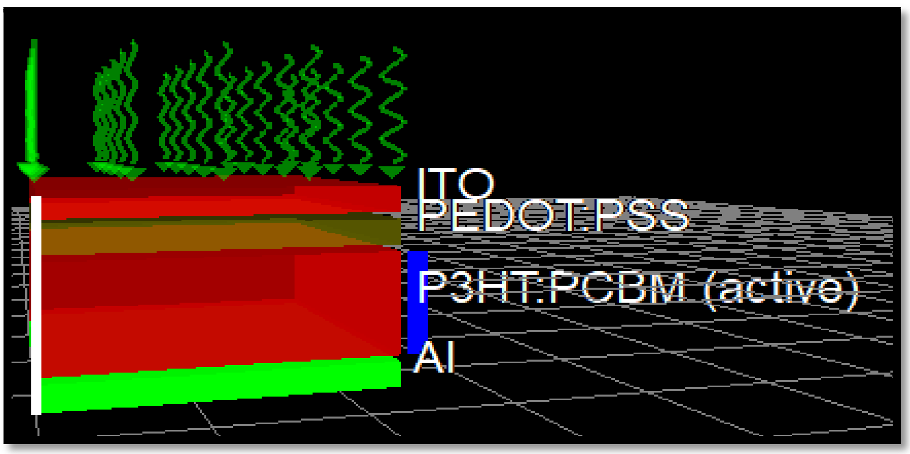

Figure (5.23): device structure of the simulated BHJ solar cell.

The input parameters are shown in the following table:

Table (5.10) Input parameters of organic solar cell based on P3HT:PCBM.

Parameter	Parameter's value
Temperature ($\boldsymbol{K}$)	300
Shunt resistance ($\boldsymbol{\Omega}$)	1.9×10^{5}
Series resistance ($\boldsymbol{\Omega}$)	19.5
ITO thickness ($\boldsymbol{m}$)	1×10^{-7}
PEDOT:PSS thickness ($\boldsymbol{m}$)	1×10^{-7}
P3HT:PCBM (active layer) thickness ($\boldsymbol{m}$)	4×10^{-7}
Al thickness ($\boldsymbol{m}$)	1×10^{-7}
Device x size($\boldsymbol{m}$)	0.0024495
Device z size ($\boldsymbol{m}$)	0.0024495

5.4.2 J-V output curve

GPVDM offers J-V characteristic curve of the illuminated solar cell. J-V characteristic curve of the illuminated solar cell is given in figure 5.24.

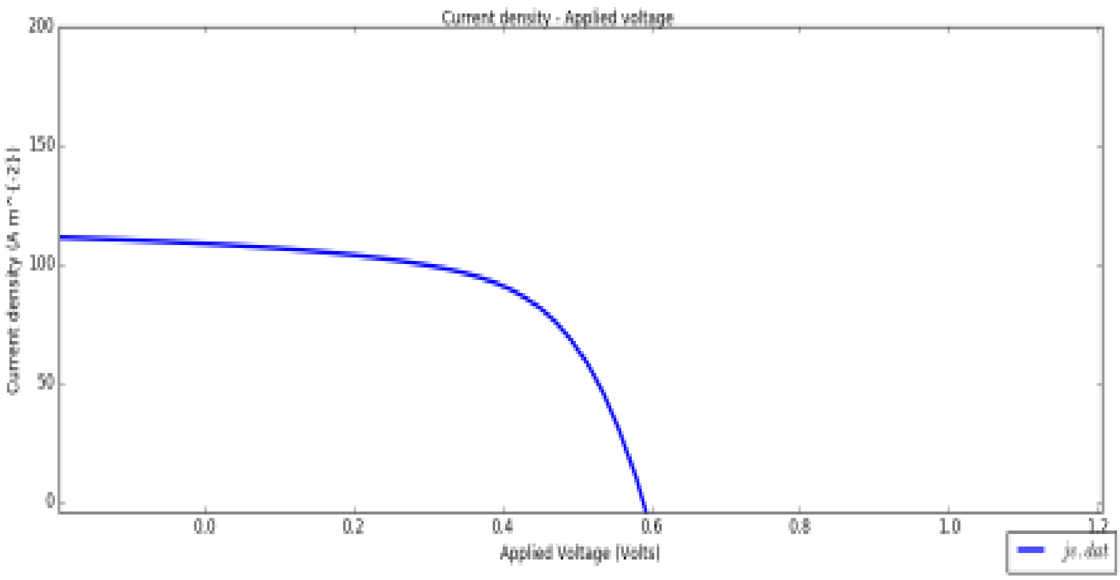

Figure (5.24): The output J-V curve of OPV cell under STC.

Table (5.11) The output electrical parameters of organic solar cell based on P3HT:PCBM.

Thickness of active layer (nm)	**400**
$J_{SC}(A/m^2)$	108.574591
$V_{OC}(Volts)$	0.588176
$J_{max}(A/m^2)$	87.32
$V_{max}(Volts)$	0.423
$P_{max}(W/m^2)$	36.441154
FF	57.063274
η %	3.644115%

The output parameters are shown in the above table. The simulation was done under $G = 1000\, W/m^2$ and $T = 300\ K$.

5.4.3 Effect of thickness of active layer on efficiency

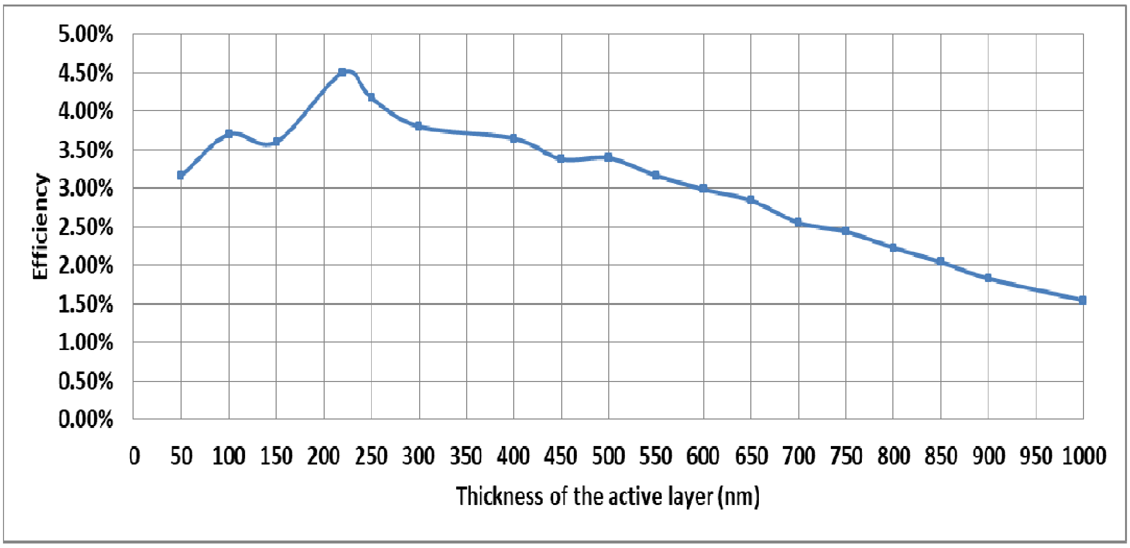

Figure (5.25) conversion efficiency versus the thickness of P3HT:PCBM.

The behavior of efficiency function with respect to thickness of active layer (P3HT:PCBM) in nm is shown in figure 5.25. The efficiency shows a periodic behavior. The efficiency increases then decreases and this behavior is repeated another time resulting two peaks one at $\boldsymbol{L = 100\ nm}$

and the other is at $\boldsymbol{L = 220\,nm}$. The maximum efficiency is $\mathbf{4.50}$ % at $\boldsymbol{L = 220\,nm}$.

With comparison to [23] the behavior of efficiency versus thickness of active layer is similar to that one resulted in [23] i.e. they're both show periodic behavior.

The data that has been obtained and drawn in figure 5.25 are summarized in table 5.12.

Table (5.12) Thickness of P3HT:PCBM against conversion of organic solar under STC.

Thickness of active layer ($\boldsymbol{nm}$)	Efficiency
50	3.16%
100	3.70%
150	3.60%
220	4.50%
250	4.17%
300	3.80%
400	3.64%
450	3.38%
500	3.39%
550	3.16%
600	2.98%
650	2.84%
700	2.55%
750	2.43%
800	2.22%
850	2.04%
900	1.83%
1000	1.54%

5.4.4 Effect of series resistance on J-V curve.

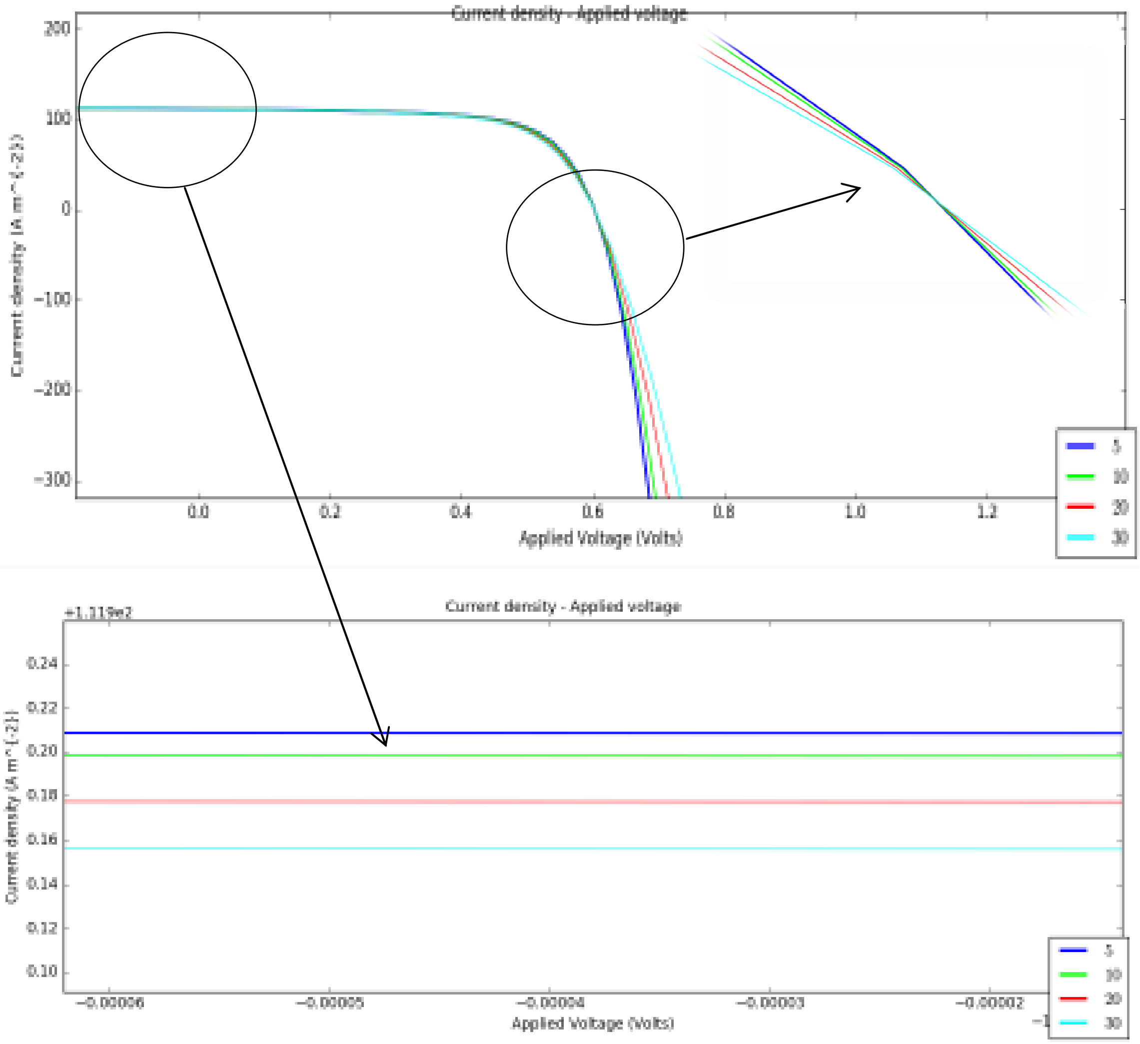

Figure (5.26): J-V curves of organic solar cell under STC through different values of series resistance.

Table (5.13): electrical parameters of simulated organic solar cell under STC against varying series resistance's value.

Series resistance value	$\mathbf{5\ \Omega}$	$\mathbf{10\ \Omega}$	$\mathbf{20\ \Omega}$	$\mathbf{30\ \Omega}$
$\boldsymbol{J_{SC}}$ $(\boldsymbol{A/m^2})$	111.660084	111.649345	111.634329	111.574267
$\boldsymbol{V_{OC}(Volts)}$	0.602238	0.602238	0.602238	0.602238
$\boldsymbol{P_{max}(W/m^2)}$	45.924982	45.647022	45.091103	44.535184
$\boldsymbol{FF}$	68.294072%	67.887253%	67.069498%	66.278271%
$\boldsymbol{\eta}$	4.592498%	4.564702%	4.509110%	4.453518%
Thickness of active layer ($\boldsymbol{nm}$)		220		

According to table 5.13 the best series resistance is $\mathbf{5\ \Omega}$. It gives the maximum short circuit current density, maximum power point, filling factor and efficiency. At all series resistances open circuit voltage has the same value.

5.4.5 Outcomes of section IV

I. An electrical simulation of $P3HT\colon PCBM$ based BHJ solar cell was done under STC with accuracy.

II. As expected J-V curve of nanoscale active layer based solar cell is similar to that of crystalline silicon based solar cells.

III. It was observed that organic BHJ solar cell has an open circuit voltage similar of the value in crystalline silicon solar cell.

IV. As expected, thickness of active layer does affect conversion efficiency of the solar cell.

V. It was found that the best thickness of active layer is $220\ nm$ which gives an efficiency of 4.5%.

VI. As expected, series resistance does affect the behavior of the solar cell.

VII. The efficiency of the solar cell raised from 4.509110% to 4.592498% when series resistance is dropped from 20Ω to 5Ω.

VIII. Raising series resistance does result in a drop in short circuit current density while open circuit voltage doesn’t affect by this raise.

IX. Raising series resistance from 5Ω to 30Ω results in a decrease in power of the cell.

X. As expected, power decreasing results in decreasing of FF and efficiency of the cell.

XI. It is inefficient to fabricate the solar cell with an active layer with thickness above 220 nm. As mentioned previously active layer with thickness more than 220 nm will not increase the efficiency.

XII. In improving efficiency researches, it is not significant to raise the thickness of active layer above 220 nm. Actually this will just consumes material and time.

Chapter Six

Conclusion

Chapter Six
Conclusion

This thesis has been provided an investigation of various models of PV cells based on datasheet information. Three types of solar cells were simulated and studied which they are:

1. Monocrystalline silicon solar cell (four various PV cell models simulated using QUCS).

2. Polycrystalline silicon solar cell (four various PV cell models simulated using QUCS).

I-V characteristic curves were studied for each simulated PV cell under STC. Also device characteristics were observed under new environmental conditions. The four various solar cell models mentioned above were used to characterize the single junction crystalline Si solar cells are:

- Single-diode – PV model (Model I)

- Single-diode with series resistance – PV model (Model II)

- Single-diode with series and parallel resistances – PV model (Model III)

- Double-diode with series and parallel resistances – PV model (Model IV)

It has been found that for single junction monocrystalline Si solar cell (I-106/12 from Isofoton) the conversion efficiency is 16.1% for model I, 14.7% for model II and model III, and 12.8% for model IV under STC.

On the other hand, the simulation results of the four models of single junction polycrystalline Si solar cell (SPM050-P) show that model I gives conversion efficiency which equals 14% while model II and model III give an efficiency of 13%, model IV yield an efficiency of 5.2%. All models were simulated under STC. Both model II and model III have the efficiency which is the nearest to the ideal model (model I).

It can be concluded that the internal losses in the solar cell cause a drop in the fill factor and the efficiency of the PV cell. In conclusion, it is evident that this study has shown how series and parallel resistances can affect efficiency.

Also, the existence of recombination effect (represented by a second diode was added in parallel to the first diode) does decrease the efficiency.

It has been shown that increasing PV cell's temperature lead to a drop of fill factor, efficiency, maximum power and open circuit voltage of the PV cell sufficiently. Moreover, the results show that increasing solar irradiation does increase fill factor, efficiency, maximum power and short circuit current of the PV cell.

Chapter 5 contains the results and the outcomes of simulation of solar cells under STC. Summing up the results, it can be concluded that single diode – PV cell model or the ideal model has the highest value of conversion efficiency. The outcome electrical characteristics of simulated solar cells were expected and they are very similar to those published in the datasheet. This research has clearly shown that monocrystalline Si solar cells are more efficient than polycrystalline ones. The data obtained indicate that the behavior of solar cell is affected by the external conditions like temperature and irradiance.

3. Organic solar cell (one PV model simulated using GPVDM).

In the last part of thesis organic BHJ solar cell has been studied under STC by GPVDM software. J-V curve was detected and the electrical characteristics were extracted. Moreover, it was shown how the conversion efficiency is affected by the thickness of active layer of the solar cell. Finally, J-V curve behavior was observed while changing series resistance value.

The simulation results show that the conversion efficiency of BHJ organic solar cell based on $P3HT{:}PCBM$ of $400\,nm$ thickness is approximately 3.64% under STC.

Also, it has been found that the thickness of active layer does affect efficiency of the PV cell and the data obtained indicate that the maximum efficiency equals 4.5% at thickness of $220\,nm$. There is no point in increasing thickness of BHJ organic solar cell above $220\,nm$ (refer to the figure 5.25).

From the research that has been conducted, it is possible to conclude that increasing series resistance does decrease short circuit current, maximum power, filling factor and efficiency of the solar cell.

Series resistance and the thickness of the active layer have a good impact on the behavior of the organic solar cell which helps to enhance conversion efficiency of the cell.

This research presented useful way to study efficiency of different generations of solar cells. Since it contains information about the dependence of solar cell on temperature and sun radiation and how the characteristics of PV cell are affected by them this research is a base to launch future experimental work. And also it could be a platform for many solar cells' manufacturers and researchers. The next stage of our research will be experimental confirmation of our theoretical work.

References

[1] Arno Smets, Klaus Jäger, Olindo Isabella, Miro Zeman, René van Swaaij, S**olar Energy: Fundamentals, Technology and Systems**, UIT Cambridge, 2016.

[2] A. Zekry, **A course on photo-voltaic array systems**, 1998.

[3] Priambodo, P. S., Sukoco, D., Purnomo, W., Sudibyo, H., & Hartanto, D, "***Electric Energy Management and Engineering in Solar Cell System***," in **Solar Cells-Research and Application Perspectives**, InTech, 2013.

[4] Nema, S., Nema, R. K., & Agnihotri, G, "***Matlab/simulink based study of photovoltaic cells/modules/array and their experimental verification***.," **International journal of Energy and Environment**, vol. 1, no. 3, pp. 487-500, 2010.

[5] "S**olar Panels Characteristics**," [Online]. Available: http://www.samlexsolar.com/learning-center/solar-panels-characteristics.aspx.

[6] Soucase, B. M., Pradas, I. G., & Adhikari, K. R., "***Numerical Simulations on Perovskite Photovoltaic Devices***," **InTech, 2016.**

[7] K. Mertens, Photovoltaics: **Fundamentals, Technology, and Practice**, John Wiley & Sons, 2018.

[8] Shah, A., Torres, P., Tscharner, R., Wyrsch, N., & Keppner, H., "***Photovoltaic technology: the case for thin-film solar cells***," **Science**, pp. 692-698, 1999.

[9] Chin, V. J., Salam, Z., & Ishaque, K., "***Cell modelling and model parameters estimation techniques for photovoltaic simulator application: A review.***," **Applied Energy**, pp. 500-519, 2015.

[10] Parida, B., Iniyan, S., & Goic, R, "***A review of solar photovoltaic technologies***," **Renewable and sustainable energy reviews**, pp. 1625-1636, 2011.

[11] Tsai, H. L., Tu, C. S., & Su, Y. J., "***Development of generalized photovoltaic model using MATLAB/SIMULINK***," **In Proceedings of the world congress on Engineering and computer science,** pp. 1-6, 2008, October.

[12] Tamrakar, V., Gupta, S. C., & Sawle, Y., "***Single-Diode PV Cell modeling and study of characteristics of single and two-diode equivalent circuit***," **Electrical and Electronics Engineering: An International Journal,** 2015.

[13] Sarkar, M. N. I., "***Effect of various model parameters on solar photovoltaic cell simulation: A SPICE analysis***.," **Renewables: Wind, Water, and Solar**, vol. 3, no. 1, 2016.

[14] Dobrzański, L. A., Szczęsna, M., Szindler, M., & Drygała, A., "***Electrical properties mono-and polycrystalline silicon solar cells***," **Solar cells**, pp. 67-74, 2013.

[15] Lineykin, S., Averbukh, M., & Kuperman, A., "***Five-parameter model of photovoltaic cell based on STC data and dimensionless***," **IEEE***,* pp. 1-5, 2012.

[16] Saloux, E., Teyssedou, A., & Sorin, M., "***Explicit model of photovoltaic panels to determine voltages and currents at the maximum power point***," **Solar energy***,* pp. 713-722, 2011.

[17] Ishaque, K., Salam, Z., & Taheri, H., "***Accurate MATLAB simulink PV system simulator based on a two-diode model***," **Journal of Power Electronics***,* pp. 179-187, 2011.

[18] Celik, A. N., & Acikgoz, N., "***Modelling and experimental verification of the operating current of mono-crystalline photovoltaic modules using four-and five-parameter models***," **Applied energy***,* pp. 1-15, 2007.

[19] Rodrigues, E. M. G., Melício, R., Mendes, V. M. F., & Catalão, J. P. S, "**Simulation of a solar cell considering single-diode equivalent circuit model**," in International Conference on Renewable Energies and Power Quality 2011, April.

[20] Dang, M. T., Hirsch, L., & Wantz, G., "***P3HT: PCBM, best seller in polymer photovoltaic research***," **Advanced Materials***,* 2011.

[21] Rastogi, N., Singh, N., & Saxena, S., "***Analysis of Organic Photovoltaic Device at Different Series Resistances***," *U***niversal Journal of Materials Science***,* pp. 83-87, 2017.

[22] Narender Singh, Ashish Chaudhary, Sandeep Saxena, Manish Saxena and Nikhil Rastogi, "***Electrical Simulation of Organic Solar Cell at Different Charge Carrier Mobility***," *I***OSR Journal of Applied Physics***,* vol. 9, no. 2, pp. 1-4, 2017.

[23] Moulé, A. J., Bonekamp, J. B., & Meerholz, K, "***The effect of active layer thickness and composition on the performance of bulk-heterojunction solar cells***," **Journal of applied physic***s,* 2006.

[24] Shockley, W., & Queisser, H. J., "***Detailed balance limit of efficiency of p□n junction solar cells***," **Journal of applied physics***,* vol. 32, no. 3, pp. 510-519, 1961.

[25] [Online]. Available: http://qucs.sourceforge.net/download.html.

[26] [Online]. Available: https://www.gpvdm.com/download.php.

[27] Goswami, D. Y., Kreith, F., & Kreider, J. F. **Goswami, Principles of solar engineering**, CRC Press, 2000.

[28] Hersch, P., & Zweibel, K., B**asic photovoltaic principles and methods**, Solar Energy Research Inst., Golden, CO (USA), 1982.

[29] Archer, M. D., & Green, M. A, **Clean electricity from photovoltaic**s, Imperial College Press, 2001.

[30] "**The Air Mass used in Engineering Testing**," [Online]. Available: https://www.e-education.psu.edu/eme810/node/469.

[31] Duffie, J. A., & Beckman, W. A., **Solar engineering of thermal processes**, John Wiley & Sons, 2013.

[32] M. A. Green, P**V modules: operating principles, technology and system applications**, UNSW, 1992.

[33] "**PVEducation,**" [Online]. Available: https://pveducation.org/pvcdrom/solar-cell-operation/effect-of-temperature.

[34] Bonkoungou, D., Koalaga, Z., & Njomo, D., "***Modelling and Simulation of photovoltaic module considering single-diode equivalent circuit model*** in **MATLAB**," vol. 3, no. 3, pp. 493-502, 2013.

[35] Benmessaoud, M. T., Zerhouni, F. Z., Zegrar, M., "***New approach modeling and a maximum power point tracker method for solar cells***," **Computers & Mathematics with Applications***,* vol. 60, no. 4, 2010.

[36] Villalva, M. G., Gazoli, J. R., & Ruppert Filho, E., "***Comprehensive approach to modeling and simulation of photovoltaic arrays***.," **IEEE Transactions on power electronics***,* vol. 24, no. 5, pp. 1198-1208, 2009.

[37] Sera, D., Teodorescu, R., & Rodriguez, P., "***PV panel model based on datasheet values***," **IEEE** *,* 2007.

[38] PAREJA APARICIO, M. I. G. U. E. L., Pelegrí Sebastiá, J., Sogorb Devesa, T. C., Sanjuan, L., & Vicente, J., "***Modeling of Photovoltaic Cell Using Free Software Application for Training and Design Circuit in Photovoltaic Solar Energy***," **New developments in renewable energy***,* pp. 121-139, 2013.

[39] Nagel, L. W., & Pederson, D. O., "***Simulation program with integrated circuit emphasis (SPICE)***," In **16th Midwest Symposium on Circuit Theory,** 1973.

[40] T. R. Kuphaldt, "**Chapter 3 - Diodes and Rectifiers/ SPICE models," in free electrical engineering textbook**, vol. III .

[41] M. Pareja, "**Photovoltaic Cell simulation with QUCS**," [Online]. Available: http://qucs.sourceforge.net/examples.html.

[42] "**Reviews and Pricing on Solar Panels and Inverters**," [Online]. Available: http://www.isofoton.com/productos-celulas.html..

[43] "**Solar Power Mart**," [Online]. Available: http://solarpower-mart.com/.

[44] Yu, G., Gao, J., Hummelen, J. C., Wudl, F., & Heeger, A. J., "***Polymer photovoltaic cells: enhanced efficiencies via a network of internal donor-acceptor heterojunctions***," **Science***,* 1995.

[45] Kim, K., Liu, J., Namboothiry, M. A., & Carroll, D. L., "***Roles of donor and acceptor nanodomains in 6% efficient thermally annealed polymer photovoltaics***," **Applied Physics Letters***,* 2007.

[46] Rafique, S., Abdullah, S. M., Sulaiman, K., & Iwamoto, M., "***Fundamentals of bulk heterojunction organic solar cells: An overview of stability/degradation issues and strategies for improvement***," **Renewable and Sustainable Energy Reviews***,* pp. 43-53, 2018.

[47] Mayer, A. C., Scully, S. R., Hardin, B. E., Rowell, M. W., & McGehee, M. D., "***Polymer-based solar cells***," **Materials today***,* pp. 28-33, 2007.

[48] Brabec, C. J., Cravino, A., Meissner, D., Sariciftci, N. S., Rispens, M. T., Sanchez, L., ... & Fromherz, T, "***The influence of materials work function on the open circuit voltage of plastic solar cells,***" **Thin solid films***,* pp. 368-372, 2002.

[49] "**General-purpose Photovoltaic Device Model - gpvdm**," [Online]. Available: https://www.gpvdm.com/.

[50] Krebs, F. C., Gevorgyan, S. A., & Alstrup, J., "***A roll-to-roll process to flexible polymer solar cells: model studies, manufacture and operational stability studies***," **Journal of Materials Chemistry***,* pp. 5442-5451, 2009.

[51] Dongue, S. B., Njomo, D., Tamba, J. G., & Ebengai, L., "***Modeling of electrical response of illuminated crystalline photovoltaic modules using four-and five-parameter models***," **International Journal of Emerging Technology and Advanced Engineering***,* vol. 2, no. 11, pp. 612-619, 2012.

APPENDIX

Table 1: Diode SPICE parameters

Symbol	Name	Parameter	Units	Default
I_S	IS	Saturation current (diode equation)	A	1E-14
R_S	RS	Parasitic resistance (series resistance)	Ω	0
N	N	Emission coefficient, 1 to 2	-	1
τ_D	TT	Transit time	S	0
$C_D(0)$	CJO	Zero-bias junction capacitance	F	0
φ_0	VJ	Junction potential	V	1
M	M	Junction grading coefficient	-	0.5
-	-	0.33 for linearly graded junction	-	-
-	-	0.5 for abrupt junction	-	-
E_g	EG	Activation energy:	eV	1.11
-	-	Si: 1.11	-	-
-	-	Ge: 0.67	-	-
-	-	Schottky: 0.69	-	-
p_i	XTI	IS temperature exponent	-	3.0
-	-	pn junction: 3.0	-	-
-	-	Schottky: 2.0	-	-
k_f	KF	Flicker noise coefficient	-	0
a_f	AF	Flicker noise exponent	-	1
FC	FC	Forward bias depletion capacitance coefficient	-	0.5
BV	BV	Reverse breakdown voltage	V	∞
IBV	IBV	Reverse breakdown current	A	1E-3

جامعة النجاح الوطنية
كلية الدراسات العليا

تطوير نماذج مختلفة من الخلايا الشمسية الكهروضوئية الفعالة

إعداد
اية محمود عبدالفتاح ابوبكر

إشراف
د. منى حاج يحيى
د. معن اشتيوي

قدمت هذه الأطروحة استكمالاً لمتطلبات الحصول على درجة الماجستير في الفيزياء بكلية الدراسات العليا في جامعة النجاح الوطنية في نابلس، فلسطين.

2019م

تطوير نماذج مختلفة من الخلايا الشمسية الكهروضوئية الفعالة

إعداد

اية محمود عبدالفتاح ابوبكر

إشراف

د. منى حاج يحيى

د. معن اشتيوي

الملخص

يتناول هذا البحث ثلاثة أنواع مختلفة من الخلايا الكهرضوئية (photovoltaic cells) وهي السيليكون أحادي البلورة (monocrystalline silicon) والسيليكون متعدد البلورات (polycrystalline silicon) والخلايا الكهروضوئية العضوية. لقد تم دراسة أربعة نماذج للدارات المكافئة لكل من الخلايا الكهروضوئية السيليكونية أحادية البلورة ومتعددة البلورات بواسطة برنامج QUCS.

تم استخراج معاملات الإدخال للخلايا الكهروضوئية من ورقة البيانات المعطاة لكل خلية. الهدف الرئيسي من هذا البحث هو الحصول على النموذج الأكثر كفاءة للخلايا الكهروضوئية للحصول على أعلى نقطة قدرة قصوى (maximum power point).

يتناول هذا البحث أيضاً العوامل الرئيسية التي تؤثر على أداء وفاعلية الخلية الكهروضوئية من أهمها: درجة حرارة الخلية (cell temperature) والإشعاع الشمسي (sun irradiance). لقد تم رسم منحنيات التيار-الفولتية (I-V) تحت تغير درجة الحرارة والإشعاع مع ملاحظة التغيرات التي تطرأ على معاملات الخلايا الشمسية.

ألقت هذه الدراسة الضوء على الجيل الثالث من الخلايا الكهروضوئية و هي الخلايا الشمسية العضوية. تم إجراء محاكاة كهربائية لخلية كهروضوئية عضوية باستخدام P3HT:PCBM كطبقة نشطة. تم إجراء المحاكاة باستخدام برنامج GPVDM تحت شروط الإختبار القياسية (STC). تم دراسة الكفاءة للخلايا العضوية تحت تغير سماكة الطبقة النشطة.

أيضاً لقد تم دراسة خصائص الخلية الكهروضوئية العضوية تحت تغير قيمة المقاومة الموصلة على التوالي (R_s).

أكدت نتائج المحاكاة، كما هو متوقع، أن الخلايا الشمسية السيليكونية أحاديـــة البلـــورة (monocrystalline) أكثر كفاءة من الخلايا الشمسية متعددة البلـــورات (polycrystalline) في حين أن كفاءة الخلايا الشمسية متعددة البلورات أعلى من كفاءة الخلايـــا الشمســـية أحاديـــة البلورة. وخلص هذا البحث إلى أن الخلايا الشمسية العضوية (غبر البلورية) ليست بنفس كفاءة الخلايا البلورية لكنها أقل تكلفة.